Die approbierte Originalversion dieser Dissertation ist an der Hauptbibliothek der Technischen Universität Wien aufgestellt (http://www.ub.tuwien.ac.at).

The approved original version of this thesis is available at the main library of the Vienna University of Technology (http://www.ub.tuwien.ac.at/englweb/).

TECHNISCHE UNIVERSITÄT WIEN

VIENNA UNIVERSITY OF TECHNOLOGY

Dissertation

Neurocontrol of Standing and Walking:

Analysis of the Electrically Stimulated Lumbar Generator for Extension in Paraplegic Human

ausgeführt zum Zwecke der Erlangung des akademischen Grades eines Doktors der technischen Wissenschaften unter der Leitung von

Ao. Univ.-Prof. DDr. Frank Rattay
Institut E114
Institut für Analysis und Technische Mathematik

eingereicht an der Technischen Universität Wien,
Fakultät für Technische Naturwissenschaften und Informatik,
von

Dipl.-Ing. Bernhard Jilge

Matrikelnummer 8801501
Inzersdorfer Straße 125/17
A-1100 Wien

Wien, am 1. September 2003

Kurzfassung der Dissertation

Neuronale Steuerung des Stehens und Gehens: Analyse des elektrisch stimulierten lumbalen Mustergenerators in Querschnittsverletzten

Für die Rehabilitation verloren gegangener Funktionen (insbesondere des Stehens und Gehens) nach Rückenmarksverletzungen ist die Erforschung der zugrundeliegenden neuronalen Kontrollmechanismen von großer Bedeutung. Die vorliegende Arbeit untersucht, inwieweit das von supraspinalen Einflüssen getrennte, elektrisch stimulierte lumbosakrale Rückenmark in der Lage ist, jenes motorische Aktivierungsmuster hervorzubringen, das zum Strecken der Beine führt. Modelle dafür, wie das Rückenmark die Aktivität der Beinmuskulatur kontrolliert, werden präsentiert.

Ziele: 1. Festzustellen, unter welchen Bedingungen epidurale Stimulation des Lumbalmarks geeignet ist, eine Streckung der unteren Extremitäten komplett Querschnittsverletzter auszulösen und aufrechtzuerhalten.

2. Das für die induzierte Streckung charakteristische Muster elektromyographischer (EMG) Aktivität (in Raum und Zeit) zu bestimmen und seine „innere Struktur" zu beschreiben.

3. Die Hypothese, das interneuronale Netzwerkes des lumbalen Rückenmarks sei maßgeblich an der Auslösung und Kontrolle der evozierten Streckung beteiligt, zu untermauern.

4. Ein Modell für die der induzierten Streckung zugrundeliegenden neurophysiologischen Mechanismen des Lumbalmarks zu entwerfen und die wesentlichen Annahmen dieses Modells durch Computersimulation zu überprüfen.

Methoden: Neurophysiologische Daten über das Input-Output-Verhalten des epidural stimulierten Rückenmarks komplett Querschnittsverletzter wurden retrospektiv ausgewertet.

Fünf Patienten mit chronischen Rückenmarksläsionen wurden im Bereich der lumbalen Rückenmarksegmente epidural stimuliert. Die Wirkung der Stimulation wurde durch die elektromyographische Aktivität (zusammengesetzte Muskelaktionspotentiale) der Ober- und Unterschenkelmuskulatur dokumentiert. Induzierte Bewegungen der Beine wurden durch Winkelmessung erfasst.

Die EMG-Daten wurden zunächst dahingehend analysiert, welches (relative) Aktivitätsniveau in den einzelnen Muskelgruppen durch verschiedene Kombinationen der Stimulationsparameter ausgelöst wurde. Um Erkenntnisse über die neuronale „Verschaltung" innerhalb des Lumbalmarks zu gewinnen, wurden Latenzzeit, Dauer und Morphologie einzelner EMG-Potentiale ermittelt. Die Potentiale während der eigentlichen Streck*bewegung* wurden einer Hauptkomponentenanalyse unterzogen, die dynamische Aspekte der evozierten Extension offenlegen sollte.

Auf Basis der bisherigen Ergebnisse wurde schließlich ein Simulationsmodell für die frequenzabhängige Selektion neuronaler Rückenmarkspfade entwickelt. Mit Hilfe dieses Modells sollte abgeschätzt werden, welche Rolle grundlegende neurophysiologische Mechanismen (zeitliche Summation postsynaptischer Potentiale, präsynaptische Hemmung

afferenter Nervenendigungen) bei der lumbalen Kontrolle von Bewegungen in komplett Querschnittsverletzten spielen. Ein vereinfachtes neuronales Netzwerk wurde mathematisch-theoretisch und durch Computersimulation analysiert.

Ergebnisse: 1. Elektrische Stimulation des lumbosakralen Rückenmarks mit einer Frequenz von 5–15 Hz und einer Intensität, bei der in den Oberschenkelmuskeln Zuckungen ausgelöst wurden, induzierte eine rasche, kraftvolle Streckbewegung der Beine. Eine Streckung, die anhielt, solange stimuliert wurde, konnte auch mit höheren Frequenzen evoziert werden, wenn die Stimulation hinreichend schwach war. Andernfalls wurde das Bein im Anschluss an eine kurze, unvollständige Streckung wieder gebeugt.

2. Im EMG ließen sich verschiedene Phasen der induzierten Streckbewegung (die unmittelbare Antwort auf die Stimulation, die eigentliche Bewegung und das aktive Beibehalten der gestreckten Position) unterscheiden, in denen die Muskelaktivität auf charakteristische Weise moduliert wurde. Dabei war die EMG-Aktivität der Extensoren (Hüfte, Fuß) stets größer als die der Flexoren. Die Vergrößerung des EMG entlang der Zeitachse zeigte einzelne „zusammengesetzte Muskelaktionspotentiale", die den einzelnen Stimulationsimpulsen direkt zugeordnet werden konnten.

3. Die Beteiligung des lumbalen interneuronalen Netzwerkes an der Auslösung und Kontrolle der evozierten Streckung wurde mehrfach bestätigt:

(i) Die bei 5–10 Hz evozierten zusammengesetzten Muskelaktionspotentiale (EMG-Potentiale) hatten eine kürzere Dauer als die bei 2 Hz oder Frequenzen über 10 Hz ausgelösten. Dieses Ergebnis deutet auf eine zentral gesteuerte Synchronisation der motorischen Einheiten hin, deren Aktivität den Potentialen zugrunde liegt.

(ii) Die EMG-Aktivität der Extensoren (im Verhältnis zu jener der Flexoren) erreichte bei einer Stimulationsfrequenz von 5–10 Hz ein Maximum. Außerhalb dieses Frequenzbereichs zeigten alle Muskelgruppen mit zunehmender Stimulationsfrequenz abnehmende Aktivität.

(iii) Während der eigentlichen Streckbewegung änderte sich die Morphologie der EMG-Potentiale. Die Hauptkomponentenanalyse wies diese Veränderungen als zweidimensional aus. Die gleichzeitig in mehreren Muskelgruppen beobachteten Veränderungen waren im hohem Maße korreliert. Latenzzeit, Amplitude, Dauer und Morphologie der EMG-Potentiale blieben konstant, sobald die Bewegung abgeschlossen war.

4. Grundlegende Input-Output-Eigenschaften des lumbalen Rückenmarks konnten vom Simulationsmodell reproduziert werden: Die einzelnen Netzwerkantworten konnten den Impulsen des Eingangssignals (den „Stimuli") direkt zugeordnet werden und strebten einem Gleichgewichtszustand zu. Ihre Latenzzeit hing von der Frequenz des Eingangssignals ab. Nach Erweiterung der Summationsprozesse um ein stochastisches Element wurden auch Antworten erzeugt, die zwei Komponenten mit unterschiedlicher Latenz enthielten. Die relative Größe dieser Komponenten wurde wiederum von der Stimulationsfrequenz bestimmt.

Schlussfolgerungen: Die in ihrer Amplitude modulierten während der induzierten Streckung gemessenen EMG-Potentiale stellten monosynaptische Reflexantworten auf die Stimulation dicker afferenter Axone in den Hinterwurzeln dar.

Dieselben afferenten Nervenimpulse wurden synaptisch an das interneuronale Netzwerk des Lumbalmarks weitergeleitet, das Bewegungen der unteren Extremitäten kontrolliert. Durch elektrische Impulsfolgen mit einer Frequenz von 5–15 Hz wurden die lumbalen Interneuronenpools zu neuen „funktionalen Einheiten" konfiguriert. Diese bestimmten—über synaptische und präsynaptische Mechanismen—die gegenüber den Flexoren erhöhte Erregbarkeit der Extensoren, die für die evozierte Streckung charakteristisch war. Das sich

während der eigentlichen Streckbewegung verändernde sensorische Feedback wurde in die spinale Kontrolle der Bewegung integriert und trug damit zur beobachteten zeitlichen Modulation der EMG-Aktivität bei.

Frequenzabhängige Selektion alternativer neuronaler Rückenmarkspfade auf der Basis von zeitlicher Summation postsynaptischer Potentiale und präsynaptischer Hemmung afferenter Nervenendigungen scheint dabei eine Rolle zu spielen.

Summary

Study Design: Neurorehabilitative procedures to restore standing and walking after traumatic spinal cord injury demand extensive neurophysiological research on the neurocontrol of these motor functions. The present work aimed at elucidating the capabilites of the isolated human lumbosacral cord with regard to the generation of lower limb extension in response to sustained electric stimulation. Neurophysiological models on the control strategies adopted by the lumbar cord to implement this motor task in complete paraplegics should be developed.

Objectives: 1. To investigate whether and under what conditions a sustained extension of the lower limbs can be induced by epidural stimulation of the lumbar cord in complete spinal cord injured subjects.

2. To define the spatiotemporal electromyographic (EMG) pattern which is characteristic for induced lower limb extension, and to describe its „internal" structure on different time scales.

3. To provide evidences for the involvement of spinal interneuronal circuitry in the initiation and control of the evoked extension movement.

4. To develop a neurophysiological model on the control strategy adopted by the lumbar interneuronal network to generate the induced extension. Furthermore, to test fundamental assumptions of this model by means of computer simulation of the network behaviour.

Methods: Neurophysiological data on the input-output behaviour of the isolated lumbar cord in response to epidural stimulation were retrospectively analysed.

Electric stimulation of the lumbosacral cord was applied in five subjects with long-standing complete spinal cord injury. The effects of spinal cord stimulation (SCS) were captured by EMG recording of induced compound motor unit potentials (CMUPs) from the main thigh and leg muscles, as well as by goniometric recording of the knee joint angle.

Evoked EMG patterns were analysed with respect to the relative amount of CMUP activity induced in different muscle groups in dependence on the applied configuration of stimulus parameters. To investigate spinal circuitry involved in the control of evoked extension, individual (stimulus-locked) CMUP responses were examined with regard to amplitude, latency time, duration and shape. Principal component analysis was performed on sequences of CMUP responses recorded during actual movement to study the dynamical properties of the induced motor task.

On the basis of the previous findings, a biology-based computational model on frequency-dependent spinal pathway selection was developed. Therewith, the potential role of elementary neurophysiological mechanisms in the control of different motor tasks by the isolated lumbar cord should be estimated. The behaviour of a simplified neuronal network, involving temporal summation of postsynaptic potentials and presynaptic inhibition, was analysed theoretically and by computer simulation.

Results: 1. Sustained, non-patterned electric stimulation of the lumbosacral cord—applied at a frequency of 5–15 Hz and a strength above the thresholds for twitches in the thigh muscles—initiated a strong and rapid extension movement of the lower limbs. An extension which was

sustained for as long as the external stimuli were applied was also evoked at higher stimulus frequencies provided that stimulation was sufficiently weak. Otherwise, the extension was soon replaced by a flexion movement (preparing rhythmical activity).

2. The EMG recording during the SCS-evoked motor task demonstrated distinct phases (immediate response, actual movement, and retention of extended position) in which well-defined temporal modulations of the EMG pattern were observed. Thereby, the amount of rectified and integrated EMG activity in the hip and ankle extensors was always larger than in the flexors. Examination on an enlarged time scale revealed the EMG trace to be composed of single CMUPs, which could be related directly to the individual pulses within the stimulus train.

3. Several observations independently suggested the involvement of spinal interneuronal circuitry in the generation of induced lower limb extension:

(i) CMUP responses to 5–10 Hz stimulation had a shorter duration than single CMUPs or responses to higher frequencies, indicating centrally controlled synchronisation of motor unit activity.

(ii) Hip/ankle extensor responses were selectively augmented compared to the flexor muscles as the stimulus frequency approached 5–10 Hz. Outside this range, the EMG amplitudes in all studied muscle groups decreased as the interstimulus interval was reduced.

(iii) During the actual movement, the CMUP responses underwent repeatable morphologic changes. In terms of principal components, the changes in either muscle group were basically two-dimensional. The modulations simultaneously recorded in different muscle groups were highly correlated. As soon as extension was implemented, consecutive CMUP responses revealed fairly constant latency time, amplitude, duration and shape.

4. Fundamental input-output features of the lumbar cord were reproduced by the computational network model: The network output was phase-locked to the input signal, and eventually converged toward a steady state. Depending on the frequency of the network input, either short- or long-latency responses were obtained. By assuming the summation processes to be stochastic, responses including components at both short and long latency were obtained as well. The relative size of these components was determined by the interstimulus interval.

Conclusions: The amplitude-modulated CMUPs observed during epidurally evoked sustained lower limb extension reflect monosynaptic responses to the stimulation of large afferents in the posterior roots.

Probably, the same primary afferent volleys were synaptically transmitted to the intrinsic spinal circuitry which is involved in the generation of lower limb movements. Stimulus trains at 5–15 Hz configured this interneuronal network in such a way that it set up—via presynaptic and synaptic mechanisms—the difference in the responsiveness between the flexor and extensor nuclei reflected in the characteristic EMG extension pattern. During the unfolding SCS-evoked movement, varying sensory feedback was integrated by the newly-organised functional units of spinal interneurones, and thus controlled the observed temporal modulations in the excitability of flexor and extensor motoneurones.

Frequency-dependent selection between alternative spinal pathways, based on temporal summation of postsynaptic potentials and presynaptic inhibition of primary afferent terminals, appears to contribute to this control.

Acknowledgements

I am grateful to Professor DDr. Frank Rattay and Professor Milan R. Dimitrijevic, MD, DSc, for their supervision and mentorship, their patient advice, and for steadily encouraging me to explore the field of human neurosciences.

Many thanks to Dozent Dr. Michaela M. Pinter, Maria Auer and Renate Preinfalk for their readiness to answer my questions on the neurophysiological data and the clinical neurophysiological assessment procedures.

Table of Contents

Kurzfassung der Dissertation 2
Summary 5
Acknowledgements 7
Table of Contents 8
Abbreviations 10

Introduction 11

The spinal cord constitutes the "lower motor centre", which integrates peripheral and central input 11
Different neurorehabilitative procedures aim at restoring impaired motor functions after traumatic spinal cord injuries 13
Is there a central pattern generator for locomotion in humans? 14
Technology to conduct neurophysiological studies on the neurocontrol of standing and walking in humans has become available 16
Design of the thesis 17

References 17

Chapter 1

Initiating extension of the lower limbs in subjects with complete spinal cord injury by epidural lumbar cord stimulation 20

Abstract 20
1.1 Introduction 21
1.2 Methods 24
1.2.1 Subjects 24
1.2.2 Evaluation procedure 25
1.2.3 Stimulation procedure 25
1.2.4 Data recording and analysis 26
1.3 Results 28
1.3.1 Effect of stimulation parameters on EMG output and induced movement 29
1.3.2 Degree and duration of the induced extension movement 36
1.3.3 Characteristic features of sequential EMG responses 37
1.3.4 Effect of initial limb positioning 38
1.4 Discussion 39
1.4.1 Primarily activated spinal cord structures 39
1.4.2 Possible mechanisms underlying the induced extension 42
1.4.3 Significance of the results 45

References 46

Chapter 2

Evidences for a lumbar extension pattern generator in humans: Neurophysiology of compound motor unit potentials 51

Abstract 51

2.1 Introduction 52
2.2 Methods 54
2.2.1 Subjects, evaluation and stimulation procedure, recording 54
2.2.2 Data analysis 54
Flexion threshold frequency 55
Net amount of rectified and integrated EMG activity 55
Content of compound motor unit potentials 57
Analysis of the temporal changes in the EMG patterns observed during the actual extension movement 58
2.3 Results 59
2.3.1 Which segments of the lumbosacral cord have to be activated to induce lower limb extension? 59
2.3.2 Quadriceps and hamstring respond differently to the same (common) input 61
2.3.3 Content of the responses during implemented extension 64
2.3.4 Content of the responses during the transition from flexed to extended lower limb position 67
2.3.5 Analysis of the temporal changes in the EMG patterns observed during the actual extension movement 68
2.4 Discussion 71
2.4.1 Frequency-dependent motor unit synchronisation 72
2.4.2 Frequency-dependent selective augmentation of extensor activity 75
2.4.3 Changes in motor unit recruitment as the induced movement unfolded 75
2.4.4 Reciprocal relation between stimulus strengths and frequencies inducing a sustained lower limb extension 76
Appendix: Principal component analysis of the temporal EMG patterns 77
A1 Analysis of the output of a single EMG channel 77
A2 Analysis of muscle synergies 82
References 83

Chapter 3
Frequency-dependent selection of alternative spinal pathways with common periodic sensory input 87
Abstract 87
3.1 Introduction 87
3.2 Methods 89
3.2.1 Model description 89
3.2.2 Computer simulations 91
3.3 Results 93
3.3.1 Theoretical analysis of the network behaviour 93
3.3.2 Computer simulations 97
Deterministic model 97
Stochastic model 99
Duration of the tuning phase 101
3.4 Discussion 106
Appendix: Theoretical analysis of the network behaviour 108
B1 Deterministic model 108
B2 Stochastic model 110
B3 Determination of parameter settings 113
References 114

Epilogue 117
Curriculum vitae 118

Abbreviations

1-LIFM	single-point leaky integrate-and-fire model
AP	action potential
C	cervical
CMUP	compound motor unit potential, EMG potential
CNS	central nervous system
CPG	central pattern generator
EMG	electromyography, -graphic
GOF	goodness of fit
H	hamstring
L	lumbar
LLPG	lumbar locomotor pattern generator
MLR	mesencephalic locomotor region
ON	orthonormal
PARA	paraspinal muscles
PCA	principal component analysis
PRMRR	posterior root muscle reflex response
PSI	presynaptic inhibition
PSP	postsynaptic potential
Q	quadriceps
S	sacral
SCI	spinal cord injury, -injured
SCS	spinal cord stimulation
T	thoracic
TA	tibial anterior
TS	triceps surae

Introduction

"We need not learn the complex language of the human central nervous system if we take advantage of its intrinsic 'translators'."

Professor DDr. Frank Rattay
My teacher

"It is a unique opportunity to study human neurocontrol of standing and walking on the basis of biological data."

Professor Milan R. Dimitrijevic, MD, DSc
My mentor

The spinal cord constitutes the "lower motor centre", which integrates peripheral and central input

Although our neurophysiological knowledge about the spinal cord has advanced significantly, the appearance of the latter has not changed. It is still an elongated, cylindrical portion of the central nervous system, which consists of peripheral white matter including propriospinal, long ascending and descending pathways surrounding the central gray. It has been shown that there are at least three systems of motor pathways originating in the brain and ending in the spinal cord: the systems from the cerebral cortex and the brainstem as well as the "gain-setting" system [Kuypers 1987]. The latter is diffusely organised, being activated during excessive motivational responses. The distribution pattern of descending system terminals within the dorsolateral and ventromedial parts of the intermediate zone of spinal interneurones has extensively been studied. Knowledge of the descending axon connections with spinal interneurones is relevant for the understanding of supraspinal-spinal interaction. It is speculated that different sets of interneurones in distinct parts of the intermediate zone possess the same characteristics as the descending pathways which terminate on them [Dimitrijevic 1992].

In the 1960s and '70s, the spinal interneuronal system was mainly seen as a centre of proprio- and exteroceptive reflexes, a network of excitatory and inhibitory neurones involved in changing peripheral input. Neurophysiology of the spinal cord focused on identifying reflex pathways from muscle spindle afferents, Golgi tendon organs, flexor reflex afferents etc. in healthy subjects as well as in humans with spinal cord injuries or other neurological disorders. It was not certain whether there were two separate subgroups of spinal interneurones, one involved in spinal reflex activity and another in supraspinal-spinal interaction. In the 1980s, researchers provided definite evidence that the spinal interneuronal population is *not* divided into these subgroups, but is an entity that integrates both functions in order to produce harmonious movements. The "premotoneuronal integration centre" is the last link of numerous peripheral and brain pathways, and the convergence of primary afferents and fibres of central origin upon spinal interneurones appears to be the rule [Schomburg 1990]. Individual interneurones can maintain widespread connections with a variety of motoneurones in a large portion of the spinal cord. Via spinal interneurones the degree of excitation/inhibition exerted on the motor nuclei of several flexors and extensors can be adjusted so that these muscles contract either alternately or simultaneously. On the other hand, the brain is not only involved in the control of spinal motor

activity but also in anticipating (planning) and setting motor events well before they become manifest. Spinal motor activity is finally influenced by the brain to execute tuned and well-adjusted movements (**Fig. 0.1**).

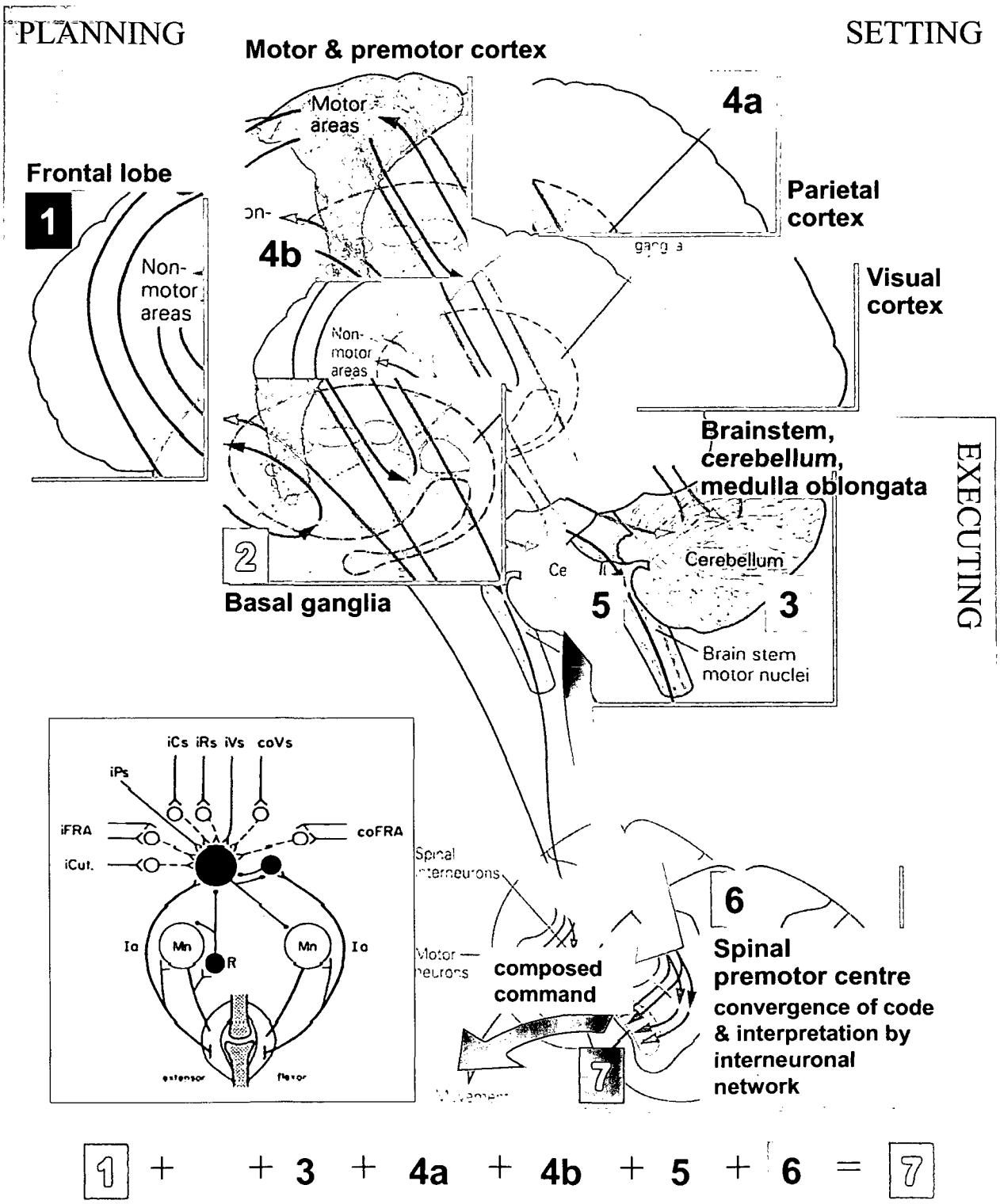

Fig. 0.1. Schematic drawing on the composition of the integral of a "movement command" (brain "motor code"). Adapted from Butler J, Lebowitz H (eds) Principles of Neural Science, 4/e, McGraw-Hill 2000, and Lundberg 1969 (inset).

Different neurorehabilitative procedures aim at restoring impaired motor functions after traumatic spinal cord injuries

In response to a spinal cord injury, particularly to one that completely or incompletely divides the "upper brain" and "lower spinal cord" motor centres, new motor control alternatives are generated as well as new features of spinal reflex activity. Neurorehabilitative intervention seeks to "direct" these changes toward minimising the effect of the injury on spinal cord functions and restoration of impaired functional capabilities. Together with the severity of the lesion, the processes of recovery supported by such procedures essentially determine the clinical outcome of traumatic injuries to the spinal cord. The percentage of subjects who recover their ability to walk after a traumatic spinal cord injury (SCI) ranges between 15 and 45 %, whereas the others stay bound to the wheelchair as the ultimate means of locomotion [Daverat *et al.* 1988]. Therefore, we have to ask ourselves to what extent we are able to „restore" lost functions, to increase the number of SCI people who become ambulatory and to improve their performance of standing and walking.

On the basis of encouraging results from animal experiments on a moving treadmill [showing that in the adult spinal cat the quality of hindlimb locomotion is improved by training, and the spinal locomotor pattern evolves with time, *cf.* Lovely *et al.* 1986 and 1990], Wernig and Müller [1992] examined whether similar training would be beneficial to humans with incomplete and chronic SCI. They found that even in severely paralysed incomplete SCI subjects bipedal stepping could be elicited after a prolonged period of time from the onset of the injury [Wernig *et al.* 1995], whereas in paraplegic, clinically complete subjects significant improvement in stepping on the treadmill was *not* observed despite daily exercise during which the limbs were set and controlled by two therapists. In parallel, Barbeau *et al.* [1992] also reported improvements in the locomotor performance of incomplete SCI subjects with locomotor training. Dobkin *et al.* [1995] confirmed that only subjects with an incomplete lesion could benefit from the training with respect to walking endurance (i.e., distance covered both on the treadmill and on a static surface), speed and necessary body weight support. During treadmill locomotion, the timing and structure of electromyographically (EMG)-recorded lower limb muscle activity in paraplegics were similar to those seen in healthy subjects [see also Dietz *et al.* 1995 and Harkema *et al.* 1997].

In parallel, other techniques such as functional electrical stimulation (FES) of peripheral nerves or intrathecal application of pharmacological substances have become available. Together with treadmill training and epidural spinal cord stimulation (see below) they constitute the repertoire of „interactive locomotor training", which is more and more often used in clinical practice. Comparing study results (and weighting for the number of subjects) one can see a gradient of effects ranging from small changes after the immediate application of FES or body weight support to larger changes when locomotor training is combined with FES and/or body weight support and/or pharmacological approaches [Barbeau *et al.* 1998].

Another approach to elicit stepping-like EMG activity from the isolated lumbar cord differs from inducing patterned, phasic sensory input from the lower limbs associated with (partial) load-bearing and manual feet movement: epidural stimulation of the lumbosacral cord with a sustained, non-patterned train of electric pulses at variable frequency, amplitude and duration. Due to Dimitrijevic's pioneering work in the 1980s, spinal cord stimulation (SCS) has become available as a clinical procedure for spasticity control in subjects with an SCI neurological syndrome. Recently, Dimitrijevic *et al.* [1998a] have shown that SCS can increase locomotor capacity in humans. The authors regarded their results as an evidence for the existence of a

spinal locomotor pattern generator in humans, which they supposed to have activated by the external stimulation.

The question whether and how the ability to *stand* can be restored after spinal cord lesions has been addressed in the literature. Pratt *et al.* [1994] and De Leon *et al.* [1998] reported an improved standing ability after daily stand training in chronic spinal cats. In humans, lower limb extension has primarily been studied as a part of the step cycle. Only a short time ago, Harkema [2001] has shown that after several weeks of step and stand training, chronic incomplete SCI subjects could eventually stand independently for several minutes though they had not been able to bear weight previously. Not least since the ability to stand is a prerequisite for walking, further studies on this matter would be desirable.

Is there a central pattern generator for locomotion in humans?

In the 1910s experimental investigations on animals indicated that the lumbar spinal cord would harbour a pacemaker („generator") inducing locomotor-like alternating movements which acted autonomously since it had been separated from suprasegmental influences by an experimentally induced trauma (transection or decerebration). In lower vertebrates as well as in mammals, complex patterns of behaviour can be performed by animals lacking a cerebral cortex. Neonatally decorticated cats move around in a way that, to the casual observer, does not appear different from that of intact cats. During the first part of the 20th century investigators asked whether basic movement synergies were generated by central networks or through some sort of reflex chain arrangement. This „either-or" way of posing the question was unfortunate in that it led even very competent researchers, such as Brown, von Holst, Gray, and Sherrington to seek evidence in favour of only one view or the other: Brown showed, for example, that rhythmic stepping-like activity observed in the acute spinal cat was not due to a succession of reflexes since it persisted after peripheral deafferentation [Brown 1911], whereas Gray put strong emphasis on sensory (feedback) mechanisms. During the 1970s it became clear that the control strategies used to implement various basic motor tasks utilise both aspects, that is, a central network that generates essential features of the motor pattern, and sensory feedback signals that form an integral and crucial part of the control system. Shik, Orlovsky and Severin [1966] had demonstrated that decerebrate cats can be made to walk if specific brainstem areas (namely the mesencephalic locomotor region) are subjected to repetitive electrical stimulation, but their movements stayed stereotyped, machine-like and not adapted to the needs of the animal [see also Grillner 1981].

Definite evidence for a „central pattern generator" (CPG) for locomotion exists in lower mammals [cat, rat, rabbit, dog; Grillner 1973, 1981, 1985]. Spinal locomotor activity was mainly observed in acute spinal preparations after injection of catecholaminergic drugs [Jankowska *et al.* 1967]. Spinal locomotor activity was also obtained in the chronic spinal cat [Barbeau *et al.* 1987], as well as in chronic spinal rats after transplanting embryonic catecholaminergic cells below the level of the spinal transection [Yakovleff *et al.* 1989, 1995]. However, the existence of a CPG in primates first remained unclear. Eidelberg *et al.* [1981] provided evidence that in acute and chronic spinal macaque monkeys it was *not* possible to evoke locomotor movement. On the other hand, Hultborn *et al.* [1993] reported to *have* evoked fictive locomotion in spinal marmoset. (The term „fictive locomotion" is used to express that peripheral segmental input has been removed, e.g., by posterior rhizotomy, in the experimental model. Since the model for fictive locomotion has not yet been established in humans with SCI, the term „lumbar locomotor pattern generator" will be used in the following.)

The question whether a „lumbar locomotor pattern generator" (LLPG) similar to the CPG found in animals exists in humans could not be answered conclusively until a short time ago [Illis 1995, Bussel *et al.* 1996]—although autonomous locomotor-like movements had been observed in embryos from the tenth week of pregnancy, and in babies immediately after their birth when they hold a certain attitude, and that these movements disappear when the suprasegmental excitatory and inhibitory influence from the brainstem increases [Forssberg *et al.* 1991]. (There appears to be a progressive inhibition of the LLPG during ontogeny.) Bussel *et al.* [1996] discussed indirect evidence for a central mechanism for stepping by demonstrating that flexor reflexes in paraplegic subjects included long-latency late-flexion reflex components. Rhythmical spinal activity was also observed in a subject with clinically complete spinal cord transection. Another indirect proof for the existence of an LLPG in humans was described in a patient with incomplete SCI and periarthritic changes in the hip [Calancie *et al.* 1994]. The patient performed involuntary (automatic) locomotor-like movements when he rested in a relaxed supine position. The movements could only be stopped by changing his position. From the synopsis of the neurophysiological evaluations presented in that study one could draw the conclusion that the periarthritic changes provided a continuous, tonic peripheral stimulus to the L2 segment of the spinal cord which led to the activation of the LLPG.

Using electrial stimulation of the human lumbar cord from the epidural space, Dimitrijevic *et al.* [1998a] were between the first who provided direct evidence for the presence of LLPG circuitry responsible for the initiation and control of rhythmic activity within the lumbosacral cord. Spinal cord stimulation had already been practiced as a method for the treatment of spasticity in spinal cord injured subjects. The authors explored whether the lumbar cord isolated from brain control could respond to a sustained, non-patterned train of electrical stimuli with the generation of rhythmically alternating lower limb movements. The actual question was whether this external tonic input could replace the suprasegmental tonic activity that was missing due to the spinal cord injury (**Fig. 0.2**). Dimitrijevic and collaborators found that such stimulation *could*

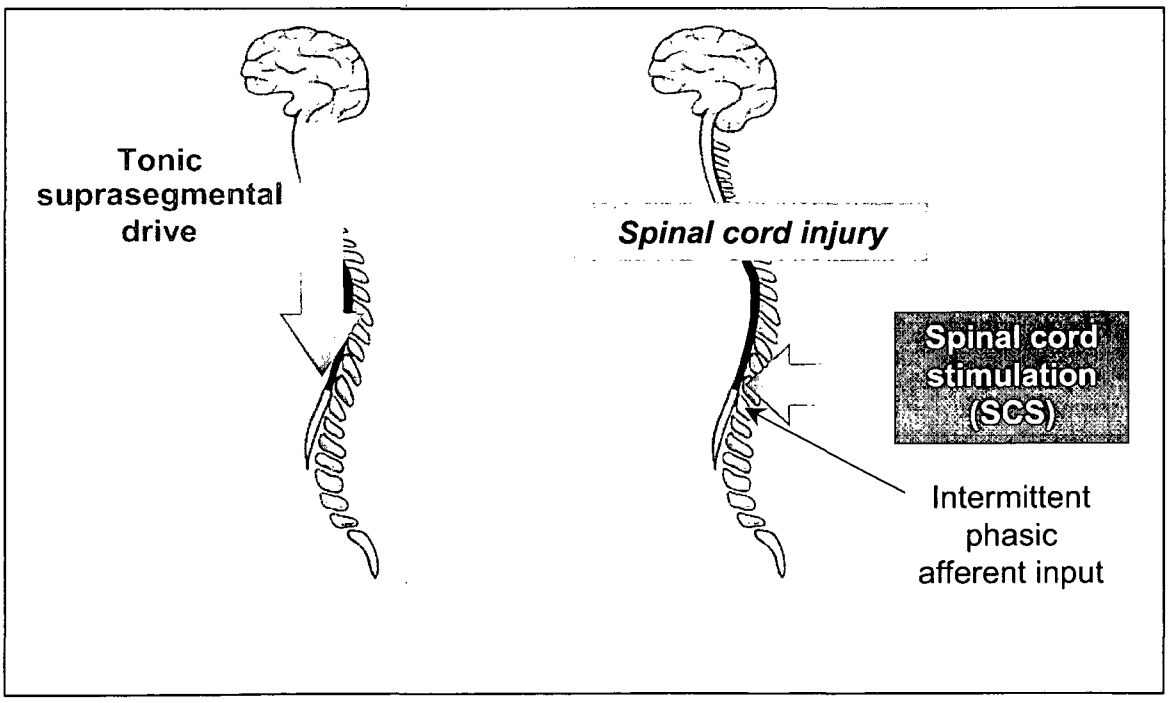

Fig. 0.2. Mimicking brainstem control of the lumbar interneuronal network. Adapted from Benner KU, Der Körper des Menschen, Weltbild Augsburg 1996.

induce stepping-like movements, which persisted for as long as the external stimuli were applied. They also examined the effect of reduced peripheral input on LLPG activity [Dimitrijevic *et al.* 1998b]. Having evoked stepping-like movements with SCS in SCI subjects, they reduced the afferent input by inducing ischemia with a temporary cuff applied over the thigh muscles. Under constant stimulation conditions, reduced peripheral input resulted in diminished amplitude and increased frequency of stepping-like EMG activity.

Technology to conduct neurophysiological studies on the neurocontrol of standing and walking in humans has become available

In his review on the spinal sensorimotor system and its supraspinal control, Schomburg [1990] pointed out that the notion of spinal reflex activity and brain motor control being integrated in an interneuronal system is not new and had already been described by Förster in 1879. What is different today is that we have the technology to study supraspinal and spinal motor activities in humans.

During the past ten years the impact of neurophysiological research on the clinical practice of spinal cord disorders has increased. On the other hand, the advances in the development of reconstructive and restorative procedures for impaired spinal cord functions demand extensive *neurophysiological evaluation* before intervention, as well as monitoring of functional capabilities during and after intervention. Moreover, if pharmacological approaches continue being more and more successful in minimising the effects of injury and disease on spinal cord functions, we shall grow more dependent upon neurophysiological methods while restoring the functional capabilities of the minimally or moderately affected spinal cord. When interacting with specific segmental spinal cord structures and their integrated functions we depend not only on clinical and radiological evaluations, biochemistry and molecular biology, but also on the electrophysiology of cellular and circuit functions as well as subclinical findings [Dimitrijevic 1992].

Today new, non-invasive techniques for the neurophysiological assessment of spinal cord functions are available. The „brain motor control assessment" (BMCA) protocol has been developed for the examination of residual functional capabilities, i.e., of the degree to which brain control is preserved below a spinal cord lesion [Sherwood *et al.* 1989 and 1996]. By using this method, a comprehensive multichannel surface EMG recording, it is possible to register objective, quantitative and reproducible data on the altered motor control after an upper motoneurone trauma. EMG patterns evoked by voluntary and passive maneuvers and by volitional modulation of reflex responses reveal features of motor control that are not apparent in the clinical examination [see, e.g., Priebe *et al.* 1996]. We define *motor control* as the voluntary, reflex, or automatic activity of the central nervous system integrated with internal and external feedback signals; i.e., the *motor task* which leads to the performance of a *motor act*. These motor acts are the ultimate expression of motor control processes, the features of which are characterised by their patterns of EMG activity.

There is continuous progress in studies on the neurocontrol of standing and walking in humans. However, the possibility to investigate particular aspects of this control by

(i) analysing EMG-recorded neurophysiological data on the input-output features of the human lumbar cord

(ii) in response to well-defined and -controlled input generated by spinal cord stimulation

(iii) under the condition of well-defined (neurophysiologically evaluated) residual supraspinal influences,

and to

(iv) develop and test biophysical/neuromathematical models on the neurocontrol of standing and walking on the basis of human neurophysiological data

is rather unique. The present work deals with the neuromathematical analysis of such data, thereby focusing on the examination of the control strategies underlying epidurally induced *extension* movements of the lower limbs.

Design of the thesis

In chapter 1, *Initiating extension of the lower limbs in subjects with complete spinal cord injury by epidural lumbar cord stimulation*, I shall define lower limb extension as a functional motor task, and explore under what conditions this task can be induced by epidural stimulation of the lumbosacral cord in complete spinal cord injured subjects. I shall describe the characteristic pattern of EMG-recorded lower limb muscle activity during epidurally evoked extension. Chapter 1 is presented as it has been accepted for publication in the peer-reviewed journal *Experimental Brain Research*.

Chapter 2, *Evidences for a lumbar extension pattern generator in humans: Neurophysiology of compound motor unit potentials*, provides several independent evidences for the involvement of spinal interneuronal circuitry in the generation and control of epidurally induced lower limb extension. These evidences are revealed by (neuromathematical) analysis of electromyographic data recorded from the lower limb muscles during evoked extension, and of their components. The content of chapter 2 is currently prepared for publication.

In chapter 3, *Frequency-dependent selection of alternative spinal pathways with common periodic sensory input*, a computational model based on neurophysiological results in chapters 1 and 2 is presented. Theoretical analysis and simulation of a simplified neuronal network demonstrate in what way elementary mechanisms could contribute to the differential responsiveness of the lumbar cord to distinct neuronal codes, and to the control of evoked extension movements in particular. Chapter 3 will be submitted to the peer-reviewed journal *Biological Cybernetics*.

References

Barbeau H, Rossignol S (1987) Recovery of locomotion after chronic spinalization in the adult cat. Brain Res 412: 184–186

Barbeau H, Dannakas M, Arsenault B (1992) The effects of locomotor training in spinal cord injured subjects: A preliminary study. Restor Neurol Neurosci 12: 93–96

Barbeau H, Norman K, Fung J, Visintin M, Ladouceur M (1998) Does neurorehabilitation play a role in the recovery of walking in neurological population? In: Kiehn O, Harris-Warrick RM, Jordan L, Hultborn H, Kudo N (eds) Neuronal Mechanism for Generating Locomotor Activity. Annals of the New York Academy of Sciences, vol 860, pp 377–392

Brown TG (1911) The intrinsic factors in the act of progression in the mammal. Proc roy Soc B 84: 308–319

Bussel B, Roby-Brami A, Neris OR, Yakovleff A (1996) Evidence for a spinal stepping generator in man. Paraplegia 34: 91–92

Calancie B, Needham-Shropshire B, Jacobs P, Willer K, Zych G, Green BA (1994) Involuntary stepping after chronic spinal cord injury. Evidence for a central rhythm generator for locomotion in man. Brain 117: 1143–1159

Daverat P, Sibrac MC, Dartigues JF, Mazaux JM, Marit E, Debelleix X, Barat M (1988) Early prognostic factors for walking in spinal cord injuries. Paraplegia 26: 255–261

De Leon RD, Hodgson JA, Roy RR, Edgerton VR (1998) Full weight bearing hindlimb standing following stand training in the adult spinal cat. J Neurophysiol 80: 83–91

Dietz V, Colombo G, Jensen L, Baumgartner L (1995) Locomotor capacity of spinal cord in paraplegic patients. Ann Neurol 37: 574–582

Dimitrijevic MR (1992) Development of neurophysiological aspects of the spinal cord during the past ten years. Paraplegia 30: 92–95

Dimitrijevic MR, Gerasimenko Y, Pinter MM (1998a) Evidence for a spinal central pattern generator in humans. In: Kien O, Harris-Warwick RM, Jordan LM, Hultborn H, Kudo N (eds) Annals of the New York Academy of Sciences, vol 860, pp 360–376

Dimitrijevic MR, Gerasimenko Y, Pinter MM (1998b) Effect of reduced afferent input on lumbar CPG in spinal cord injury subjects. Soc Neurosci Abstr 24: 654

Dobkin BH, Harkema S, Requejo P, Edgerton VR (1995) Modulation of locomotor-like EMG activity in subjects with complete and incomplete spinal cord injury. J Neurol Rehab 9: 183–190

Eidelberg E, Walden JG, Nguyen LH (1981) Locomotor control in macaque monkeys. Brain 104: 647–663

Forssberg H, Hirschfeld H, Stokes VP (1991) Development of human locomotor mechanisms. In: Armstrong DM, Bush BMH (eds) Locomotor Neural Mechanisms in Arthropodes and Vertebrates. Manchester University Press, Manchester, pp 313–331

Grillner S (1973) Locomotion in the spinal cat. In Stein RB, Pearson KG, Smith RS, Redford JB (eds) Advances in behavioral biology, vol 7. Control of posture and locomotion. Plenum New York, pp 515–535

Grillner S (1981) Control of locomotion in bipeds, tetrapods, and fish. In: Brooks VB (ed) Handbook of Physiology. The Nervous System. Motor Control. American Physiological Society, Bethesda, pp 1179–1236

Grillner S (1985) Neurological bases of rhythmic motor acts in vertebrate. Science 223: 143–149

Harkema SJ, Hurley SL, Patel UK, Requejo P, Dobkin BH, Edgerton VR (1997) Human lumbosacral spinal cord interprets loading during stepping. J Neurophysiol 77(2): 797–811

Harkema SJ (2001) Neural plasticity after human spinal cord injury: application of locomotor training to the rehabilitation of walking. Prog Clin Neurosci 7(5): 455–468

Hultborn H *et al.* (1993) Evidence of fictive spinal locomotion in the marmoset (*Callithrix jacchus*). Soc Neurosci Abstr 19: 539

Illis LS (1995) Is there a central pattern generator in man? Paraplegia 33: 239–240

Jankowska E, Jukes MGM, Lund S, Lundberg A (1967) The effect of DOPA on the spinal cord. V: Reciprocal organisation of pathways transmitting excitatory actions to alpha motoneurones of flexor and extensors. Acta Physiol Scand 70: 369–388

Kuypers HGJM (1987) Some aspects of the organization of the output of the motor cortex. In: Motor Areas of the Cerebral Cortex, CIBA Foundation Symposium 132. John Wiley & Sons, pp 63–82

Lovely RG, Gregor R, Roy RR, Edgerton VR (1986) Effects of training on the recovery of full-weight-bearing stepping in the adult spinal cat. Exp Neurol 92: 421–435

Lovely RG, Gregor R, Roy RR, Edgerton VR (1990) Weight-bearing hindlimb stepping in treadmill-exercised adult spinal cats. Brain Res 514: 206–218

Lundberg A (1969) Convergence of excitatory and inhibitory actions on interneurones in the spinal cord. In: Brazier MAB (ed) The interneuron. University of California, Berkeley, pp 231–265

Mori S (1987) Integration of posture and locomotion in acute decerebrate cats and in awake, freely moving cats. Prog Neurobiol 28: 161–195

Pratt CA, Fung J, Macpherson JM (1994) Stance control in the chronic spinal cat. J Neurophysiol 71: 1981–1985

Priebe MM, Sherwood AM, Thornby JI, Kharas NF, Markowski J (1996) Clinical assessment of spasticity in spinal cord injury: a multi-dimensional proble. Arch Phys Med Rehab 77: 713–716

Sherwood AM, Dimitrijevic MR (1989) Brain motor control assessment. Proc IEEE Eng Med Biol Soc 11: 953–944

Sherwood AM, McKay WB, Dimitrijevic MR (1996) Motor control after spinal cord injury: assessment using surface EMG. Muscle Nerve 19: 966–979

Shik ML, Severin FV, Orlovsky GN (1966) Control of walking and running by means of electrical stimulation of the mid-brain. Biophysics 11: 756–765 (cited by Mori 1987)

Schomburg ED (1990) Spinal sensorimotor systems and their supraspinal control. Neurosci Res 7: 265–340

Wernig A, Müller S (1992) Laufband locomotion with body weight support improved walking in persons with severe spinal cord injuries. Paraplegia 30: 229–238

Wernig A, Müller S, Nanassy A, Cagol E (1995) Laufband therapy based on ‚rules of spinal locomotion' is effective in spinal cord injured persons. Euro J Neurosci 7: 823–829

Yakovleff A, Roby-Brami A, Guézard B, Mansour H, Bussel B, Privat A (1989) Locomotion in rats transplanted with noradrenergic neurons. Brain Res Bull 22: 115–121

Yakovleff A, Cabelguen JM, Orsal D, Gimenez M, Rajaoftra N, Drian MJ, Bussel B, Privat A (1995) Fictive motor activities in chronic spinal rats transplanted with foetal monoaminergic neurones. Exp Brain Res 106: 69–78

Chapter 1

Initiating extension of the lower limbs in subjects with complete spinal cord injury by epidural lumbar cord stimulation

Bernhard Jilge[1], Karen Minassian[1,2], Frank Rattay[1], Michaela M. Pinter[3], Franz Gerstenbrand[4], Heinrich Binder[4], Milan R. Dimitrijevic[4,5,6]

[1] TU-BioMed Association for Biomedical Engineering, Vienna University of Technology, Vienna, Austria

[2] Ludwig Boltzmann Institute for Electrical Stimulation and Physical Rehabilitation, Vienna, Austria

[3] Neurological Rehabilitation Center Rosenhügel, Vienna, Austria

[4] Ludwig Boltzmann Institute for Restorative Neurology and Neuromodulation, Vienna, Austria

[5] University Institute for Clinical Neurophysiology, Clinical Centre Ljubljana, Slovenia

[6] Department of Physical Medicine and Rehabilitation, Baylor College of Medicine, Houston, Texas, USA

Abstract. We provide evidence that the human spinal cord is able to respond to external afferent input and to generate a sustained extension of the lower extremities when isolated from brain control. The present study demonstrates that sustained non-patterned electric stimulation of the lumbosacral cord—applied at a frequency in the range of 5–15 Hz and a strength above the thresholds for twitches in the thigh and leg muscles—can initiate and retain lower limb extension in paraplegic subjects with a long history of complete spinal cord injury. We hypothesise that the induced extension is due to tonic input applied by the epidural stimulation to primary sensory afferents. The induced volleys elicit muscle twitches (posterior root muscle reflex responses) at short and constant latency times and co-activate the configuration of the lumbosacral interneuronal network, presumably via collaterals of the primary sensory neurones and their connectivity with this network. We speculate that the volleys induced externally to the lumbosacral network at a frequency of 5–15 Hz initiate and retain an "extension pattern generator" organisation. Once established, this organisation would recruit a larger population of motor units in the hip and ankle extensor muscles as compared to the flexors, resulting in an extension movement of the lower limbs. In the electromyograms of the lower limb muscle groups, such activity is reflected as a characteristic spatiotemporal pattern of compound motor unit potentials.

Key words. Spinal cord injury – spinal cord stimulation – lower limb extension

Abbreviations used in this chapter

C	cervical
CMUP	compound motor unit potential, EMG potential
CNS	central nervous system
EMG	electromyography, -graphic
H	hamstring
L	lumbar
MLR	mesencephalic locomotor region
PARA	paraspinal muscles
Q	quadriceps
S	sacral
SCI	spinal cord injury, -injured
SCS	spinal cord stimulation
T	thoracic
TA	tibial anterior
TS	triceps surae

1.1 Introduction

In several animal models it has been shown that muscles which are paralysed due to impaired upper motor neurone function can be induced to exhibit rhythmical activity, and even to perform locomotion, by stimulating certain structures of the central nervous system (CNS). Back in 1966, Shik *et al.* reported that electric stimulation (at 10–20 μA and 20–60 Hz) of the mesencephalic locomotor region (MLR) triggered a complete quadrupedal locomotor pattern in a decerebrate cat placed on a moving treadmill belt [Shik *et al.* 1966, Shik and Orlovsky 1976]. Jordan *et al.* [1979] moved one step further demonstrating that a "fictive" locomotor pattern could be induced by stimulating the MLR even when any phasic input from the periphery was excluded.

As long ago as 1910, Roaf and Sherrington used repetitive electric stimulation of the feline cervical cord in studies on the neurocontrol of locomotion. Later in the century it was demonstrated in numerous preparations that stimulation with sustained non-patterned (i.e. tonic) electric stimuli can be effective when applied to dorsal roots and/or columns of the spinal cord or to peripheral nerves [Grillner and Zangger 1979]. The same authors succeeded in evoking alternating rhythmical electromyographic (EMG) activity and stepping patterns closely resembling the pattern of normal hindlimb locomotion in deafferented acute and chronic spinal cats, who had received DOPA prior to the stimulation. A similar approach of studying spinal cord stimulation (SCS) for eliciting locomotor-like activity in spinalised and decerebrate adult cats has been used by Garcia-Rill *et al.*, who suggested that stimulation of the lumbar enlargement may activate an intrinsically organised system [Iwahara *et al.* 1991]. In 1983, Kazennikov *et al.* reported that stepping could be evoked in the decerebrate cat by electrically stimulating a specific portion of fibres in the dorsolateral funiculus at the cervical or thoracic level, also known as the "locomotor strip" [see also Shik 1997]. Recently an effort has been made to elicit movements in different spinal preparations (frog, rat, cat) by direct electric micro-stimulation of the interneuronal network within the lumbar grey matter [Giszter *et al.* 1993, Bizzi *et al.* 1995, Tresch and Bizzi 1999]. Mushahwar *et al.* [2000] reported functional movements by stimulating the spinal cord through electrodes (microwires) implanted in the lumbar cord enlargement of the intact cat.

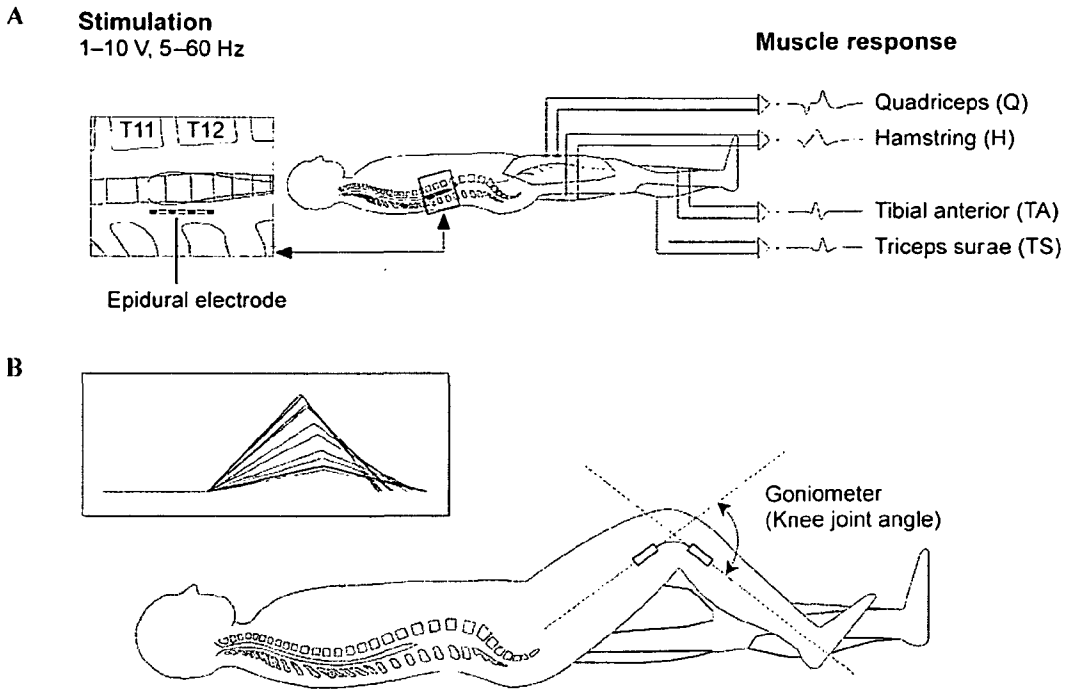

Fig. 1.1. Outline of the clinical assessment design. **A**, The subjects were placed in supine position. Pairs of surface EMG electrodes were placed over the bellies of the lower limb muscle groups to record the effects of epidural stimulation. **B**, Goniometers were applied bilaterally to the knee to monitor leg movements. The stick figure (see inset) illustrates how the position of the lower limb is shifting during induced movements.

In this way, animal experiments had revealed that sustained electric stimulation of the MLR, the grey matter of the lumbar cord enlargement, or the posterior roots or columns of the lumbar cord, could induce rhythmical motor activity. From these three approaches of stimulating the CNS, the latter is closest to the already well-established clinical procedure for spasticity control in humans after a spinal cord injury (SCI) by electric stimulation of the posterior cord from the epidural space [Barolat *et al.* 1995]. For this effective method of treatment to be successful it is crucial to evaluate the optimal simulation settings (site, strength and frequency) on a case-by-case basis. Stimulation below the SCI—particularly of the lumbar cord segments—was found to control spasticity more effectively than stimulation above the injury level [Richardson and McLone 1978, Barolat *et al.* 1995, Dimitrijevic 1998]. Pinter *et al.* [2000] demonstrated that SCS would be effective for the control of spinal spasticity if *(i)* the stimulating electrode is located over the upper lumbar cord segments (L1–L3), and *(ii)* the applied stimulus train has a frequency of 50–100 Hz, an amplitude of 2–7 V, and a pulse width of 210 μs.

When SCS was the clinical choice for spasticity control in a patient with complete SCI, we took advantage of the available clinical practice and, while evaluating the optimal parameter configurations, recorded the motor effects elicited by the stimulation. In the course of the evaluation procedure we noticed that the stimulation sometimes evoked rhythmical, locomotor-like EMG activity in the patient's paralysed lower limb muscles. This happened when we applied frequencies somewhat lower than the ones effectively controlling spasticity *without* changing the site of the stimulation [Rosenfeld *et al.* 1995, Gerasimenko *et al.* 1996]. Meanwhile, we have performed several retrospective and prospective studies on the potential effect of SCS in eliciting

Table 1.1. Subjects included in the study

Table 1.1a. Demographic and clinical data

Subject No.	Sex	Date of Birth	Date of SCI	Cause of SCI	ASIA Classification	Data collected in
1	f	12/1965	04/1996	car accident	A	1999
2	m	04/1973	01/1997	ski accident	B	1999
3	f	07/1975	01/1996	car accident	A	2001/2002
4	m	04/1973	01/1995	car accident	A	2001
5	f	03/1978	12/1994	car accident	A	2002

Table 1.1b. X-ray documentation of injury level and epidural electrode position

Subject No.	Vertebral Level of Fracture	Stabilisation of Vertebrae	Electrode Position (Vertebral Level)
1	T5/6, and T10	T4–7, and T9–11	T12/L1
2	C5/6	C4–7	T12
3	T7	T6–8	T12, slightly left
4	C4/5	C3–6	L1
5	T4/5, with dislocation	T3–6	T12

motor activity in the lower extremities of complete SCI subjects. These studies have shown that a frequency of 25–50 Hz and a strength of 7–10 V (210 μs pulse width) had to be applied to the upper lumbar cord segments to initiate and retain rhythmical stepping-like hip-knee flexion movements of the subject's paralysed limbs [Dimitrijevic *et al.* 1998a and b, Pinter *et al.* 1998, Dimitrijevic *et al.* 2001]. Moreover, while evaluating the optimal settings for spasticity control, a strong and brisk extension movement of the lower limbs was evoked by stimulus trains involving even lower frequencies (< 15 Hz) [Jilge *et al.* 2001].

From these observations it was clear that the lumbosacral cord isolated from supraspinal input would be capable of generating at least three different types of motor output in response to epidural stimulation at the same segmental level but different frequencies (and an adjusted stimulus amplitude). They led us to speculate that different stimulus frequencies would "open" different inhibitory and/or excitatory spinal pathways controlling *(i)* the suppression of excitability within particular motor nuclei (thus reducing spasticity after SCI)—induced at stimulus frequencies between 50 and 100 Hz, *(ii)* the generation of rhythmical locomotor-like activity [Minassian *et al.* 2001a and 2003]—induced at stimulus frequencies around 30 Hz, and *(iii)* the generation of sustained lower limb extension—induced at stimulus frequencies below 15 Hz [Jilge *et al.* 2002]. In the present study we investigated, the effect of SCS at frequencies between 5 and 15 Hz. We analysed previously recorded EMG data with respect to the question whether and under what conditions it was possible to initiate and retain lower limb extension in subjects with trauma-related SCI whose lumbosacral cord was isolated from brain control.

1.2 Methods

1.2.1 Subjects

The analyses performed in this study are based on EMG and goniometric data collected while routinely conducting a clinical protocol for the evaluation of the optimal site and parameters of SCS for spasticity control in subjects who were resistant to other treatment modalities. For the present retrospective study, we selected recordings obtained in five subjects who were neurologically classified as having a complete (ASIA A or B) spinal cord lesion at the cervical or thoracic level with no motor functions below the lesion. Pertinent demographic and clinical data are listed in **Table 1.1a**.

At the time of data collection the subjects met the following criteria: *(i)* They were healthy adults with closed post-traumatic spinal cord lesions; *(ii)* the lesion was at least one year old; *(iii)* no antispastic medication was being used; *(iv)* the stretch and cutaneomuscular reflexes were preserved; *(v)* there was no voluntary activation of motor units below the level of the lesion as confirmed by brain motor control assessment [Sherwood *et al.* 1996] while lumbosacral evoked potentials were present [Beric 1988]; and *(vi)* there was no sensory function below the level of the lesion in four of the subjects studied, while one subject showed tactile impairment below the level of the SCI, and not altered cortical somatosensory evoked potentials elicited by stimulation of the peroneal and tibial nerves.

To control their spasticity, all subjects had an epidural electrode array implanted (see Methods) at some vertebral level ranging from T12 down to L1, as verified by X-ray picture (**Table 1.1b**). The implantation as well as the clinical protocol to evaluate the optimal stimulation parameters was approved by the local ethics committee. All subjects gave their informed consent.

Table 1.2. Results of the neurophysiological evaluation

							Brain Motor Control Assessment											
Subject	LSEP				SSEP		Voluntary				Tendon Jerk				Withdrawal			
No.	RP		SP				Hip-Knee		Ankle		Knee		Ankle		w/o supp		w supp	
	R	L	R	L	R	L	R	L	R	L	R	L	R	L	R	L	R	L
1	+	+	+	+	–	–	–	–	–	–	+	+	+	+	+	+	+	+
2	+	+	+	+	+	+	–	–	–	–	+	+	+	+	+	+	+	+
3	+	+	+	+	–	–	–	–	–	–	+	+	+	+	+	+	–	–
4	+	+	+	+	–	–	–	–	–	–	+	+	+	+	+	+	+	+
5	+	+	+	+	–	–	–	–	–	–	+	+	+	+	+	+	–	–

LSEP, Lumbosacral evoked potentials: RP, Root potential; SP, Stationary potential. SSEP, Somatosensory evoked potentials. +/–: Evoked potential present/absent. Voluntary, Voluntary movement: Hip-Knee, Unilateral leg (hip and knee) flexion and extension. Ankle, Unilateral ankle dorsi- and plantar flexion. +/–: EMG response present/absent.

Tendon Jerk: Knee, Patellar tendon tap. Ankle, Achilles tendon tap. Withdrawal, Plantar withdrawal reflex: w supp, The subject was instructed to attempt to suppress any reflex movement. w/o supp, Without attempting to suppress the reflex movement. +/–: Reflex response present/absent in the EMG.

R/L, Right/Left lower limb.

1.2.2 Evaluation procedure

Within the Clinical Program of Restorative Neurology, a neurologist examined the subjects' spinal cord functions and assessed their functional status. In addition, the following clinical neurophysiological procedures for the assessment of motor and sensory functions were applied:

1. Simultaneous recording of compound motor unit potentials (CMUPs) from muscle groups of the limbs and trunk using 16 pairs of surface electrodes and EMG channels, while a standardised protocol for the evaluation of voluntary and reflex motor tasks was executed [Sherwood *et al.* 1996].

2. To assess posterior column functions, cortical evoked potentials elicited by tibial and peroneal nerve stimulation were conducted [Dimitrijevic *et al.* 1983].

3. Lumbosacral evoked potentials were used to assess the functions of the spinal grey matter. They were recorded after tibial nerve stimulation [Beric 1988, Lehmkuhl 1984] with silver-silver chloride surface electrodes placed at the T12, L2, L4, and S1 spinous processes referenced to an electrode at T6. Results of the neurophysiological evaluation are listed in **Table 1.2**.

1.2.3 Stimulation procedure

For spasticity control, quadripolar electrode arrays (PISCES-QUAD, Model 3487A, MEDTRONIC)—hereinafter referred to as "electrodes"—were percutaneously placed in the posterior epidural space at vertebral levels T12 through L1 under local anesthesia. The implantation procedure has been described in detail previously [Murg *et al.* 2000]. The position of the electrode relative to the vertebral column was monitored intraoperatively by fluoroscopy and elicitation of muscle twitches. The position of the electrode relative to the spinal cord was verified based on the previous finding that the spatial relation between the active cathode of the electrode and the corresponding segmental input-output of the spinal cord can be usefully monitored by EMG recordings of muscle twitch patterns [Dimitrijevic *et al.* 1980, Murg *et al.* 2000]. During the postoperative test phase the stimulus threshold values for muscle twitches were measured. Single muscle twitches were elicited with the epidural electrode connected to an external stimulator (Model 3625, MEDTRONIC) and the amplitude of the generated stimulus being increased to the point of eliciting brief muscle contractions. As mentioned above, the results of these routinely performed measurements provided the basis for estimating the position of the stimulating electrode relative to the spinal cord (see "Data recording and analysis" below). Finally, the electrode was connected to the implanted pulse generator (ITREL 3, Model 7425, MEDTRONIC) to form a fully integrated closed system.

The four independent contacts of the quadripolar electrodes were set at a distance of 9 mm. They were labelled 0, 1, 2, 3, such that contact #0 was at the top and contact #3 at the bottom of the electrode. The stimulator was operated in bipolar mode by connecting the cathode and anode to a pair of contacts. The motor output elicited by SCS was captured for stimulus frequencies of 5–60 Hz (incrementally increased by about 5 Hz between 5 and 20 Hz, and by about 10 Hz between 20 and 60 Hz), amplitudes of 1–10 V (increased in 1 V steps; bipolar electrode impedance of about 1 kΩ), and pulse widths of 210 and 450 μs. However, intensities which caused discomfort to the subject under examination were never applied. An overview of actually used parameter configurations is given in **Table 1.3a**.

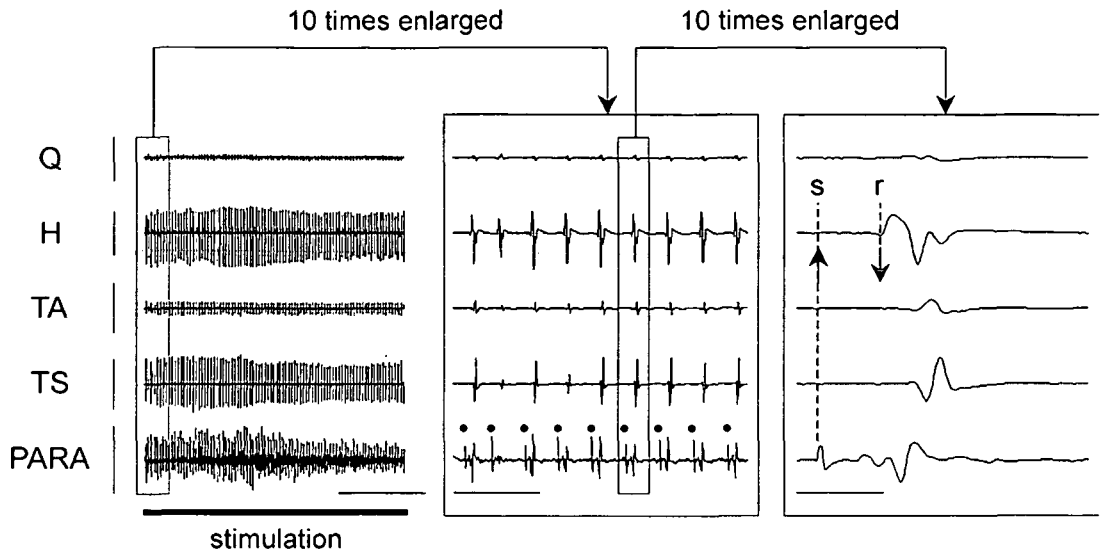

Fig. 1.2. Presentation of EMG recordings. Electromyographic recording from the lower limb (Q, quadriceps; H, hamstring; TA, tibial anterior; TS, triceps surae) and paraspinal ('PARA') muscles, presented on three different time scales. The bar at the bottom of the figure on the left hand side indicates the time interval when SCS was applied. On the intermediate scale it is apparent that each pulse within the stimulus train triggered a single CMUP (in each muscle group). The stimulus artefacts (marked by dots) recorded from the paraspinal muscles were used as indicators of the moments when the stimulus pulses were applied. The labels 's' and 'r' on the right hand side denote the application of a stimulus pulse, and the onset of an evoked response, respectively. The time between these two moments will be referred to as the latency time of the evoked CMUP. Vertical markers: 2000 μV (Q, H); 3000 μV (TA, TS); 400 μV (PARA). Horizontal markers: 2 s, 200 ms, 20 ms. The EMG was recorded in subject #1 (estimated segmental level of stimulation: L4/5) in response to the following stimulation parameters: polarity of the active contacts 2+3–, 7 V, 14 Hz, 210 μs pulse width.

1.2.4 Data recording and analysis

Fig. 1.1 illustrates the patient setup used, according to the clinical protocol, for the evaluation of the optimal stimulation parameters for spasticity control, with the stimulating electrode placed in the epidural space, and the recording sites for the surface EMG of the thigh and leg muscles (**Fig. 1.1A**). Goniometers were bilaterally applied to the knee (**Fig. 1.1B**). The subjects were placed on a comfortable examination table covered with soft sheepskin in a supine position. This configuration allowed flexion/extension movements of the lower limbs to unfold smoothly and minimised friction between the heel and the supporting surface.

The subjects' lower limbs were manually moved to the point of complete flexion or extension before stimulation was applied at certain configurations of the stimulus parameters. Throughout the induced unilateral or bilateral extension movements, the subject's legs were manually protected by a technologist (when necessary) in order to prevent injury of the joints during electrically evoked extension of the lower limbs, which was rather strong and sudden, resembling a ballistic movement.

A typical evaluation session to systematically test the effect of different stimulation sites (i.e. contact combinations), intensities and frequencies lasted 1–2 hours. The stimulation cycles themselves, during which one parameter (usually the stimulus frequency) was varied while the

others (site and strength) were kept constant, lasted 1–5 min and were followed by appropriate resting intervals of 2–4 min. Within each stimulation cycle, the individual stimulation trials were separated by intervals of at least 10 seconds.

The effects of SCS were captured by EMG recording of induced CMUPs using pairs of recessed, silver-silver chloride surface electrodes placed 3 cm apart over the midlines of the quadriceps ('Q'), hamstring ('H'), tibial anterior ('TA') and triceps surae ('TS') muscle bellies on both lower limbs. Paraspinal ('PARA') muscles were covered in the same way. The skin was slightly abraded such that an electrode impedance of < 5 kΩ was reached to avoid artifacts. In subjects #3–5, goniometers (Model XM-180, and K100 AMPLIFIER SYSTEM, PENNY & GILES BIOMETRICS LTD.) were used to record knee movements (**Fig. 1.1B**). The measurements were performed with a GRASS 12D-16-OS NEURODATA ACQUISITION SYSTEM (GRASS INSTRUMENTS) using a gain of 2000 over a bandwidth of 30–1000 Hz (–3 dB). The data were digitised at 2048 samples/s for each channel at a bit depth of 12 bits using a CODAS ADC system (DATAQ INSTRUMENTS). The amplified and processed EMG and goniometer signals were monitored on-line and stored for subsequent analysis. **Fig. 1.2** gives an example of EMG-recorded induced CMUPs. The same data are presented on three different time scales illustrating *(i)* a whole series of EMG responses to SCS, *(ii)* the stimulus-response relationship, and *(iii)* characteristics of single responses.

The cord-based positions of the epidural electrodes placed in the five subjects under study were estimated as follows: subject #1: L4/5; subject #2: L3/4; subject #3: L4/5; subject #4: S1/2; subject #5: L5. As described above under "Stimulation procedure", we arrived at these positions by analysing the muscle twitch patterns elicited by the electrodes. This workaround was necessary because, failing appropriate neuroimaging techniques, spinal cord segments cannot be visualised directly, nor can they be accurately mapped by fluoroscopic visualisation of the vertebrae involved. X-ray imaging is only useful to the extent that it hints at the cord level of the epidural electrode if we assume that the spinal cord has "standard" spatial relations between vertebral and cord structures [Kameyama *et al.* 1996, Lang and Geisel 1983].

In the present study, a refined approach to this issue was used by combining two evaluation techniques that are described in detail elsewhere [Murg *et al.* 2000, Rattay *et al.* 2000]. First, the muscle twitch patterns obtained by EMG recording were analysed for the recruitment order of the lower limb muscles in response to incremental stimulus amplitudes, based on the demonstration by Murg *et al.* [2000] of two distinct recruitment orders depending on whether the stimulating cathode was placed over the upper (= initial response by quadriceps and/or adductor) or the lower (= initial response by tibial anterior and triceps surae) lumbar cord segments. Second, the muscle twitch patterns were additionally evaluated as described by Rattay *et al.* [2000], who used computer modelling techniques to analyse the segmental position of a bipolar electrode in relation to the recruitment order of lower limb muscles. Depending on the rostro-caudal level of stimulation, the authors discriminated at least four distinct muscle recruitment patterns.

The recorded EMG potentials were analysed off-line using WINDAQ WAVEFORM BROWSER (DATAQ INSTRUMENTS). The responses induced by the external stimuli did not interfere with each other, regardless of the stimulus frequency, as long as it did not exceed approximately 30 Hz. (Illustrative examples at 5 and 21 Hz will be given in **Fig. 1.4B**.) Each CMUP could be related unequivocally ('1 : 1') to the pulse which had triggered it. In other words, each (sufficiently strong) pulse within the applied stimulus train evoked one single EMG response per muscle group (**Fig. 1.2**). For the *integrated activity* of single responses, the original EMG record was divided into successive time windows of equal length, each covering a single muscle twitch

response. The margins of the time windows were defined by the moments when the external stimuli had been applied. These moments were reflected in the EMG as volume-conducted artifacts of the stimulus pulses recorded from the paraspinal muscles. Then the samples $V_1,...,V_M$ of the EMG potential within each window were replaced by a single value $\mathrm{IA}(V_1,...,V_M)$, calculated as

$$\mathrm{IA}(V_1,...,V_M) = \frac{l}{M} \cdot \sum_{k=1}^{M} |V_k|$$

where M depends on the length l of the time window, which was selected based on the stimulus frequency f:

$$l = \frac{1}{f},$$
$$M = 2048l,$$

if l is given in seconds. (Note that the EMG recordings were digitised at a rate of 2048 samples per second.)

The goniometer recordings were used to quantify the degree of extension incorporated in the induced movements based on the maximum deflection of the knee-joint angle:

$$\Delta\varphi = \max \varphi(t) - \min \varphi(t)$$

where $\varphi(t)$ is the time course of the joint angle as it is given by the goniometer curve. The *average slope* of this curve over an interval from $t = a$ to $t = b$ was calculated as follows:

$$\frac{\varphi(b) - \varphi(a)}{b - a}$$

1.3 Results

In the present communication, we are going to demonstrate that rhythmical motor unit activity, which is induced by SCS at frequencies of 25–50 Hz, is converted to a tonic one by lowering the frequency of the stimulus train to about 5–15 Hz *without* changing the site and intensity of the stimulation (see **Fig. 1.3**). As a visible correlate of this tonic output, the lower limbs undergo an extension that persists for as long as the external stimulus is sustained. In some of our recordings, the paralysed limbs remained extended for up to 52 seconds of continuous stimulation, which readily happened when lower stimulus frequencies of 5–10 Hz were used.

In this context, "rhythmical" ideally refers to the periodical alternation of burst-like phases of CMUP activity with "silent" ones in which no EMG activity is observed in a given muscle group. A "tonic" pattern, on the other hand, is characterised by continuous CMUP activity without any interruption, the individual discharges within this pattern being separated by a constant time interval. During the transition from rhythmical to tonic motor unit activity or vice versa, an interference between these two elementary features is observed (see **Fig. 1.4A**, 21 Hz).

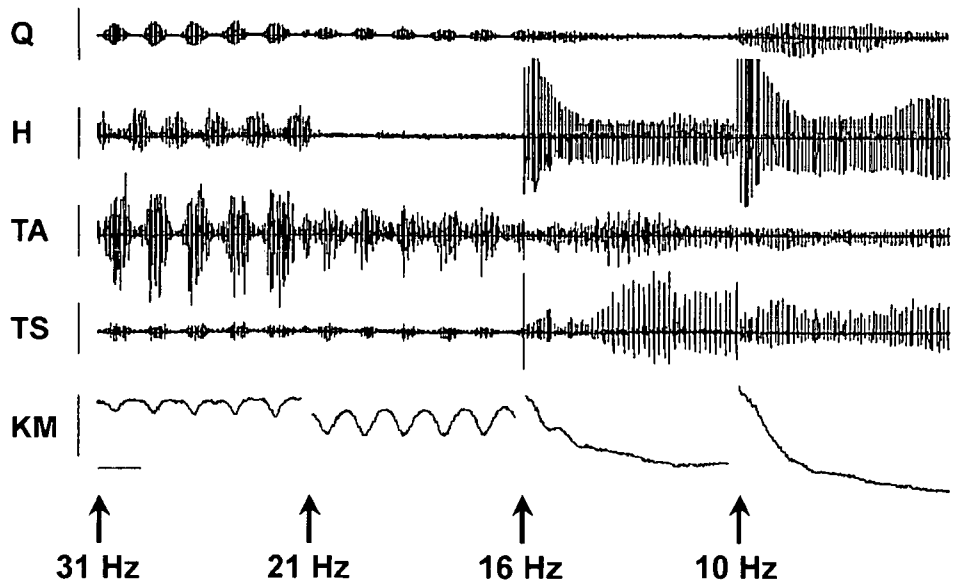

Fig. 1.3. Rhythmical and tonic EMG activity of paralysed lower limbs induced by spinal cord stimulation. EMG recordings obtained from the lower limb muscle groups during spinal cord stimulation at frequencies of 31 and 21 Hz (rhythmical activity) as compared to 16 and 10 Hz (tonic activity). The goniometer traces below illustrate the corresponding rhythmical and extension movements, respectively, of the lower limbs. The other stimulation parameters (site and strength) were never changed during the recording session. Note that during the "flexion phases" induced at 31–21 Hz the amplitudes in quadriceps and tibial anterior are larger than the ones in hamstring and triceps surae, respectively. This dominance is reversed in response to stimulus frequencies of 16–10 Hz. Recorded in subject #3 (estimated segmental level of stimulation: L4/5); stimulation parameters: 0–3+, 10 V, 210 μs pulse width. Vertical markers: 500 μV (Q, H, TA, TS); 45 ° (KM, knee movement). Horizontal marker: 1 s.

Table 1.3 surveys the results obtained in each of the five subjects under study. The following sections will give a detailed description of the evoked lower limb extension, particularly in terms of the CMUP patterns induced in the thigh and leg muscles in response to specific stimulus parameters. As will be apparent from **Table 1.3**, the findings we shall be presenting were observed in a large number of recordings provided that appropriate parameter settings were applied.

1.3.1 Effect of stimulation parameters on EMG output and induced movement

When the subjects' lower extremities were manually moved to the point of complete (i.e. maximum possible) flexion, and a train of electric stimuli was subsequently applied to the posterior structures of the lumbosacral cord at a frequency of about 5–15 Hz, and a strength which was above the thresholds for twitches in the thigh and leg muscles (4–10 V), a sudden strong and brisk extension movement of the lower limbs occurred. When the endpoint of the actual movement was reached, and the stimulation was sustained, the limbs remained in the extended position, with the muscles visibly and strongly contracting. Any attempt to flex a limb in this condition manually in the knee and hip failed due to the strong muscle contraction induced by the stimulation. The strong and brisk extension was observed in the absence of any manual support of the lower extremities; it happened as soon as the appropriate stimulus

parameters were applied. When the electric stimulation was turned off, the lower limb muscles relaxed immediately, and the limbs could be manually flexed and extended.

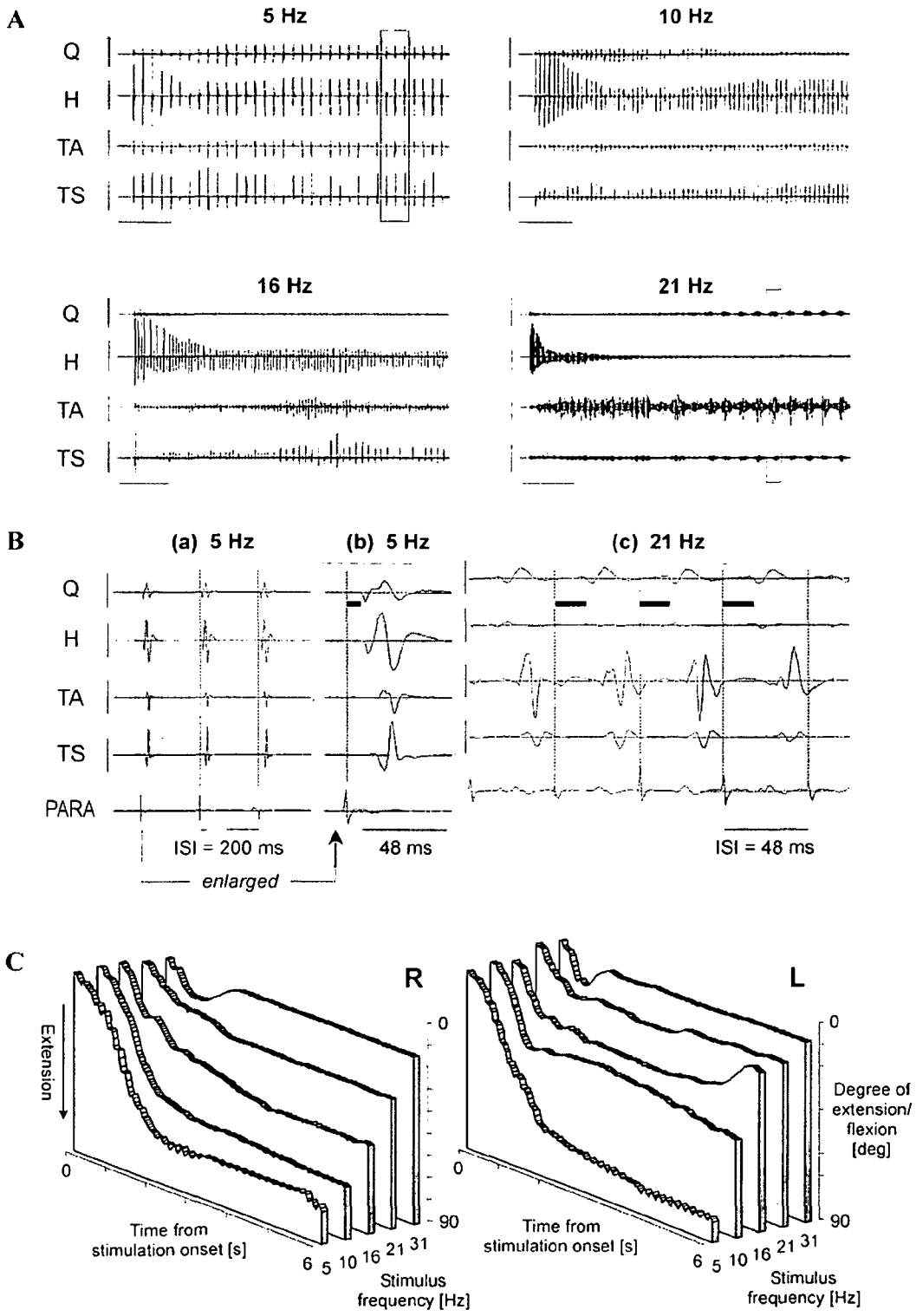

Fig. 1.4. EMG and goniometric recordings in response to SCS at different frequencies. **A**, EMG recordings in response to different stimulus frequencies (5–21 Hz). The subject's lower limbs had been placed in complete flexion prior to the stimulation. The stimulus trains at 5, 10 and 16 Hz evoked an EMG pattern with hamstring and triceps surae dominating over quadriceps and tibial anterior, respectively, which is referred to as the EMG "extension pattern". In addition, the recordings reveal temporal modulation of the amplitude relation between quadriceps and hamstring as the induced extension movement unfolds: independently from the applied stimulus frequency, hamstring loses while quadriceps gains momentum until a fairly parallel course is established. At 21 Hz, in contrast, the extension pattern is replaced by a flexion/extension (i.e. stepping) pattern. Recorded in subject #3 (estimated segmental level of stimulation: L4/5); stimulation parameters: 0–3+, 10 V, 210 μs pulse width. Vertical markers: 800 μV. Horizontal markers: 1 s (5–16 Hz); 3 s (21 Hz). **B**, CMUPs taken from the windows entered in **A** (see the recordings for 5 and 21 Hz, respectively) are shown on a larger time scale. The corresponding EMG recordings from the paraspinal muscles are given in addition. A magnification of the first CMUPs in **(a)** is given in **(b)**. **(c)** Although each phase of "burst-like" activity included about 15 CMUPs per muscle group, only 4 of them are illustrated. Note the prolonged latency time of the quadriceps responses at 21 Hz as compared to 5 Hz—see the bars. (The CMUPs under **(b)** and **(c)** are shown on the *same* time scale.) Vertical markers: 600 μV (5 Hz); 300 μV (21 Hz). ISI, interstimulus interval. **C**, Goniometer traces covering the first 6 seconds of movements induced by SCS at different frequencies (5–31 Hz). The 5–21 Hz goniometer curves recorded from the left (L) limb belong to the EMG traces in **A**. The degree of flexion/extension is illustrated by a gradient of 0–90 °. Downward deflection indicates lower limb extension (see arrow), upward deflection indicates flexion. As one can see, the degree of the induced extension was larger for lower stimulus frequencies. Trains at 31 Hz evoked a fleeting extension which was not sustained but quickly reversed to a pronounced flexion. The slightly different responses obtained in the right (R) versus left (L) lower limbs suggest that the posterior structures were not stimulated symmetrically from the midline of the spinal cord. Recorded in subject #3 (estimated segmental level of stimulation: L4/5); stimulation parameters: 0–3+, 10 V, 210 μs pulse width.

← *previous page* —

The parameter settings for which the goniometer recordings (and the annotations to these recordings) revealed a *sustained* extension of the initially flexed lower limbs in subjects #3–5 are given in **Table 1.3b**. At the effective stimulus strengths, all four lower limb muscle groups responded with muscle twitches. The corresponding EMG recordings confirmed the co-activation of (hip and ankle) flexors and extensors, with the CMUP amplitudes being larger in the latter as soon as specific stimulus frequencies were applied (see **Fig. 1.2**). With respect to the initiation of a goniometrically verified sustained lower limb extension, the effective frequencies ranged between 5 and 21 Hz. Frequencies above 21 Hz were effective only in subject #4 when low-intensity (5 V) stimuli were applied (using one particular combination of anode and cathode). However, a fleeting extension movement, i.e. one which was *not* sustained, *was* repeatedly evoked by 21–50 Hz trains (see footnote "d" in **Table 1.3**).

Fig. 1.4A shows EMG recordings of subject #3 whose spinal cord was stimulated at the level of L3/4 (estimated segmental position of the cathode) at frequencies of 5–21 Hz and a stimulus strength of 10 V (210 μs pulse width). **Fig. 1.5A** compares different recordings in the same subject using the same strength and a frequency of 10 Hz, whereas **Fig. 1.5B** was recorded in subject #4, who was stimulated at the segmental level of S1/2 (7 V, 16 Hz). The recordings for 5, 10 and 16 Hz (**Fig. 1.4A**), 10 Hz (**Fig. 1.5A**), and 16 Hz (**Fig. 1.5B**), respectively, revealed at least two distinct phases of the extension induced in the flexed limbs. In the first phase, the corresponding EMG pattern was characterised by substantial temporal modulation. The induced muscle contractions within the hamstring muscle group were immediately generated, resulting in a fast extension of the knee—as documented by the corresponding goniometer recording, **Figs. 1.5A** and **B**—and a progressive decrease of the EMG amplitude in hamstring while the one in

quadriceps gradually increased. During the following seconds a steady amplitude relation is established between these muscles (second phase).

In both phases, based on the amplitudes of recorded CMUPs, hamstring had a larger output than quadriceps, and triceps surae had a larger output than tibial anterior. By way of contrast, tibial anterior dominated over triceps surae during the rhythmical activity induced at a frequency of 21 Hz. Moreover, by incrementally increasing the stimulus frequency it is possible to demonstrate the transition from induced steady extension (**Fig. 1.4A**/5 Hz) of the lower limbs to the onset of alternating flexion-extension movements (**Fig. 1.4A**/21 Hz). Most interestingly, SCS which could effectively initiate stepping-like activity initially also evoked a tonic, "extension-like" CMUP pattern, with hamstring exhibiting larger amplitudes than quadriceps (and the limbs extending to a certain extent). Within 10–12 seconds, however, this tonic output turned rhythmical, with quadriceps and tibial anterior dominating over hamstring and triceps surae, respectively. (We call this a "fleeting extension movement".) **Fig. 1.4B** compares the CMUPs observed during implemented extension at 5 Hz with the ones during rhythmical activity elicited at 21 Hz. Apart from changes in shape and amplitude of the evoked CMUPs, they revealed significantly different latency times, the latter being prolonged by about 10 ms as compared to the former. A more detailed analysis of this observation will be presented in a separate communication.

In **Table 1.3a** the parameter configurations which induced an EMG pattern with hamstring and triceps surae dominating over quadriceps and tibial anterior, respectively, are listed for each of the five subjects included in this study. We are going to refer to this characteristic pattern of amplitude relations between antagonistic muscle groups as the EMG "extension pattern". It was generally observed in response to frequencies in the range of 5–15 Hz. However, on some occasions this range was slightly shifted toward higher frequencies (10–21 Hz). Applying stimulus trains above 21 Hz, the extension pattern could still be induced immediately after the onset of the stimulation, but it reversed very soon to one with the (hip and/or ankle) flexors dominating over the extensors (see **Fig. 1.4A**/21 Hz and footnote a in **Table 1.3**).

—— *Table 1.3a, next page* ——→

Column 'Initial position': Position of the subject's lower limbs prior to the stimulation. Column 'Polarity': Electrode contacts used as anode (+) and cathode (–). Column 'Tested Strengths/Frequencies': Tested parameter values, and – in squared brackets – total number of recordings using different parameter configurations. (Unless otherwise specified, the stimuli had a pulse width of 210 µs.) Column 'Effective Strengths/Frequencies': Parameter values which effectively induced an EMG pattern in which hamstring and triceps surae exhibited larger CMUP amplitudes than quadriceps and tibial anterior, respectively. In addition, the number of supportive recordings is given in squared brackets. E.g., '8–10 V/10–21 Hz [12/14]' denotes that the EMG extension pattern was observed in 12 out of 14 recordings in which a stimulus amplitude between 8 and 10 V, and a stimulus frequency between 10 and 21 Hz was used. In subject #3, the analysed data had been collected in two sessions ('Sess #1 and 2'). Whether the results for the right or left lower limb are presented in this table has arbitrarily been chosen for each subject.

[a] Parameter values which induced the EMG extension pattern immediately after the onset of the stimulation, but not necessarily also during subsequent phases.

[b] Parameter values which induced the EMG extension pattern in the thigh muscles, but not necessarily also in the leg muscles.

[c] Parameter values which induced the EMG extension pattern in the thigh muscles immediately after the onset of the stimulation.

Table 1.3. Overview of the stimulus parameters used and of the results recorded in the subjects under study

Table 1.3a. Parameter configurations tested and settings effectively inducing the EMG extension pattern

Subject No.	Initial Position	Polarity	Tested Strengths	Tested Frequencies		Effective Strengths	Effective Frequencies	
1	Extended	2–3+	5–10 V	10–31 Hz	[33]	8–10 V	10–21 Hz	[12/14]
		2+3–	5–8 V	14 Hz	[5]	5–8 V	14 Hz	[4/5]
			1–10 V	21 Hz	[11]	6–10 V	21 Hz	[5/5]
		1–2+	1–10 V	21 Hz	[10]	–	–	
		1+2–	1–10 V	21 Hz	[10]	9–10 V	21 Hz	[2/2]
2	Extended	0–3+	6–8 V	10–60 Hz	[18]	7–8 V	10 Hz	[2/2]
						[a]6–8 V	16–60 Hz	[11/13]
		0+3–	6–8 V	10–60 Hz	[18]	7–8 V	16–21 Hz	[4/4]
3/Sess #1	Extended	0–3+	1–10 V	10 Hz	[10]	7–10 V	10 Hz	[5/5]
	Flexed	0–3+	5, 10 V (210 µs)	5–50 Hz	[30]	10 V	5–10 Hz	[6/6]
						[c]10 V	5–50 Hz	[15/15]
			5, 10 V (450 µs)	5–50 Hz	[12]	5, 10 V	5–16 Hz	[5/6]
						[a]5, 10 V	5–21 Hz	[7/8]
						[c]5, 10 V	5–30 Hz	[9/10]
		0+3–	5, 10 V (450 µs)	5–50 Hz	[10]	5 V	10–20 Hz	[3/3]
						10 V	5–10 Hz	[2/2]
						[a]5, 10 V	5–31 Hz	[9/9]
3/Sess #2	Extended	0–3+	6–10 V	5–50 Hz	[35]	8–10 V	5–16 Hz	[9/9]
						[a]7–10 V	5–50 Hz	[23/27]
						[c]7–10 V	5–50 Hz	[28/28]
		0+3–	4–9 V	5–50 Hz	[42]	4–9 V	10–21 Hz	[13/16]
						[c]4–9 V	5–50 Hz	[40/40]
	Flexed	0–3+	7–10 V	10–51 Hz	[21]	9–10 V	10–16 Hz	[5/5]
		0+3–	8, 10 V	16–50 Hz	[7]	8 V	16 Hz	[1/1]
						[a]8, 10 V	16–31 Hz	[5/6]
4	Flexed	0–3+	5, 7 V	5–50 Hz	[14]	7 V	10–31 Hz	[4/4]
						[a]5, 7 V	5–50 Hz	[12/14]
						[c]5, 7 V	5–50 Hz	[14/14]
		0+3–	5, 7 V	5–50 Hz	[12]	5 V	16–21 Hz	[2/2]
						[a]5, 7 V	5–50 Hz	[11/12]
5	Extended	0–3+	4–6 V	5–31 Hz	[15]	–	–	
		0+3–	4–6 V	5–31 Hz	[15]	–	–	
						[a]4–5 V	5 Hz	[2/2]
						[b]4–5 V	5–16 Hz	[6/6]
	Flexed	0–3+	4, 6 V	5–31 Hz	[10]	4 V	5–16 Hz	[3/3]
		0+3–	4, 6 V	5–31 Hz	[10]	–	–	
						[b]4, 6 V	5–10 Hz	[4/4]
						[c]4, 6 V	5–16 Hz	[6/6]

Table 1.3b. Parameter settings which effectively induced an extension movement, and temporal changes in the EMG pattern observed during the movement

Subject No.	Polarity	Effective Strengths	Effective Frequencies	Temporal changes in the EMG pattern: Immediate	Movement	Steady state	
1		No goniometer recordings available.					
2		No goniometer recordings available.					
3/Sess #1	0–3+	10 V	5–16 Hz	+	–	*	[8/9]
		[d]10 V	21–50 Hz				
		5 V (450 µs)	5–16 Hz	+	–	*	[2/3]
	0+3–	5, 10 V (450 µs)	5–10 Hz	*	–	*	[3/4]
		[d]5 V (450 µs)	16–31 Hz				
3/Sess #2	0–3+	8–10 V	10–21 Hz	+ (10–16 Hz)[c]		*	[6/9]
				* (21 Hz)[c]		*	[4/4]
		[d]10 V	31–50 Hz				
	0+3–	–	–				
		[d]8 V	16–31 Hz				
4	0–3+	5 V	5–50 Hz	+	–	*	[8/8]
		7 V	5–10 Hz	+	–	*	[2/2]
		[d]7 V	16–31 Hz				
	0+3–	5, 7 V	5–21 Hz	+	–	*	[7/8]
		[d]5, 7 V	31 Hz				
5	0–3+	6 V	5–16 Hz	+	–	*	[2/3]
		[d]6 V	21–31 Hz				
	0+3–	–	–				

Column 'Effective Strengths/Frequencies': Parameter values which effectively induced a *sustained* extension of the flexed lower limbs (as documented by goniometer recording). Let 'H–Q' denote the difference between the EMG amplitudes in hamstring and quadriceps. Under 'Temporal changes in the EMG pattern' we indicate whether H–Q increased (+), decreased (–) or remained constant (*) during successive phases of the induced extension, i.e. immediately after the onset of the stimulation ('Immediate'), during the actual movement ('Movement'), and as soon as the EMG output remained temporally stable ('Steady state'). In addition, the number of recordings in which the described modulations were actually observed is given in squared brackets. E.g., '+ – * [8/9]' denotes that in 8 out of 9 recordings H–Q first increased, then decreased, and finally remained constant.

[d] Immediately after the onset of the stimulation, an extension movement was induced, but it immediately reversed to a pronounced flexion.

[c] When a stimulus frequency of 10–16 Hz was applied, H–Q slowly increased until it remained fairly constant. At 21 Hz, the EMG amplitudes in the thigh muscles remained essentially constant throughout the recording.

Both the EMG output and the extension movement became increasingly weaker as the stimulus strength was reduced without changing the site and frequency of the stimulation. The minimum stimulus level inducing lower limb extension would appear to be influenced by two factors: (i) the rostro-caudal position of the cathode based on spinal cord segments, and (ii) the electric contact between its active poles and the surrounding tissue influencing the impedance of the electrode. These two factors are also reflected in the routinely measured threshold values initiating single muscle twitches (see Methods); hence we used the results of these recordings as a reference in examining the relation between the segmental position of the stimulating electrode and the elicited CMUP output. The question within what segmental range the lumbosacral cord has to be stimulated to induce extension of the lower limbs was addressed by comparing the results obtained for different levels of the stimulating electrode. It emerged that there was no single "optimal" site to elicit and retain such extension.

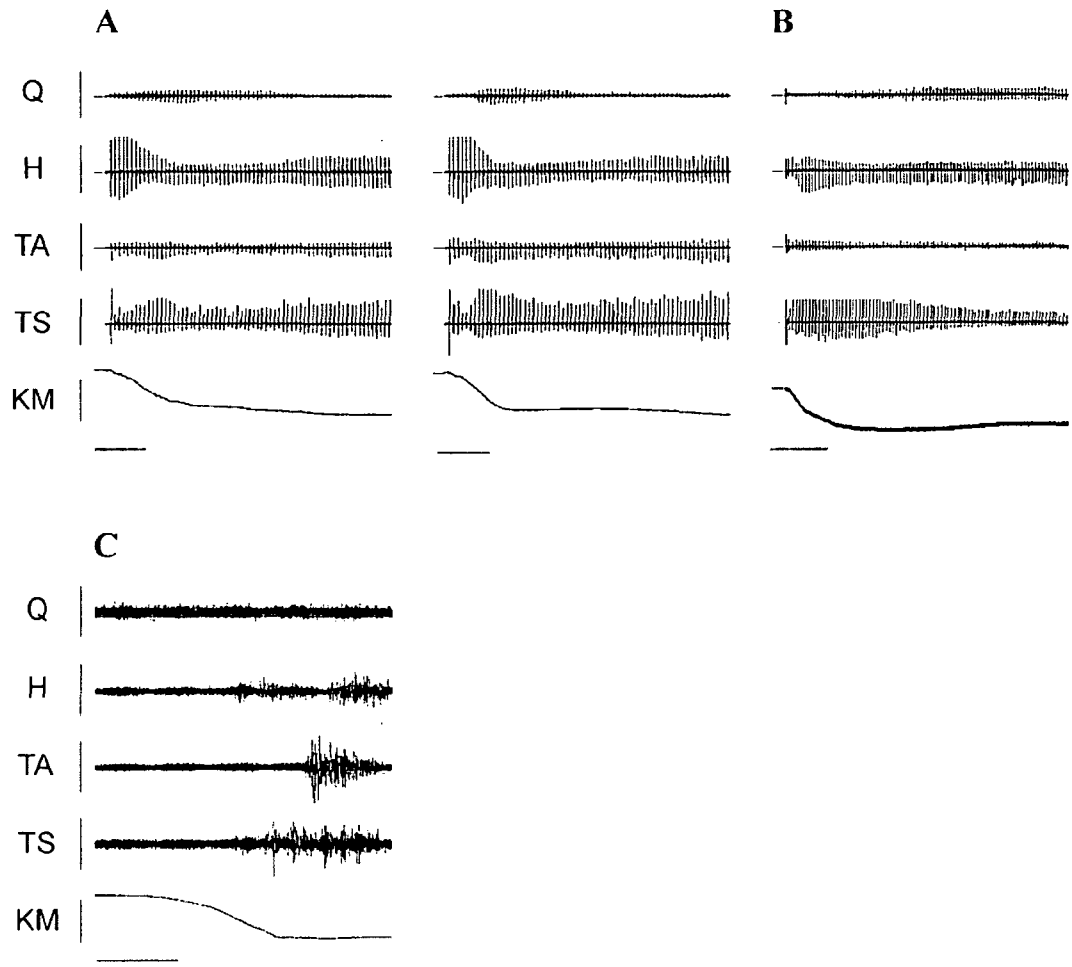

Fig. 1.5. EMG recordings during electrically induced vs. manually controlled lower limb extension. **A**, EMG recordings during electrically induced lower limb extension, obtained in two different trials using the same parameter settings (subject #3, estimated segmental level of stimulation: L4/5; stimulation parameters: 0–3+, 10 V, 10 Hz, 210 μs pulse width). Note the similarities between the two recordings with respect to the dominance of the extensors over the flexors, and the temporal modulations during the actual movement. Vertical markers: 1200 μV (Q, H); 600 μV (TA, TS); 60 ° (KM, knee movement). Horizontal markers: 1 s. **B**, EMG recording during electrically induced lower limb extension obtained in a different subject (subject #4, estimated segmental level of stimulation: S1/2; stimulation parameters: 0–3+, 7 V, 16 Hz, 210 μs pulse width). It reproduces the features observed in **A**. Vertical markers: 6000 μV (Q, H, TA, TS); 90 ° (KM). Horizontal marker: 1 s. **C**, EMG recording during manually controlled lower limb extension (subject #3; stimulation off). In contrast to the frequency-following (stimulus-triggered) CMUPs observed in **A** and **B** it reveals low-amplitude phasic-tonic stretch reflex responses. (Note the different scaling of the vertical axes as compared to **A** and **B**.) Vertical markers: 80 μV (Q, H, TA, TS); 60 ° (KM). Horizontal marker: 1 s.

On the contrary: the cord-based locations at which stimulation was successful covered a relatively long distance, ranging from L2/3 to L5. In one case (subject #4), the electrode was placed as low as S1/2 and still evoked powerful extension movements at 5–50 (!) Hz. In another subject, a strong extension was observed with the electrode at L4/5 when a stimulus of moderate strength (5 V) was applied at an increased pulse width (450 μs); again, the response remained essentially constant over a wide range of frequencies (5–31 Hz). Differences in the EMG output due to different levels of the stimulating cathode could be studied also *within* each subject to

some extent by comparing the results obtained for different combinations of the electrode contacts used as anode and cathode. Curiously enough, using the '0–3+' polarity (or '2–3+', or '1–2+', respectively) the lowest stimulus intensity required to evoke the EMG extension pattern was always higher than the one required for the reverse polarity ('0+3–', '2+3–', or '1+2–', respectively—see **Table 1.3a**). Whether this observation means that activation of the lower (rather than the upper) lumbar cord is required for lower limb extension to be initiated needs to be investigated further.

The parameter configurations found to evoke the *EMG* extension pattern (as given in **Table 1.3a**) largely coincide with the ones that the *goniometer recording* revealed to elicit sustained extension (as given in **Table 1.3b**). We may therefore summarise that in all five subjects included in this study, repetitive stimulation of the lumbosacral cord using particular parameter settings reproducibly induced lower limb extension as documented by EMG and, in subjects #3–5, also by goniometer recording. **Fig. 1.5A** demonstrates that the above-described characteristics of the induced sustained extension (particularly the dominance of the extensors, different phases of the movement, and the temporal modulations) were consistently observed in different trials under constant stimulation conditions. Applying the same protocol in different subjects revealed similar features, as can be seen by comparing **Figs. 1.5A** and **B**. If the same movement from full flexion to extension was, however, performed by passive (i.e. manually controlled) extension of the paralysed limb instead of SCS, the EMG was of a quite different feature. It exhibited phasic-tonic stretch reflex responses of low amplitude (10–100 times below the ones in **Fig. 1.5A**) which were most prominent when the extended position of the limb had already been reached (**Fig. 1.5C**).

1.3.2 Degree and duration of the induced extension movement

The maximum deflection of the knee-joint angle, which was used to quantify the degree of extension obtained in our trials, turned out to depend on the frequency of the stimulus train. **Fig. 1.4C**/'R' illustrates a series of recordings in which a stimulus of 10 V was applied with the cathode placed over L3/4 (estimated segmental position). The frequency of the stimulus train went from 5 up to 31 Hz. Each recording was started with the subject's lower limbs in complete flexion. The goniometer recordings clearly confirmed that both the degree and the duration of the induced extension movements decreased as the stimulus frequency was increased. In response to 5 Hz stimulation, lower limb extension was expressed at maximum degree. **Fig. 1.4C**/'L' represents the goniometric recordings which were obtained at the same time from the contralateral limb. The differences to the right limb ('R'), particularly in the traces at 10 and 16 Hz, can be explained by the asymmetric position of the stimulating cathode. In the five subjects under study, the best results, including the most powerful extension movements, were obtained at frequencies of about 5–10 Hz.

Interestingly, the curves for all extension movements started with a steep slope (see Methods). In the curve shown for 16 Hz in **Fig. 1.4C** (left limb), it amounted to 36 ° per second based on the first 0.5 s. Although this initial slope was observed at all frequencies, the curves as a whole became increasingly flatter as higher frequencies were used. In the first phase of the extension movement, the slope of the goniometer curve was more or less constant, which implies that the average amount of extension *per muscle twitch* monotonically decreased as the stimulus frequency increased.

Although an extension movement was still observable at 31 Hz, this was, as pointed out above, a rather fleeting response immediately reversing to a pronounced flexion movement. A

minor flexion peak right after the initial extension slope was also observed at 21 and 16 Hz, but the definitive flexion movement started markedly later in these cases (after around 5 and 3.5 s, respectively, compared to around 1 s at 31 Hz—see **Fig. 1.4C**, left limb).

1.3.3 Characteristic features of sequential EMG responses

Comparing **Figs. 1.4A** and **C** (the EMG traces in A belong to the 5–21 Hz traces in C/'L') it becomes apparent that the temporal EMG pattern during induced lower limb extension was well in accordance with the "movement trajectory", i.e. the time course of the joint angles during the induced extension movement. During the first phase, in which hamstring decreased and quadriceps increased in activity, the actual *movement* of the lower limb unfolded while the subsequent phase could be related to the active *retention* of the extended position (see also **Figs. 1.5A** and **B**). The temporal changes in the CMUP patterns were further analysed by calculating the integrated activity of single muscle twitch responses during different phases of the movement.

Fig. 1.6B illustrates the first 24 muscle twitches evoked in the thigh and leg muscle groups by a stimulus train of 5 Hz, which effectively induced an extension movement of the subjects' lower limbs. As can be seen from the goniometer curve, the first 12 of these responses covered the actual extension phase. It emerges that, after an initial phase of divergence (primarily due to certain augmentation in hamstring), the integrated activities of the thigh muscle groups tended toward each other during the extension movement, with hamstring losing and quadriceps gaining momentum (**Fig. 1.6A**). Once the limbs were in end position, the activity within each muscle group remained fairly constant. Continued stimulation actively maintained this position, which was reflected in a stable EMG pattern, with the activity still being greater in hamstring than in quadriceps. For subjects #3–5, a qualitative description of the changing amplitude relations between these two muscle groups during induced extension is given in **Table 1.3b**. In all analysed recordings (except the ones during session #2 in subject #3 when the '0–3+' electrode polarity was used) much the same spatiotemporal CMUP pattern was observed—as also illustrated in **Figs. 1.5A** and **B**.

As is apparent from **Fig. 1.6C**, the temporal modulations of the CMUP output during extension were not confined only to the EMG amplitude, but the shape of the individual responses elicited by repeated stimuli was changing as well. Analysing these changes was beyond the scope of this study but may help to understand the observed modifications. Preliminary studies of the EMG features of muscle responses during different types of induced activity have been performed. Results of these studies have been presented in abstract form [Minassian *et al.* 2001b, Jilge *et al.* 2002, Minassian *et al.* 2002].

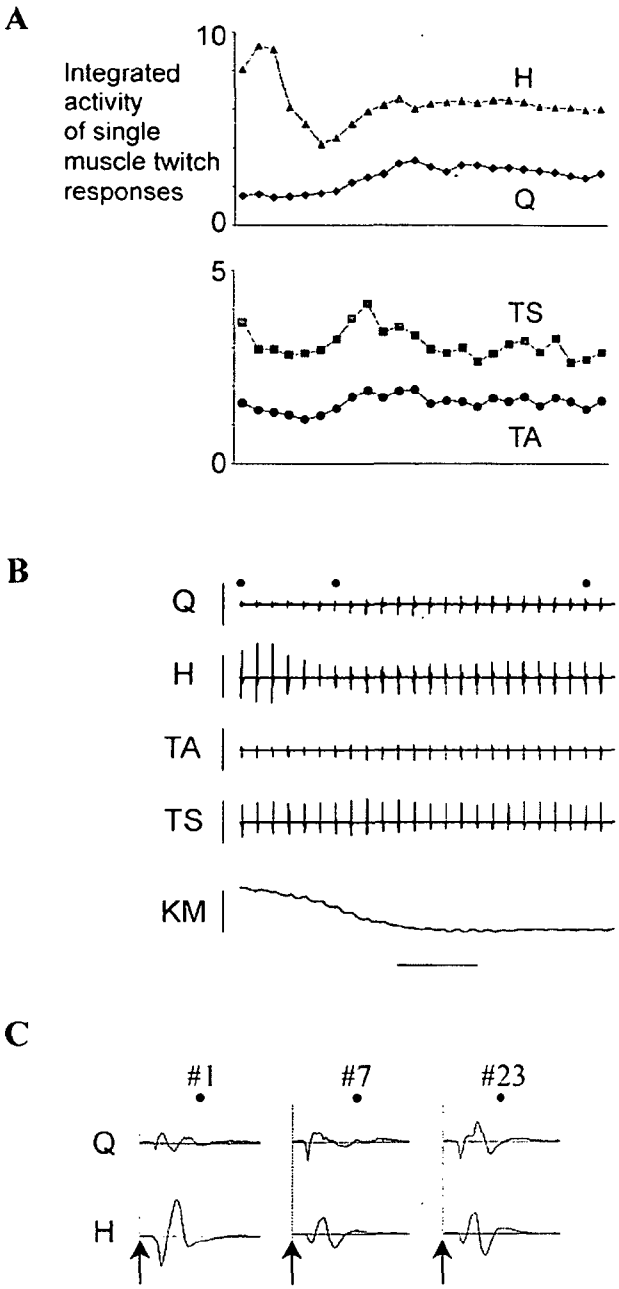

Fig. 1.6. EMG activity during the induced extension. Sequential EMG responses during the first 5 seconds of the induced extension. The first 12 CMUPs following the onset of the stimulation covered the actual movement phase, while during the next 12 CMUPs the extension was sustained. Recorded in subject #3 (estimated segmental level of stimulation: L4/5); stimulation parameters: 0–3+, 10 V, 5 Hz, 210 μs pulse width. **A**, Integrated activity ([in microvolt-seconds] = electric potential [in μV] × time [in s]) of single CMUPs. Note the difference in the amount of EMG activity in hamstring and quadriceps at the onset of the induced motor task. As the limbs approach the point of sustained extension a parallel course is gradually established. **B**, Original EMG data from which the histograms in **A** were calculated. Vertical markers: 1600 μV (Q, H, TA, TS); 90 ° (KM, knee movement). Horizontal marker: 1 s. **C**, Presentation of single CMUPs, selected from the EMG record in B, on a larger time scale. CMUP #1 immediately followed the onset of the stimulation, CMUP #7 was taken from the actual movement phase, and CMUP #23 was recorded during sustained extension. The arrows indicate the moments when the external stimuli were applied. Note that the temporal modulations in the EMG pattern were not confined to the integrated activity of the individual responses, but their morphology (shape) was changing as well. Vertical markers: 400 μV (Q); 800 μV (H). Horizontal marker: 50 ms.

1.3.4 Effect of initial limb positioning

At that point of the study, the question remained to what extent the recordings revealing lower limb extension may have been influenced by the initial position of the lower limbs. To address this question, we analysed an extra set of recordings in which a different initial position was used: instead of being flexed, the subjects' lower limbs were moved to the point of complete extension and were left resting on the examination bed without manual support. The subsequently applied stimuli, while not evoking any visible extension *movements*, did raise the muscle tone due to isometric contraction, thus actively *retaining* the extended position of the lower limbs. Accordingly, the recorded EMG pattern was temporally stable, with hamstring and

triceps surae showing a level of integrated activity of the single responses well above the one exhibited by quadriceps and tibial anterior, respectively (**Fig. 1.7B**). This latter result was similar to the pattern observed in the regular recordings after the extension movement starting from complete flexion had been completed (**Fig. 1.7A**).

As we have pointed out earlier, the extension phase in response to frequencies higher than around 20 Hz tended to be very short, quickly reversing to a flexion movement that, in some cases, was sustained until the limb was back to where it started from. **Fig. 1.7C** illustrates the transition from the initially flexed position to extension and back to flexion again. The point where the integrated activity curves (i.e. the sequential histograms of integrated activity of single responses) for quadriceps and hamstring intersect coincides with the point where the corresponding goniometer curve for the knee joint angle has its valley, indicating the transition from the extension to the flexion movement. Tibial anterior and triceps surae showed an analogous pattern (**Fig. 1.7C**). A similar EMG pattern and flexion movement were also induced when the stimuli were applied with the lower limbs fully extended (**Fig. 1.7D**). Overall, initial limb positioning did not have a noticeable effect on the characteristic EMG histograms once the induced movement (whether flexion or extension) had been completed.

1.4 Discussion

Qualitatively equal results were repetitively obtained in different recording sessions (which were several months apart) both in the same subjects and in different subjects. The consistency of our findings only depended on the appropriate stimulus parameters. On account of this fact it is particularly unlikely that the observed temporal modulations of CMUP amplitudes and shapes were basically a function of changing geometrical relations around the surface electrodes during the unfolding extension movement. Moreover, such an explanation cannot be reconciled with our finding that the EMG amplitude changed much more rapidly at higher frequencies of the stimulus train (compare **Fig. 1.4A**: 5 Hz and 21 Hz), whereas the initial velocity of the actual movement did not vary depending on the stimulus frequencies used. The latter argument follows from the observation that the goniometer curves recorded in parallel started with a slope which was more or less constant when different interstimulus intervals were applied (see **Fig. 1.4C**).

1.4.1 Primarily activated spinal cord structures

These observations immediately raise the question as to the mechanisms which are involved in the generation of the artificially induced lower limb extension. First of all, which neural structures have been directly activated by the externally applied pulse train? It had been suggested by clinical observations [Maccabee *et al.* 1996, Troni *et al.* 1996] and demonstrated by theoretical studies [Coburn 1985, Strujik *et al.* 1993, Rattay *et al.* 2000] that specific geometric and electric conditions would result in so-called "hot spots" for electric stimulation (i.e. sites which have a low activation threshold). These sites would coincide with the entry points of the dorsal root fibres into the spinal cord. In fact, due to the dorsomedial position of the epidural electrode in the present study, the sensory afferents in the dorsal roots and their axonal branches in the dorsal columns are the largest fibres closest to the electrode, and therefore exceptional candidates among the possible targets for direct activation.

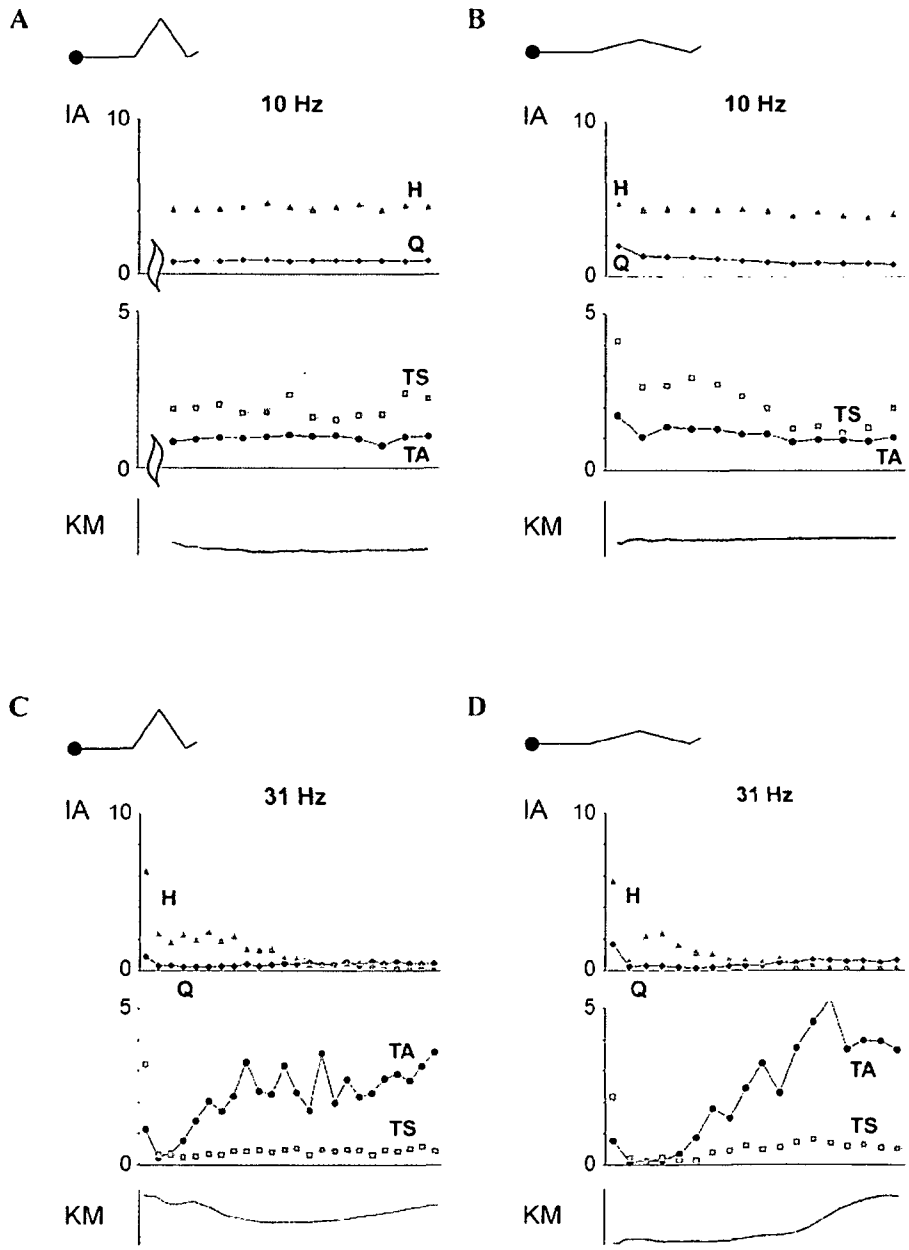

Fig. 1.7. Effect of initial limb positioning. **A**, At low frequencies (10 Hz), when stimulation is started with the limbs *flexed*, extension of lower limbs is actively retained after the actual extension movement has been completed. The first 12 CMUPs, covering the movement from the flexed to the extended position, have been omitted from the diagram. **B**, At low frequencies (10 Hz), when stimulation is started with the limbs *extended*, this extension is actively retained. **C**, At high frequencies (31 Hz), when stimulation is started with the limbs *flexed*, the induced extension quickly gives way to flexion (developing stepping movement). **D**, At high frequencies (31 Hz), when stimulation is started with the limbs *extended*, a flexion movement is induced. In the insets to the diagrams, the respective initial position of the lower limbs is indicated. Note the characteristic relationship between the integrated activities of quadriceps, hamstring, tibial anterior and triceps surae when extension is induced (see **A** and **B**), which is in contrast to the patterns obtained when flexion is induced (see **C** and **D**). Vertical markers: 30 ° (KM, knee movement). IA, integrated activity of single responses [in microvolt-seconds]. The original EMG data were recorded in subject #3 (estimated segmental level of stimulation: L4/5) in response to the following stimulation parameters: 0–3+, 10 V, 210 μs pulse width.

By analysing EMG data which had been collected to define the segmental level of the epidural electrode in subjects with impaired sensory functions, Murg *et al.* [2000] demonstrated that electrodes placed at vertebral levels T11–12 predominantly induced muscle twitches in quadriceps and adductors while stimuli delivered from T12–L1 levels resulted in a stronger activation of tibial anterior and triceps surae. A comparable relationship between the cathode level and the recruitment order of the lower limb muscles was obtained by Rattay *et al.* [2000] by assuming solely dorsal root stimulation in a computer model. Furthermore, the authors provided evidence for the following conclusions: *(i)* With regard to the least stimulus strength ("threshold") required to initiate an action potential in a particular neural structure from the epidural space, dorsal root fibres have the lowest threshold values while ventral root fibres do not respond until much higher stimulus intensities are applied. *(ii)* For a cathode which is close to or above the entry level of a target fibre into the spinal cord, spike initiation putatively occurs at the border between the cerebrospinal fluid and the white matter. Cathodes positioned (essentially) below the entry level of a target fibre cause spike initiation at a point which is close to the cathode, in a region where the fibre follows the ascending/descending course within the cerebrospinal fluid.

By way of contrast, the activation of dorsal column fibres is general rather than localised to afferents of any specific segmental origins. This can be seen on a clinical basis in the application of SCS in chronic pain management. There, medially placed electrodes elicit a widespread distribution of paraesthesiae in body areas at the level of stimulation and well caudally to it [He *et al.* 1994]. The reason is that at any cord level all dermatomes corresponding to that level and caudally are represented in the dorsal columns by ascending projections of their large cutaneous afferents. It was also demonstrated that dorsal column stimulation can result in a non-selective plurisegmental facilitation of motor neurones of different lower limb muscles. Guru *et al.* [1987] and Hunter and Ashby [1994] reported that thigh and leg muscles could be recruited with electrodes at T9–10 or even more rostral vertebral levels, at which point the cord segments and associated roots innervating the lower limbs are located well below the electrode. The authors attributed this non-specific muscle activity to antidromic activation of the rostral projections of muscle afferents in the dorsal columns.

These findings demonstrate that the direct effect of epidural lumbosacral cord stimulation is typically restricted in two respects. First, the electric (cathodal) field generated by the epidural electrode (directly) affects neural structures within a specific, limited range of segmental levels. It is focused to the cord segment(s) in the vicinity of the cathode if the stimulation is applied at threshold level. Using higher stimulus intensities, adjacent rostro-caudal levels will be excited as well. Second, it is primarily the large axons within the dorsal roots which are excited. If at all, activation of dorsal column fibres or interneurones plays a minor role. Meanwhile, further evidence has been reported that the muscle responses obtained by lumbosacral cord stimulation using a bipolar electrode placed dorsomedially in the epidural space are primarily due to the activation of large afferent fibres within the posterior roots [Minassian *et al.* 2001c and 2003]. We therefore suggest that, in the present study, dorsal roots of a restricted range of lumbosacral cord segments were primarily recruited in response to different sites and strengths of the stimulation. Moreover, we expect that, within each recording session, those spinal structures which were *directly* activated by the stimulation were *the same* in response to a constant stimulus amplitude.

In this context, it is also important to ask if the occasional manual support applied in order to protect skin and joint injury could have contributed to the extension that was induced from the flexed limb position. The answer to this question is no, which is immediately apparent from **Fig. 1.5**. It illustrates the differences in the EMG activity induced in the lower limb muscles during

electrically evoked (**Fig. 1.5A** and **B**), and passive (**Fig. 1.5C**), extension (with SCS OFF) of the lower extremities, respectively. The characteristic distribution of motor unit activity within the lower limb muscle groups, with the (hip and ankle) extensors dominating over the flexors, as well as the temporal modulations in the EMG amplitude during the electrically induced movement are absent if SCS is OFF. The outstanding differences in the EMG pattern suggest that epidural lumbar dorsal root stimulation on the one hand, and passive movement of the lower extremity on the other hand provide quite different input to the spinal cord. Moreover, an actual extension of the lower limb was evoked only when appropriate stimulus parameters were applied. Even when we did not support the limbs during SCS, we were nevertheless able to observe a strong and brisk, ballistic-like extension movement. However, in order to prevent any limb injury it was essential to add the protective – but not activating – manual antigravity support. **Fig. 1.7A** demonstrates that the CMUP output in hamstring and triceps surae was larger than the one in quadriceps and tibial anterior, respectively, also when the legs lay on the examination bed (without additional support) throughout the electric stimulation.

It is worth mentioning that the CMUP output induced in complete SCI people by epidural stimulation in supine position is much larger than the one observed in the same category of subjects during locomotor training in vertical position with partial body weight support (*cf.*, e.g., Dobkin *et al.* 1995, Harkema *et al.* 1997, or Dietz *et al.* 1998 where the reported EMG amplitudes are by a factor of 10–100 lower than the ones we recorded). This observation suggests that the mechanisms underlying these two approaches are very different, and further investigation to clarify this difference will be necessary.

1.4.2 Possible mechanisms underlying the induced extension

What about the possibility that the SCS-induced extension was the result of a series of massive reflex responses to the stimulation of several types of extensor and flexor afferents? Early studies on the motor control in subjects with chronic spinal cord injuries of different severity revealed that massive reflex extension is rare in complete SCI people [Riddoch 1917, Walsh 1919, Kuhn 1950, Dimitrijevic and Nathan 1967, Dimitrijevic 1994]. Even if such strong extensor reflex responses were after all evoked by the constant and regular stimulus pulses we applied, they would habituate rapidly due to the regular repetition of these pulses at the same site and with the same strength, rather than remaining present for 50 or more seconds of sustained stimulation [Dimitrijevic et al. 1972]. Furthermore, it would be unusual to observe a massive reflex extension revealing EMG features within the thigh and leg flexors and extensors which were the same in subjects #3–5 on many occasions (*cf.* **Table 1.3**). In addition, a non-selective, strong activation of several types of extensor and flexor afferents – through the dorsal columns, for example – seems unlikely in the light of the described selectivity of lumbosacral cord stimulation.

The CMUPs recorded during SCS-evoked lower limb extension were actually short-latency posterior root muscle reflex responses. However, what mechanism could account for the dominance of the extensor forces which ultimately resulted in an extension of the limb? If a more complex interneurone system was not involved in its production, the higher forces in the antigravity muscles could, in principle, be generated at three different levels: *(i)* The extensor afferents could have been exposed to a stronger electric field than the flexor afferents. It this were the case one would expect the success of SCS with respect to the initiation of lower limb extension to hinge on a particular rostro-caudal location of the stimulating cathode. However, our investigations did not reveal a single "optimal" site, but the spinal cord levels at which extension was effectively induced covered a relatively long stretch of lumbar segments (L2/3–

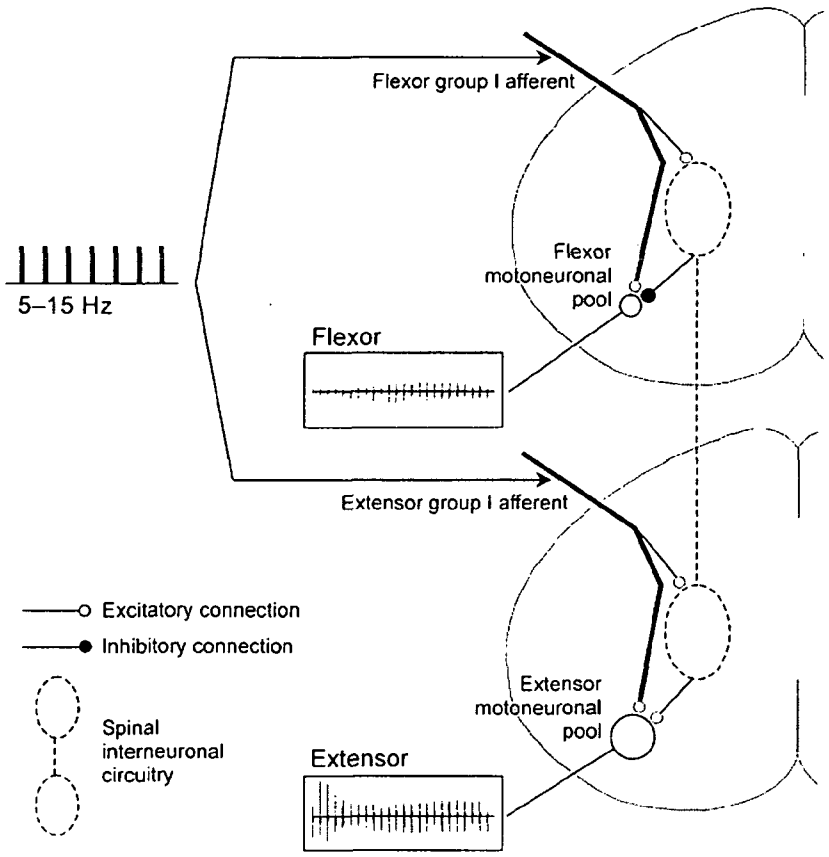

Fig. 1.8. Speculative scheme of the mechanisms underlying the induced extension. Probably both peripheral and central mechanisms were involved in the generation of the evoked lower limb extension. We hypothesise that the CMUPs recorded during the induced motor task reflect monosynaptic responses to dorsal root stimulation of large primary afferents of flexor and extensor muscles. In parallel, the external stimulus would have triggered central processing via these afferents which gave rise to the observed amplitude relation between flexors and extensors and its modulation over time.

L5). *(ii)* It could be an inherent property of the monosynaptic reflex arc of the extensors that the latter are activated stronger than the flexors in response to the same stimulus strength (and frequencies of 5–15 Hz). *(iii)* It could be an inherent property of the extensor muscles to generate larger forces than the flexor muscles in response to the same level of input to the muscle fibres. Explanations *(ii)* and *(iii)*, however, still leave the described temporal changes in the relationship between quadriceps and hamstring activity to be explained.

From the present study it emerges that the human lumbar cord is capable of producing at least two very different functional movements in response to sustained non-patterned stimulation. In other words, there are two different "codes" inducing the isolated lumbar cord to respond with two different motor tasks (**Fig. 1.3**). It has previously been shown that a stimulus train with a frequency of 25–50 Hz can evoke rhythmical, even stepping-like activity in the muscles of the lower limbs [Dimitrijevic *et al.* 1998b, Dimitrijevic 2001]. The presented results demonstrate that the lumbar spinal cord can also be induced to respond with a non-patterned type of motor output in the form of sustained lower limb extension. No less remarkably, this "reconfiguration"

is brought about just by lowering the stimulus frequency and without departing from the same sustained and non-patterned mode of input application *to the same spinal cord structures.*

During the transition between the two motor tasks (see **Fig. 1.4A**/21 Hz) a new spatial and temporal distribution of excitation and inhibition is developed. In addition to the already discussed features of epidurally evoked lower limb extension, several observations indicate that both peripheral *and central* mechanisms could be involved in the neurocontrol of the above SCS-induced movements: *(i)* The dominance of the EMG activity in the extensor muscles over the one in the flexors evoked at 5–15 Hz is reversed during the "flexion phases" of the induced rhythmical EMG patterns as frequencies of 25–50 Hz are applied (**Fig. 1.3**). *(ii)* As opposed to alternating reciprocal activation of flexors and extensors during stepping-like activity, the lower limb muscles are simultaneously activated during sustained extension. Thereby, the degree of co-activation is gradually reinforced as the movement unfolds in order to stabilise the involved joints and thus retain the extended position (**Fig. 1.6A** and **B**). Changes in the shape of the individual CMUPs recorded in parallel also suggest that a dynamic process takes place within the spinal cord (**Fig. 1.6C**). *(iii)* The latency times of the CMUPs recorded from the flexor muscles during rhythmical activity are significantly (about 10 ms) longer than the ones during extension (**Fig. 1.4B**; see also Minassian 2001a, b, 2002 and 2003). Only the latter can be explained in a simple manner considering the respective length of the efferent part of the monosynaptic reflex arc and "a single synaptic time lag": During implemented extension, the thigh and leg muscle groups responded at a constant latency time of approx. 10 and 15 ms, respectively (see **Fig. 1.2**/right hand side, **Fig. 1.4B**/5 Hz (b), and Murg *et al.* 2000). In contrast, necessary delays between flexor and extensor muscles are provided during rhythmical activity.

On the basis of this evidence we hypothesise that the amplitude-modulated CMUPs observed during epidurally evoked sustained lower limb extension actually reflect monosynaptic responses to the stimulation of large afferents in the posterior roots. However, the same primary afferent volleys will be synaptically transmitted to the intrinsic spinal circuitry which is involved in the generation of lower limb movement patterns. Stimulus trains at particular frequencies (namely 5–15 Hz) will configure this interneuronal network (or at least part of it) in such a way that it sets up—via presynaptic and synaptic mechanisms—the difference in the responsiveness between the flexor and extensor nuclei reflected in what has been termed the EMG "extension pattern". During the unfolding SCS-evoked movement, varying sensory feedback from the muscle, tendon and joint afferents will be integrated by the newly-organised "functional units" of spinal interneurones [see Hultborn 2001] and thus control the observed temporal modulations in the excitability of flexor and extensor motoneurones [see Jankowska 2001]. A speculative scheme to illustrate this hypothesis is given in **Fig. 1.8**.

Certain support for the existence of an interneuronal system within the mammalian lumbar cord which is – when properly stimulated – capable of generating extension movements has recently been provided by Mushahwar *et al.* [2000]. They reported to have elicited coordinated, weight-bearing whole hind limb extensor synergies in healthy, adult cats by stimulating the spinal cord through a microelectrode implanted in the caudal half of the lumbar enlargement. Following their argumentation, the induced multi-joint movements were not due to direct stimulation of motoneurones but resulted from the activation of interneuronal networks within the motoneuronal pools [Mushahwar *et al.* 2002]. A similar approach was used by Tresch and Bizzi [1999] who were successful in eliciting (isometric) forces which "drive the limb away from the body" in chronically spinalised rats by stimulation of a particular region within the posterior lumbar cord.

One might finally ask how it can be that the same procedure of epidural lumbar cord stimulation is effective for both the suppression of spasticity and the implementation of lower limb extension. It has to be noticed, however, that distinct stimulus frequencies have to be applied to achieve these different goals. Partial elimination of afferent input has been shown to reduce spasticity [Dimitrijevic and Nathan 1967]. Apparently, SCS at 50–100 Hz induces some kind of "electrophysiological rhizotomy" by strongly activating spinal interneurones which have an inhibitory—putatively presynaptic—influence on primary afferents of the lower limbs. In the control of several movement tasks, presynaptic mechanisms are known to play an important roll, being integral parts of their "central programs". Thus, presynaptic suppression of sensory transmission may be involved in the generation of SCS-induced lower limb extension, too. Low frequency stimulation (5–15 Hz), however, does not allow this mechanism to predominate the motor output. It is rather integrated in the organisation which is induced by the regular train of stimuli. The *steady* difference in the excitability of the flexor and extensor motor nuclei during implemented extension is replaced by *alternating* excitation/inhibition of these nuclei during epidurally evoked rhythmical flexion/extension movements of the lower limbs.

1.4.3 Significance of the results

The question whether and how the ability to stand can be restored after spinal cord lesions has been addressed in the literature. Pratt *et al.* [1994] investigated the effect of daily stand training on the weightbearing capacity of a chronic spinal cat. De Leon *et al.* [1998] revisited the same design to find out whether the observed recovery was really due to the training or whether it may have been spontaneous. They suggested that the improved standing ability seen after rote repetition of a specific hindlimb task was due to the training, which presumably gave rise to long-term changes in specific spinal pathways. More recently, Harkema [2001] showed that after several weeks of step and stand training, chronic incomplete SCI subjects who had not been able to bear weight previously were eventually able to stand independently for several minutes.

Our results illustrate that a sustained extension of the lower limbs can be obtained by epidural stimulation of the lumbar cord in subjects who are resting in supine position. This approach does not require any preparatory (conditioning) procedure to be carried out, but the movement is elicited immediately after the onset of stimulus application. Moreover, the opportunity to induce an extension of the lower limbs by epidural cord stimulation remains intact even if the SCI occurred many years back (2–8 years in our population). However, the studies on the effect of SCS on spasticity, or with respect to the possibility to induce lower limb movements, respectively, were made in supine position. We did not have the opportunity to measure the forces actually generated in the lower limb muscles in response to the stimulation. Although the extension induced in supine position was quite powerful, we are therefore not able to judge if it would have been strong enough to support the subject's body weight in standing position. Conversely, it has been shown that – at least during locomotion – the activity of both the leg and thigh muscles is powerfully controlled by afferents from load receptors [*cf.*, e.g., Pearson and Collins 1993, Harkema *et al.* 1997, Dietz *et al.* 2002]. Short latency reflex responses occur in triceps surae at that point of the step cycle where the heel of the swinging leg hits the ground and becomes the center of weight bearing. In addition, Brooke and McIlroy [1985] demonstrated that, during particular phases of the step cycle, short latency pathways between extensors of the knee and ankle open in both directions.

Obviously, the artificial "code" externally applied to the posterior roots of the lumbar cord cannot replace the complex dynamic process that underlies postural control but in a fragmentary manner. The present study included only subjects whose lower spinal cord had been isolated

from the brain by accidental trauma. Neurophysiological evaluation of their motor functions confirmed that they had no supraspinal control. All brainstem-derived descending tonic and phasic activity at the lumbosacral level had been eliminated by the injury. In particular, the presence of both the "driving" tonic input, which could provide postural tonus, and of the regulatory influences from higher centres was excluded. We have therefore not been able to address such critical questions as how to maintain balance or how to respond to unexpected postural disturbances [Mori 1987, Macpherson *et al.* 1999]. Experiments in both decerebrate and spinal cats have shown that the brainstem and spinal cord cannot by themselves ensure postural equilibrium during stance. Such preparations may be capable of weightbearing for as long as specific portions of the CNS are being stimulated, involving a short lag at best, but they cannot maintain lateral stability in the longer run [Mori *et al.* 1982, Pratt *et al.* 1994]. Since the ability to stand is a prerequisite for locomotion, epidural stimulation of the lumbosacral cord at low frequencies might nevertheless be a useful neuroaugmentative tool to support locomotor training in subjects with SCI. However, further studies are needed to learn more about the mechanisms underlying our findings and to explore their full potential for clinical neurorehabilitation.

Acknowledgements. Special thanks are due to Ms. Auer, Ms. Preinfalk and Ms. Alesch for their excellent technical support. This study was supported by the Austrian Science Fund (FWF), research project No. P15469; the Austrian Ministry of Transport, Innovation and Technology; and a grant from the Kent Waldrep National Paralysis Foundation in Addison, Texas, USA.

References

Barolat G, Singh-Sahni K, Staas WE, Shatin D, Ketcik B, Allen K (1995) Epidural spinal cord stimulation in the management of spasms in spinal cord injury. A prospective study. Stereotact Funct Neurosurg 64: 153–164

Beric A (1988) Stability of lumbosacral somatosensory evoked potentials in a long-term follow-up. Muscle Nerve 11: 621–626

Bizzi E, Giszter SF, Loeb E, Mussa-Ivaldi FA, Saltiel P (1995) Modular organization of motor behavior in the frog's spinal cord. Trends Neurosci 18: 442–446

Brooke JD, McIlroy WE (1985) Locomotor limb synergism through short latency afferent links. Electroenceph Clin Neurophysiol 60: 39–45

Brown TG (1911) The intrinsic factors in the act of progression in the mammal. Proc roy Soc B 84: 308–319

Coburn B (1985) A theoretical study of epidural electrical stimulation of the spinal cord. Part II: Effects on long myelinated fibers. IEEE Trans Biomed Eng 32: 978–986

De Leon RD, Hodgson JA, Roy RR, Edgerton VR (1998) Full weight bearing hindlimb standing following stand training in the adult spinal cat. J Neurophysiol 80: 83–91

Dietz V, Wirz M, Colombo G, Curt A (1997) Locomotor capacity and recovery of spinal cord function in paraplegic patients: a clinical and electrophysiological evaluation. Electroenceph Clin Neurophysiol 109: 140–153

Dietz V, Muller R, Colombo G (2002) Locomotor activity in spinal man: significance of afferent input from joint and load receptors. Brain 125: 2626–2634

Dimitrijevic MR (1994) Motor control in chronic spinal cord injury patients. Scand J Rehabil Med Suppl 30: 53–62

Dimitrijevic MR (1998) Chronic spinal cord stimulation for spasticity. In: Gindelberg PL, Tasker RR (eds) Textbook for Stereotactic and Functional Neurosurgery. McGraw-Hill, New York, pp 1267–1273

Dimitrijevic MR (2001) What does the human brain tell to the spinal cord to generate and control standing and walking? Proceedings of the World Congress on Neuroinformatics Vienna (Austria) (ISBN 3-901608-20-6): 53–54

Dimitrijevic MR *et al.* (1980) Study of sensation and muscle twitch responses to spinal cord stimulation. Int Rehabil Med 2: 76–81

Dimitrijevic MR, Faganel J, Gregoric M, Nathan M, Trontelj JK (1972) Habituation: Effects of regular and stochastic stimulation. J Neurol Neurosurg Psychiatry 35: 234–242

Dimitrijevic MR, Gerasimenko Y, Pinter MM (1998a) Effect of reduced afferent input on lumbar CPG in spinal cord injury subjects. Soc Neurosci 24: 654.23

Dimitrijevic MR, Gerasimenko Y, Pinter MM (1998b) Evidence for a spinal central pattern generator in humans. In: Kien O, Harris-Warrick RM, Jordan L, Hultborn H, Kudo N (eds) Neuronal Mechanism for Generating Locomotor Activity. Annals of the New York Academy of Sciences, vol 860, pp 360–376

Dimitrijevic MR, Minassian K, Murg M, Pinter MM, Rattay F, Gerasimenko Y, Binder H (2001) Study of locomotor capabilities induced by spinal cord stimulation (SCS) of the human lumbar cord isolated from the brain control by post traumatic spinal cord injury. Soc Neurosci Abstr 27: 935.6

Dimitrijevic MR, Nathan PW (1967) Studies of spasticity in man. 1. Some features of spasticity. Brain 90: 1–30

Dimitrijevic MR, Prevec TS, Sherwood AM (1983) Somatosensory perception and cortical evoked potentials in established paraplegia. J Neurol SCI 60: 253–265

Dobkin BH, Harkema S, Requejo P, Edgerton VR (1995) Modulation of locomotor-like EMG activity in subjects with complete and incomplete spinal cord injury. J Neurol Rehabil 9(4): 183–190

Gerasimenko Y, McKay B, Sherwood A, Dimitrijevic MR (1996) Stepping movements in paraplegic patients induced by spinal cord stimulation. Soc Neurosci Abstr 22: 1372

Giszter SF, Mussa-Ivaldi FA, Bizzi E (1993) Convergent force fields organized in the frog's spinal cord. J Neurosci 13(2): 467–491

Grillner S, Zangger P (1979) On the central generation of locomotion in the low spinal cat. Exp Brain Res 34: 241–261

Gurfinkel VS, Levik YuS, Kazennikov OV, Selionov VA (1998) Locomotor-like movements evoked by leg muscle vibration in humans. Europ J Neurosci 10: 1608–1612

Harkema SJ, Hurley SL, Patel UK, Requejo PS, Dobkin BH, Edgerton VR (1997) Human lumbosacral spinal cord interprets loading during stepping. J Neurophysiol 77: 797–811

Harkema SJ (2001) Neural Plasticity after Human Spinal Cord Injury: Application of locomotor training to the rehabilitation of walking. Prog Clin Neurosci 7(5): 455–468

Hultborn H (2001) State-dependent modulation of sensory feedback. J Physiol 533.1: 5–13

Iwahara T, Atsuta Y, Garcia-Rill E, Skinner RD (1991) Spinal cord stimulation induced locomotion in the adult cat. Brain Res Bull 28: 99–105

Jankowska E (2001) Spinal interneuronal system: identification, multifunctional character and reconfigurations in mammals. J Physiol 533.1: 31–40

Jilge B, Minassian K, Dimitrijevic MR (2001) Electrical stimulation of the human lumbar cord can elicit standing parallel extension of paralyzed lower limbs after spinal cord injury. Proceedings of the World Congress on Neuroinformatics Vienna (Austria) (ISBN 3-901608-20-6): 63–64

Jilge B, Minassian K, Rattay F, Dimitrijevic MR (2002) Tonic and rhythmical motor unit activity of the cord induced by epidural stimulation can alter posterior roots muscle reflex responses. Proceedings of the 7th Annual Conference of the IFESS Ljubljana (Slovenia): 164–166

Jordan LM, Pratt CA, Menzies JE (1979) Locomotion evoked by brain stem stimulation: occurrence without phasic segmental afferent input. Brain Res 177: 204–207

Kameyama T *et al.* (1996) Morphologic Features of the normal human cadaveric spinal cord. Spine 21: 1285– 1290

Kazennikov OV, Shik ML, Yakovleva GV (1983) Stepping elicited by stimulation of the dorsolateral funiculus in the cat spinal cord. Bulletin Experimentalnoy Biologii i Mediziny (Bulletin of Experimental Biology and Medicine) 96(8): 8–10 (cited by Shik 1997)

Kuhn R (1950) Functional capacity of the isolated human spinal cord. Brain 1: 1–51

Lang J, Geisel U (1983) Lumbosacral part of the dural sac and the topography of its contents. Morphol Med 3: 27–46 (in German)

Lehmkuhl D, Dimitrijevic MR, and Renoul E (1984) Electrophysiological characteristics of lumbosacral evoked potentials in subjects with established spinal cord injury. Electroencephalogr Clin Neurophysiol 59: 142–155

Maccabee PJ, Lipitz ME, Desudchit T, Golub RW, Nitti VW, Bania JP *et al.* (1996) A new method using neuromagnetic stimulation to measure conduction time within the cauda equina. Electroencephalogr Clin Neurophysiol 101: 153–166

Macpherson JM, Deliagina TG, Orlovsky GN (1999) Control of body orientation and equilibrium in vertebrates. In: Stein PSG, Grillner S, Selverston AI, Stuart DG (eds) Neurons, networks and motor behavior. MIT Press, Cambridge/Massachusetts, London, pp 257–267

Minassian K, Pinter MM, Murg M, Binder H, Sherwood A, Dimitrijevic MR (2001a) Effective spinal cord stimulation (SCS) train for evoking stepping locomotor movement of paralyzed human lower limbs due to SCI elicits a late response additionally to the early monosynaptic response. Soc Neurosci Abstr 27: 935.12

Minassian K, Rattay F, Dimitrijevic MR (2001b) Features of the reflex responses of the human lumbar cord isolated from the brain but during externally controlled locomotor activity. Proceedings of the World Congress on Neuroinformatics Vienna (Austria) (ISBN 3-901608-20-6): 55–56

Minassian K, Rattay F, Dimitrijevic MR (2001c) A computer simulation and electrophysiological methods to identify the primary stimulated spinal cord structures with epidural electrodes. Proceedings of the World Congress on Neuroinformatics Vienna (Austria) (ISBN 3-901608-20-6): 64–65

Minassian K, Jilge B, Rattay F, Pinter MM, Gerstenbrand F, Binder H, Dimitrijevic MR (2002) Effective spinal cord stimulation (SCS) for evoking stepping movement of paralyzed human lower limbs: study of posterior root muscle reflex responses. Proceedings of the 7th Annual Conference of the IFESS Ljubljana (Slovenia): 167–169

Minassian K, Jilge B, Rattay F, Pinter MM, Binder H, Gerstenbrand F, Dimitrijevic MR (2003) Stepping-like movements in humans with complete spinal cord injury induced by epidural stimulation of the lumbar cord: Electromyographic study of compound muscle action potentials. Spinal Cord (submitted)

Mori S (1987) Integration of posture and locomotion in acute decerebrate cats and in awake, freely moving cats. Prog Neurobiol 28: 161–195

Mori S, Kawahara K, Sakamoto T, Aoki M, Tomiyama T (1982) Setting and resetting of level of postural muscle tone in decerebrate cat by stimulation of brain stem. J Neurophysiol 48(3): 737–748

Murg M, Binder H, Dimitrijevic MR (2000) Epidural electric stimulation of posterior structures of the human lumbar spinal cord: 1. muscle twitches – a functional method to define the site of stimulation. Spinal Cord 38: 394–402

Mushahwar VK, Collins DF, Prochazka A (2000) Spinal cord microstimulation generates functional limb movements in chronically implanted cats. Exp Neurol 163(2): 422–429

Mushahwar VK, Gillard DM, Gauthier MJA, Prochazka A (2002) Intraspinal microstimulation generates locomotor-like and feedback-controlled movements. IEEE Trans Rehab Eng 10(1): 68–81

Pearson KG, Collins DF (1993) Reversal of the influence of group Ib afferents from plantaris on activity in medial gastrocnemius muscle during locomotor activity. J Neurophysiol 70: 1009–1017

Pinter MM, Dimitrijevic MR, Dimitrijevic MM (1998) Effect of motor task on externally induced stepping movement in spinal cord subjects. Soc Neurosci Abstr 24: 831.1

Pinter MM, Gerstenbrand F, Dimitrijevic MR (2000) Epidural electrical stimulation of posterior structures of the human lumbosacral cord: 3. Control of spasticity. Spinal Cord 38: 524–531

Pratt CA, Fung J, Macpherson JM (1994) Stance control in the chronic spinal cat. J Neurophysiol 71: 1981–1985

Rattay F, Minassian K, Dimitrijevic MR (2000) Epidural electrical stimulation of posterior structures of the human lumbosacral cord: 2. quantitative analysis by computer modeling. Spinal Cord 38: 473–489

Richardson RR, McLone DG (1978) Percutaneous epidural neurostimulation for paraplegic spasticity. Surg Neurol 9: 153–155

Riddoch G (1917) The reflex functions of the completely divided spinal cord in man compared with those associated with less severe lesions. Brain 40: 264–402

Roaf HE, Sherrington CS (1910) Further remarks on the spinal mammalian preparation. Quart J Physiol 3: 209–211

Rosenfeld JE, McKay WB, Halter JA, Pollo F, Dimitrijevic MR (1995) Evidence of a pattern generator in paralyzed subjects with spinal cord injury during spinal cord stimulation. Soc Neurosci Abstr 21: 688

Sherwood AM, McKay WB, Dimitrijevic MR (1996) Motor control after spinal cord injury: Assessment using surface EMG. Muscle Nerve 19: 966–979

Shik ML, Orlovsky GN (1976) Neurophysiology of locomotor automatism. Physiol Rev 56: 465–501

Shik ML, Severin FV, Orlovsky GN (1966) Control of walking and running by means of electrical stimulation of the mid-brain. Biophysics 11: 756–765 (cited by Mori 1987)

Shik ML (1997) Recognizing propriospinal and reticulospinal systems of initiation of stepping. Motor Control 1: 310–313

Struijk JJ, Holsheimer J, Boom HB (1993) Excitation of dorsal root fibers in spinal cord stimulation: A theoretical study. IEEE Trans Biomed Eng 40: 632–639

Tresch MC, Bizzi E (1999) Responses to spinal microstimulation in the chronically spinalized rat and their relationship to spinal systems activated by low threshold cutaneous stimulation. Exp Brain Res 129(3): 401–416

Troni W, Bianco C, Moja MC, Dotta M (1996) Improved methodology for lumbosacral nerve root stimulation. Muscle Nerve 19: 595–604

Walsh FM (1919) On the genesis and physiological significance of spasticity and the disorders of motor innervation with a consideration of the functional relationship to the pyramidal tract. Brain 42: 1–28

Chapter 2

Evidences for a lumbar extension pattern generator in humans: Neurophysiology of compound motor unit potentials

Bernhard Jilge[1], Karen Minassian[1,2], Frank Rattay[1], Milan R. Dimitrijevic[3,4,5]

[1] TU-BioMed Association for Biomedical Engineering, Vienna University of Technology, Vienna, Austria

[2] Ludwig Boltzmann Institute for Electrical Stimulation and Physical Rehabilitation, Vienna, Austria

[3] Ludwig Boltzmann Institute for Restorative Neurology and Neuromodulation, Vienna, Austria

[4] University Institute for Clinical Neurophysiology, Clinical Centre Ljubljana, Slovenia

[5] Department of Physical Medicine and Rehabilitation, Baylor College of Medicine, Houston, Texas, USA

Abstract. It has been shown in complete spinal cord injured subjects that epidural stimulation of the lumbosacral cord at 4–10 V and 5–15 Hz initiated a strong and rapid extension movement of the lower extremities which was sustained for as long as the external stimulus was applied. Parallel electromyographic recordings revealed single compound motor unit potentials (CMUPs) which were identified as temporally modulated "posterior root muscle reflex responses". The present study explored the physiological content of these CMUPs with regard to their latency time, duration and shape in dependence on the stimulus parameters (site, strength, and frequency of stimulation). The EMG responses were analysed both under stationary conditions (i.e., when lower limb extension was implemented) and during the unfolding movement. Several lines of evidence independently suggest participation of the lumbar interneuronal network in the initiation and control of the epidurally evoked extension. At stimulus frequencies within the particular range of 5–10 Hz, CMUPs were significantly shorter, indicating increased synchronisation of the involved motor units. Moreover, extensor activity was greatly augmented, whereas flexor activity was continuously suppressed as frequencies above 2 Hz were applied. During the actual movement the initial CMUP shape in each muscle group was gradually replaced by another. Thereby, a high correlation was found between the temporal modulations observed in different muscle groups. As soon as extension was implemented the spatiotemporal EMG pattern remained remarkably constant. Taken together, we hypothesise that epidural stimulation of the human lumbosacral cord at 5–15 Hz and sufficient strength induced previously inactive interneuronal circuits to reorganise and form a "functional unit" capable of generating lower limb extension.

2.1 Introduction

In a range of limbed and nonlimbed animals, different motor patterns are produced by their nervous systems in the absence of afferent feedback [*cf.*, e.g., Delcomyn 1980, Grillner 1981, Rothwell *et al.* 1982, Sanes *et al.* 1985]. As a motor pattern generated by a nervous system which has been deprived of all peripheral feedback must be of central origin, the concept of "central pattern generation" has been introduced [reviewed by Grillner and Wallén 1985]. Central pattern generators (CPGs) serve as relatively simple model systems which help to explain how neuronal networks within the central nervous system produce complex motor behaviour [Kien and Kjaerulff 1998]. Although peripherally reduced preparations are usually not able to reproduce all aspects of the normal pattern, the question if some part is missing is not important in the definition of a central pattern generator.

Central pattern generators for different motor behaviours have extensively been studied. There are some questions that are usually addressed to a CPG under study: *(i)* how to "drive" the CPG, i.e., which supraspinal and/or spinal structures have to be stimulated in order to activate the CPG? *(ii)* Where is the CPG located? Is its spatial extension limited to a restricted area within the central nervous system? *(iii)* How is the CPG internally organised, and how does it work?

The internal organisation and functioning of central pattern generators has been investigated at many different levels from ion channels and single cells over synaptic (and presynaptic) mechanisms to neuronal circuitry and global functioning [*cf.*, e.g., Grillner and Wallén 1985, Selverston and Moulins 1985, Feldman 1986, Grillner *et al.* 2000]. The investigation of phase-dependent modulation of spinal reflexes has proven as a powerful tool in the assessment of spinal circuitry [reviewed by Burke 1999, see also Burke 2001]. Fundamental principles that are common to different types of CPGs within a preparation as well as to different (invertebrate and vertebrate) preparations have been described [Kennedy and Davis 1977, Getting 1986 and 1988, Dekin 1991, Pearson 1993]. In higher vertebrates, the concept of unit pattern generators (acting at single joints) has been introduced [Grillner 1981 and 1985]. In some preparations, the generation of different types of locomotion (forward/backward, up or down slopes) has been explained by changing the sign of coupling between these unit CPGs, which has the charm of a very simple control strategy [Grillner and Wallén 1985]. In other preparations, the enormous flexibility of the central nervous system in generating locomotor patterns suggested a "fragmented or mosaic segmental motor apparatus" capable of activating individual muscles—even "synergists"—independently [Grillner 1981].

CPGs generating locomotor patterns have always been of special interest. In humans, it has been shown that the lumbar spinal cord deprived of any suprasegmental influence can be induced to generate a stepping-like motor output pattern [Dimitrijevic *et al.* 1998]. Minassian *et al.* [2003] introduced the term "lumbar locomotor pattern generator" (LLPG) instead of "locomotor CPG" to indicate that the requirement of absence of afferent feedback, which is an integral part of the definition of a CPG, has not been fulfilled in the human model. Meanwhile, the investigation of locomotor-dependent spinal reflexes has contributed to our—yet moderate—knowledge of the neuronal organisation of the LLPG [Pearson 2000, Hultborn 2001, McCrea 2001].

Lower limb extension has primarily been studied as a part of the step cycle. Examination of the plantar reflex modulation during the stance phase of the locomotor cycle [Zehr *et al.* 1997] as well as during standing [Rossi and Decchi 1994] in subjects with intact nervous system have revealed similarities between these two "states" of the central nervous system related to lower

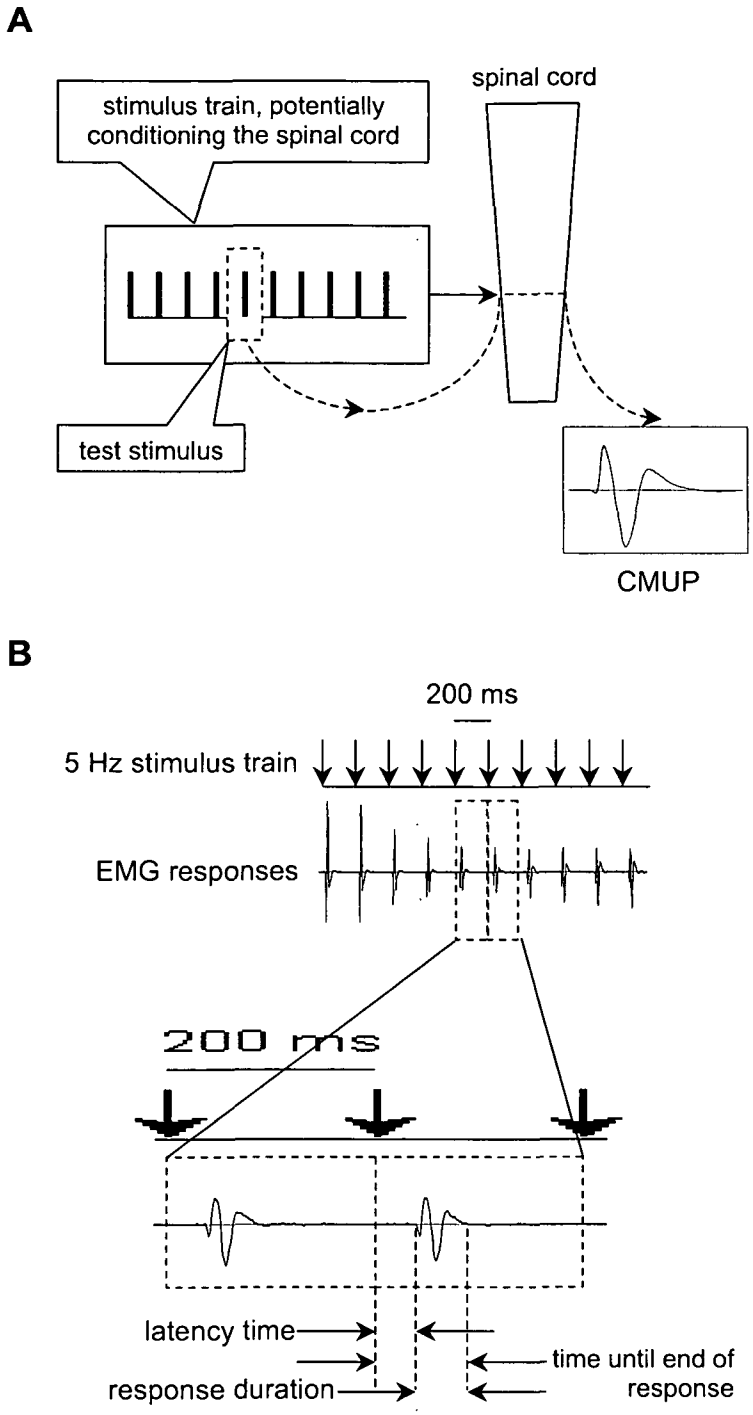

Fig. 2.1. Outline of methodology. **A**, The epidurally applied train of electric pulses was used—as a "conditioning" stimulus—to establish a certain "state" of the lumbar spinal cord. In parallel, each single pulse within the train served as a "test" stimulus capable of revealing the state-dependent reflex organisation of the cord. **B**, The EMG recorded in the lower limb muscles during SCS-induced lower limb extension revealed single compound motor unit potentials (CMUPs). Each CMUP response could unequivocally be related to the stimulus pulse which had triggered it. The EMG trace was divided into successive time windows, each covering a single CMUP. The margins of the windows were defined by the moments when the external stimuli had been applied. Enlarging the time scale allowed to analyse the physiological "content" (latency time, duration and shape) of the EMG responses.

limb extension: In both cases, the plantar reflex is reversed from a flexion reflex to an enhancement of the extension of the ipsilateral limb when the latter is to bear the load of the body. In incomplete spinal cord injured (SCI) subjects, foot contact with the floor during externally induced (air) stepping under body weight support immediately interrupts the ongoing stepping movement, initiating a strong extensor thrust of the ipsilateral limb [Pinter *et al.* 1998].

In complete paraplegics, results from the investigation of the flexor and crossed extensor reflexes support the view that the isolated human cord may be able to produce a flexion

(withdrawal) pattern in response to painful and non-painful stimuli but it cannot generate extension autonomously [Kuhn 1950, Dimitrijevic and Nathan 1967, Dimitrijevic 1994]. However, Jilge *et al.* [2003] have presented evidences for the existence of a "code" inducing the lumbosacral cord of complete SCI people to respond with lower limb extension. The authors have shown that sustained, non-patterned epidural stimulation at a frequency of 5–15 Hz and a strength between 4 and 10 V initiated a strong and rapid extension movement of the lower extremities, which was sustained for as long as the external stimuli were applied. The EMG recorded during the SCS-induced motor task demonstrated single compound motor unit potentials (CMUPs) in the main thigh and leg muscles, which could be related directly to the individual pulses within the stimulus train. It has been argued that the recorded CMUPs were due to the activation of large group I afferents in the dorsal roots [Minassian *et al.* 2003]. The stimulus-coupled responses to the epidural stimulation of the lumbosacral cord have therefore been termed "posterior root muscle reflex responses" (PRMRRs).

During SCS-induced sustained lower limb extension, the amount of rectified and integrated CMUP activity in the hip and ankle extensors was always larger than in the flexors. Furthermore, within the limits of this rule, well-defined temporal modulations of the EMG pattern were observed during the unfolding movement. These observations led the authors to formulate the following hypothesis: Although the recorded CMUPs reflected monosynaptic responses to the epidurally applied pulse train, the same afferent volleys were displayed to spinal interneuronal structures as well, thus configurating a system which set the (time-dependent) relative responsiveness of the involved motoneurone pools via premotoneuronal mechanisms.

If this is true, one would expect changes of the EMG pattern to occur not only at the level of the *overall amount of integrated activity* but also at the level of the *individual CMUP responses* as the SCS-induced extension movement unfolds. Moreover, as lower limb extension is not initiated and retained unless the epidural input is applied at a particular frequency range, these "internal" changes within a recorded sequence of CMUPs would also have to depend essentially on this stimulus parameter. In the present study we therefore investigated the physiological "content" of the single CMUPs recorded during *implemented* SCS-induced extension with respect to different variables (latency time, duration and shape) and how it depended on the applied stimulus frequency. Furthermore, we compared the features of the individual CMUPs recorded during the *unfolding* extension movement, revealing the basic "components" of these responses as the transition from the flexed to the extended lower limb position was performed.

2.2 Methods

2.2.1 Subjects, evaluation and stimulation procedure, recording

The study is based on the same subjects as in Chapter 1, using the same procedures of evaluation, stimulation and recording.

2.2.2 Data analysis

The raw EMG data (2048 samples per second) were analysed with respect to different features. As the EMG responses induced by the externally applied stimuli did not interfere with each other regardless of the stimulus frequency as long as it was not above 30 Hz, each CMUP could unequivocally ('1 : 1') be related to the pulse which had triggered it (**Fig. 2.1A**). The EMG recording was therefore divided into successive time windows of equal length, each covering one

muscle twitch response. The margins of the windows were defined by the moments when the stimulus pulses had been applied. These moments were reflected in the EMG charts as stimulus artefacts recorded in the abdominal and paraspinal muscles.

The subsequent analysis, which was performed separately for each single time window, was based on an approach which has not yet been described elsewhere. While the externally applied train of electric pulses could be regarded as potentially *conditioning* the spinal cord, we interpreted each single pulse within the train as a *test* stimulus eliciting a motor response which would give some information on the (induced) organisation of the spinal cord (**Fig. 2.1B**).

Parameters as the latency time, the duration and the shape of each motor response were of particular interest in our study, as well as the rectified and integrated activity within the respective time window. In a next step, the results obtained for different windows were compared. Mean and standard deviation of the obtained parameter values were calculated. (Further details about this stage of the analysis are given in the following sections.) For graphic representation purposes, pointwise averaging of 12–20 successive time windows was performed.

Flexion threshold frequency

It was immediately apparent from the EMG recordings under study that certain parameter settings elicited a *sustained* extension of the lower limbs while others evoked a re-flexion of the limbs immediately after the initially induced extension movement. For further analysis the "flexion threshold" frequency corresponding to a certain stimulus intensity was defined as the lowest stimulus frequency at which a stimulus train of the given strength induced such a re-flexion. As an increment of at least 5 Hz was generally used in our recordings, they provided no more than a rough estimate of this frequency. However, this was sufficient to reveal a certain relationship between the frequency and the amplitude of the stimulation in connection with a particular motor output.

Net amount of rectified and integrated EMG activity

In order to separate the "noise" included in the EMG recordings from the "net" activity induced by spinal cord stimulation (SCS), we calculated the amount of EMG activity in each of the four muscle groups under "resting" conditions first. However, an EMG recording during which the subject's spinal cord had not been stimulated for a few seconds was not available in most cases. We thus chose recordings in which a very weak stimulus (2.1 Hz, 1–2 V, well below any muscle twitch threshold) was applied over a period of 7–10 seconds. Based on the calculated average "noise level" (which was different for each muscle group) we subsequently computed the "net" amount of EMG activity within a given time window by integrating the rectified values of the electric potential above noise within the window.

When we analysed the effect of different stimulus frequencies on the amount of EMG activity induced in the lower limb muscles, this calculation was performed for 12 consecutive responses (per parameter combination), and their "net" activity values were finally added up.

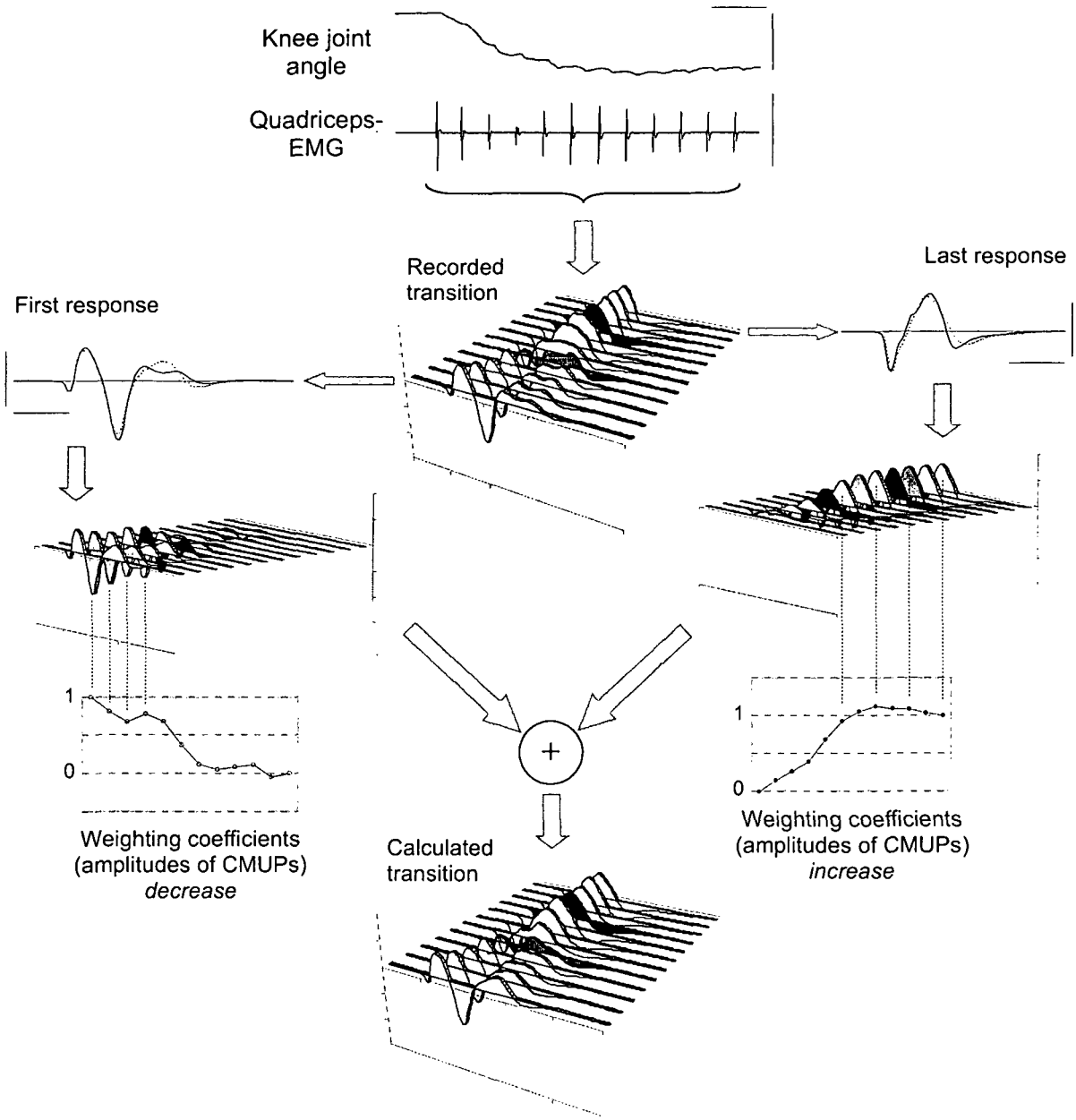

Fig. 2.2. Principal component analysis of recorded CMUP sequences. The original EMG recording during SCS-induced extension is divided into successive time windows, each covering a single CMUP. By means of a *principal component analysis* (PCA) the first and last responses are adjusted such that each CMUP is fairly reproduced by *weighted summation* of the resulting potentials. That is, one obtains two CMUP sequences – one starting with the adjusted first and another ending with the adjusted last response – the sum of which gives an approximation of the recorded data. Within these sequences, the potentials do not change their shape. Their amplitude variation is reflected in the sequential *weighting coefficients* calculated by PCA. (Recorded in subject #4, stimulus strength/frequency: 5 V/5 Hz, stimulating cathode at S4 segmental level. Vertical markers: 90 ° (knee joint angle), 4 mV (EMG trace); 2 mV (single responses). Horizontal marker: 0.4 s (EMG trace), 10 ms (single responses). Vertical axes: 1 mV/division. Horizontal axes: 10 ms/division.)

Content of compound motor unit potentials

Successive CMUPs recorded in a particular muscle group using a specific parameter combination were analysed with respect to their mean latency time and duration. Prior to the estimation of these parameters they were normalised as follows. First, the peak-to-peak amplitude of each CMUP was calculated as the difference between its largest and its smallest value. (Rectification of the electric potential was *not* performed.) Subsequently, the mean peak-to-peak amplitude was used as a reference level in such a way that we defined the latency time of a given response as the time passing between the preceding stimulus artefact and the first deflection of the electric potential from zero which was larger than 10 % of the mean peak-to-peak amplitude. We took care that this first deflection had the same direction (either positive or negative) for every CMUP within the given set. Responses which started with a deflection in the other direction (which were rare) were excluded from the analysis. Occasionally, a first deflection above the 10 % level was observed at very low latency times. Those which (randomly) occurred earlier than 3 or 7 ms post stimulus in the thigh or leg muscles, respectively, were ignored. We defined the end of each response, analogous to its onset, as the moment of its last deflection from zero larger than 10 % of the mean peak-to-peak amplitude. Finally, the time passing between the onset and the end of the response will be denoted as the "response duration".

The introduction of the requirement to exceed the 10 % level is (roughly) equivalent to the normalisation of every CMUP within the given set of responses to the same peak-to-peak amplitude. In the Results we will show that the EMG amplitude depends on the stimulus frequency underlying the set of responses. If we had used a fixed (i.e. amplitude-independent) level to be exceeded by the first and last deflections in the above definitions, differences in the latency time and duration of the responses to different stimulus frequencies would have been an "automatic" consequence. Thus, the performed normalisation removed the changes in the latency time and duration which were simply due to changes in the *overall* amplitude from those which resulted from changes in the spatiotemporal recruitment pattern of the motor units contributing to the CMUP.

When 10 % of the mean peak-to-peak amplitude were lower than the average "noise level" the application of the 10 % rule was not useful. Such weak responses were excluded from the analysis. In this connection, the average noise level was defined as the mean + 2×standard deviation of the rectified EMG potential recorded under "resting" conditions (see above).

In general, responses that were obtained at different stimulus frequencies or in response to distinct initial limb positions revealed different latency times and durations. In order to examine whether the differences between the respective mean values were significant, two-sample t-tests (on independent data) were performed. Welch's test statistic was applied instead in case of variance inhomogeneity between the samples, which was examined using the F-test. Single responses recorded during the actual movement from flexed to extended lower limb position were examined for their latency time and duration being different from the respective mean values during already implemented extension. To this end, one-sample t-tests were performed. All tests were carried out at the significance level $\alpha = 0.05$. The samples subjected to the tests generally contained 20 successive CMUPs.

Analysis of the temporal changes in the EMG patterns observed during the actual extension movement

The CMUPs recorded in response to frequencies which induced lower limb extension revealed smooth morphologic changes as the evoked movement unfolded. We subsequently formulated the hypothesis that they simply represented two superimposed processes going on in parallel, namely *(i)* the gradual suppression of the CMUP observed at the onset of the movement, and *(ii)* the gradual build-up of that CMUP which was observed at the end of the actual movement, i.e., when the extension was fully implemented (**Fig. 2.2**). In other words, the question was whether the whole sequence of (usually 12–20) CMUPs which were recorded during the implementation of lower limb extension was simply due to the successive substitution of one CMUP by another. In order to test our hypothesis we performed a linear regression analysis,

$$\mathbf{y}_j = a_j \cdot \mathbf{y}_1 + b_j \cdot \mathbf{y}_p + \Delta_j \quad (j = 1,\ldots,p), \tag{2.1}$$

in which the first and last CMUPs of the sequence, denoted as $\mathbf{y}_1$ and $\mathbf{y}_p$, served as the regressors. According to our notion, we anticipated the weights $a_1, a_2, \ldots, a_p$ to decrease from 1 to 0 while $b_1, b_2, \ldots, b_p$ would increase from 0 to 1. In fact, this was roughly the case. However, as we will describe in the Results, the goodness of fit (GOF, as documented by the value of the r^2 statistic) which was achieved by the regression was not as high as we had expected. Having cast doubt on our assumption that only two regressors (components) would be sufficient to "explain" the observed sequence of CMUPs, we investigated our data for their "dimensionality" by means of a principal component analysis (PCA; Timischl 2000). This approach allowed to test the premise that the variation contained in the data includes a certain "noise" which has to be filtered out in order to reveal the actual "components" of the recorded CMUPs. In the majority of analysed recordings the elimination of this noise yielded adjusted regressors $\tilde{\mathbf{y}}_1$ and $\tilde{\mathbf{y}}_p$ which could act as those two CMUPs the suppression resp. build-up of which resulted in the EMG responses that had been observed during the induced extension movement (**Fig. 2.2**).

Our analyses were either separately performed on the CMUPs recorded from different muscle groups, or simultaneously. In the latter case we sought to explain the whole spatiotemporal CMUP pattern during the externally induced extension movement on the basis of a small number of 'muscle synergies', i.e., suitable *sets*

$$\begin{pmatrix} \tilde{\mathbf{y}}_1^{\text{quadriceps}} \\ \tilde{\mathbf{y}}_1^{\text{hamstring}} \\ \tilde{\mathbf{y}}_1^{\text{tibial anterior}} \\ \tilde{\mathbf{y}}_1^{\text{triceps surae}} \end{pmatrix} \text{ and } \begin{pmatrix} \tilde{\mathbf{y}}_p^{\text{quadriceps}} \\ \tilde{\mathbf{y}}_p^{\text{hamstring}} \\ \tilde{\mathbf{y}}_p^{\text{tibial anterior}} \\ \tilde{\mathbf{y}}_p^{\text{triceps surae}} \end{pmatrix}$$

of (adjusted) CMUPs for the respective muscle groups. This approach is equivalent to searching for separate regressors for each muscle group which secure, however, one and the same sequence of weighting coefficients to be suitable for *all* muscles. For further information on the principal component approach we refer to the Appendix where full details of the method and its application to the data under study are given.

Sequences of weighting coefficients (see $a_1, a_2, \ldots, a_p$ and $b_1, b_2, \ldots, b_p$ above) were compared between different muscle groups using Pearson's correlation coefficient.

2.3 Results

2.3.1 Which segments of the lumbosacral cord have to be activated to induce lower limb extension?

In the following we will denote the segments innervating a given muscle group as "*activated*" by the externally applied stimulus train if they were stimulated at a strength which was *above* the previously observed muscle twitch threshold (see Methods). A stimulus train at a strength below the muscle twitch thresholds for both quadriceps and hamstring never induced a measurable extension movement of the lower limbs. Particularly, in those cases where tibial anterior and triceps surae were selectively activated (i.e., in the absence of any EMG output in the thigh muscle groups), there was no extension of the hip and knee joints in response to the stimulation.

On the other hand, spinal cord stimulation at a strength above the muscle twitch thresholds for both quadriceps and hamstring consistently induced lower limb extension within a certain range of "effective" stimulus frequencies. This was confirmed by the respective (knee joint) goniometer recording during the performance of the extension movement, and the corresponding EMG pattern in which hamstring dominated over quadriceps with respect to their EMG amplitudes. These recordings were obtained during stimulation at very different rostrocaudal levels of the stimulating cathode (vertebral levels T12 through lower L1). **Fig. 2.3B** demonstrates that a "well-expressed" EMG extension pattern (with the activity in hamstring and triceps surae dominating over the one in quadriceps and tibial anterior, respectively) as well as a pronounced (sustained) extension of the limb at the hip and knee joints could be elicited by stimulating either the upper or the lower lumbosacral cord. In both subjects the strength of the externally applied stimulus train was well above the muscle twitch thresholds for quadriceps and hamstring (shown in the left part of the figure).

Some parameter combinations underlying the recordings under study elicited a sustained extension of the lower limb, i.e., the (more) extended position of the limb was retained after the actual extension movement by the continued stimulation. Using other parameter combinations, the stimulus train evoked a re-flexion of the limb immediately after the initially induced extension movement. Looking for a rule underlying this observation we found that the range of stimulus frequencies which were effective for the induction of a *sustained* lower limb extension depended on the applied stimulus strength as follows: For stronger stimuli this range was narrower than for weaker stimuli. **Fig. 2.3C** illustrates the relation between effective stimulus strengths and frequencies in a subject whose electrode was placed at the upper lumbar cord level (identical with subject #1 in **Fig. 2.3B**). For each stimulus strength between 4 and 9 V, the approximate "flexion threshold" frequency is given. With respect to their efficiency for the initiation of a sustained extension, there is a reciprocal, generally non-linear relationship between the intensity and the frequency of the stimulation. For higher strengths, only stimulus frequencies between 5 and 15 Hz were effective, while a sustained extension movement (of the right limb) could be induced with frequencies up to 50 Hz if a low stimulus strength was applied. Note that quadriceps and hamstring were not activated with stimulus strengths below 4 V (using the 0+3– electrode polarity) in this recording session, and lower limb extension was not induced between 1 and 4 V.

As the ankle joint was not instrumented with a goniometer in the available recordings (and the foot was not placed in dorsiflexed position prior to the stimulation) we did not analyse which spinal cord segments had to be activated to induce an extension of the *ankle* joint. In the following the term "lower limb extension" will always refer to the extension of the hip and knee joints.

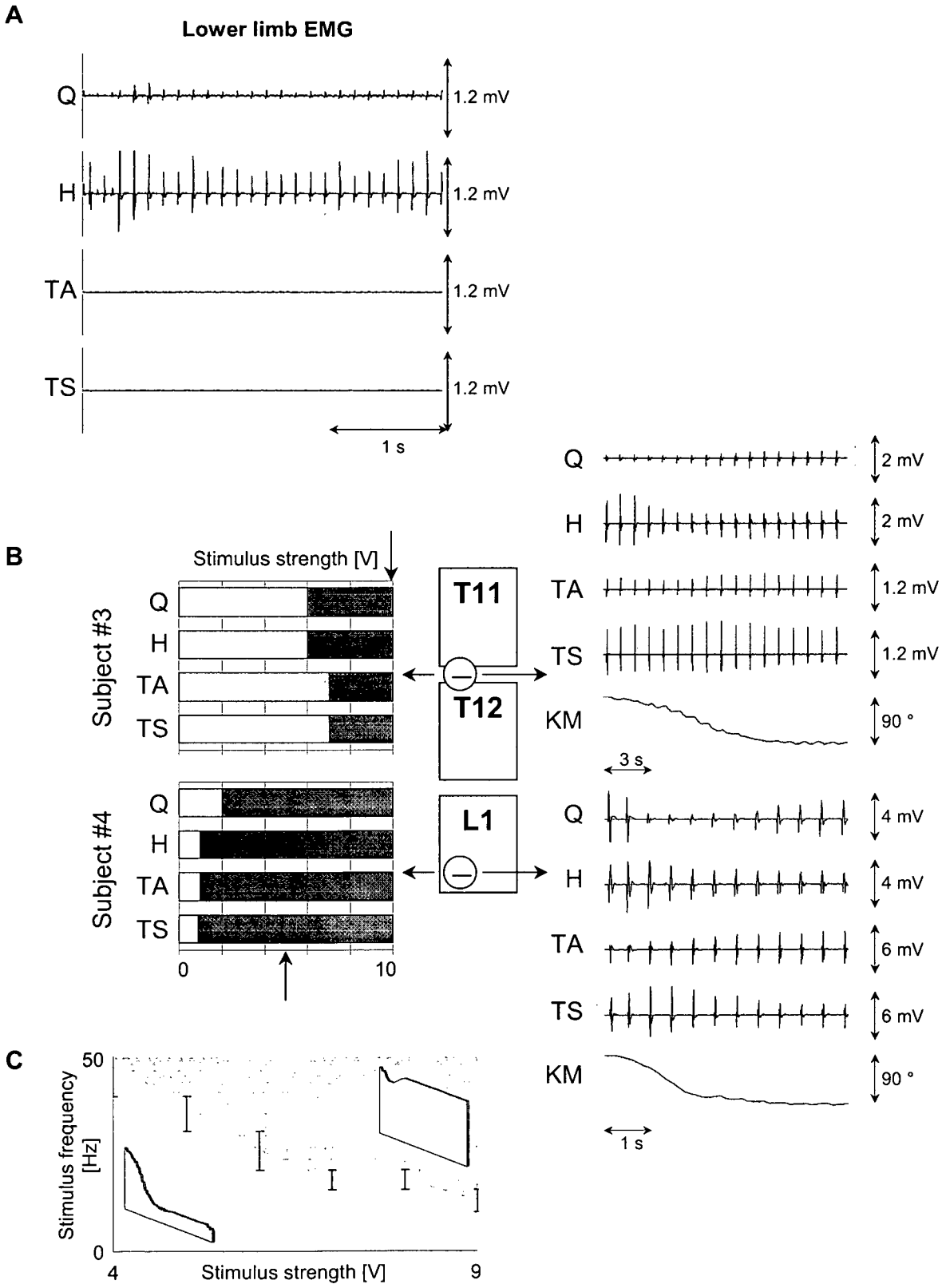
A
Lower limb EMG
Q
H
TA
TS
1.2 mV
1 s
B
Stimulus strength [V]
Subject #3
Subject #4
Q
H
TA
TS
0
10
T11
T12
L1
2 mV
1.2 mV
90 °
3 s
4 mV
6 mV
KM
1 s
C
Stimulus frequency [Hz]
50
0
4
9
Stimulus strength [V]

Fig. 2.3. Parameters which determine the initiation of a sustained lower limb extension. **A**, Lower limb EMG recording in response to SCS at 16 Hz and 6 V. At that strength, single muscle twitches were selectively induced in the thigh muscles. Subject #2, stimulating cathode at L2/3 segmental level. Q, quadriceps; H, hamstring; TA, tibial anterior; TS, triceps surae. **B**, Muscle twitch thresholds, and EMG and goniometric recording during SCS-induced lower limb extension in two subjects with the stimulating cathodes at T11/12 (L3/4) and lower L1 (S4) vertebral (segmental) level, respectively. The black bars in the left hand side panels indicate stimulus strengths at which single muscle twitches were induced. Arrows mark the intensities resulting in the right hand side recordings. Stimulus frequency: subject #3, 5 Hz; subject #4, 10 Hz. KM, knee movement: Downward deflexion indicates extension. **C**, Parameter combinations (stimulus strength and frequency) which induced a *sustained* (light grey area) or a *fleeting* (dark grey area) lower limb extension. The strength-dependent *flexion threshold* frequency is given by the border between these areas. Error markers indicate the inaccuracy of the measurement. Subject #3/session #2, stimulating cathode at L5/S1 segmental level.

← *previous page* —

2.3.2 Quadriceps and hamstring respond differently to the same (common) input

We examined the effect of changing the stimulus frequency on the amount of rectified and integrated EMG activity induced in the lower limb muscles by the externally applied stimulus. To this end, we analysed 18 sets (obtained in 3 subjects) of recordings which differed in the applied stimulus frequency only, while the other stimulus parameters were constant within each set. Only those recordings in which the strength of the stimulus train was above the muscle twitch thresholds for quadriceps and hamstring were included in this part of the study. During the recordings, the subjects' lower extremities had rested on the examination bed in extended position throughout.

According to the frequencies tested, each set of recordings was subsequently divided into three subsets: subset (1) responses to *single* stimuli or very low-frequency (not more than 2 Hz) stimulus trains (referred to as "single muscle twitches"); subset (2) responses to stimulus *trains* at a frequency which effectively induced the characteristic EMG extension pattern in the thigh and leg muscles (i.e., hamstring and triceps surae dominating over quadriceps and tibial anterior, respectively); subset (3) responses to higher-frequency stimulus trains, which did not induce lower limb extension. In this study, we were particularly interested in the differences between the responses of subsets (1) and (2), i.e., in the effect of going over from single stimuli to "low-frequency" stimulus trains.

As the EMG extension pattern was generally better pronounced for higher stimulus intensities we started the analysis with those recordings (within each subject) in which the highest stimulus strength had been applied. Responses to higher-frequency stimulus trains (subset (3)) were generally much weaker than single muscle twitch responses (subset (1); see the responses for 40 and 50 Hz in **Fig. 2.4B**). In other words, stimulus trains which did not induce lower limb extension exerted an overall suppression on the activity in the lower limb muscles as compared to single stimuli. However, this was not the case when responses to trains which *induced* the extension pattern (subset (2)) were compared with single muscle twitch responses (subset (1)). Particularly in hamstring, the decline in the amount of activity (in response to the frequency increase) was, in general, markedly weaker than in quadriceps or even converted to an increase of the EMG output (**Fig. 2.4A** and **Table 2.1**). Within the range of "effective" frequencies, which resulted in the responses of subsets (2), this "selective augmentation" of the EMG output in hamstring reached a maximum, which amounted to a factor of up to 1.47 (see Methods) in our recordings (**Table 2.1**, subject #3).

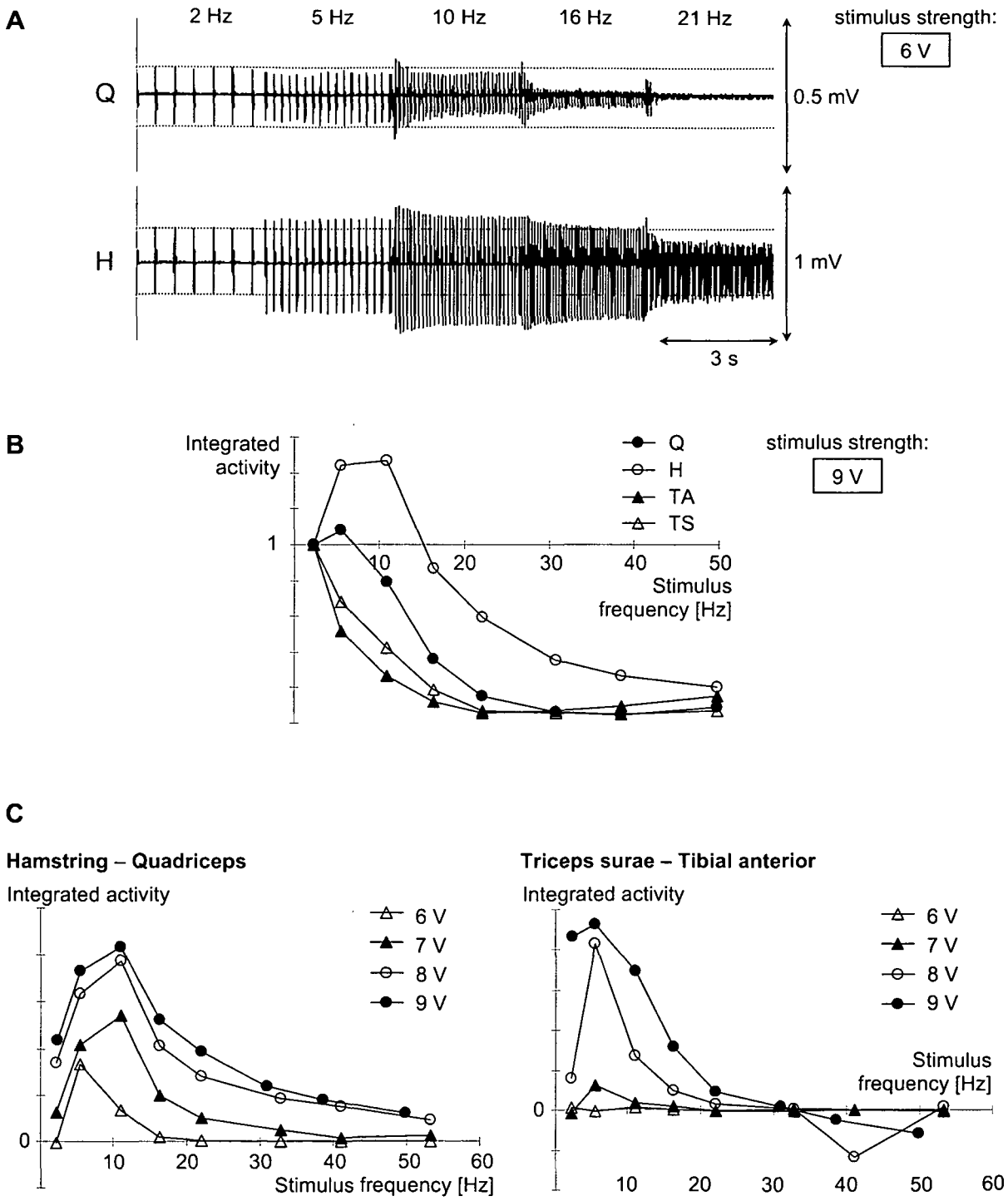

Fig. 2.4. SCS-induced selective augmentation of extensor activity. **A**, EMG recording in quadriceps and hamstring during SCS at 2–21 Hz. Subject #3/session #2, stimulating cathode at L5/S1 segmental level. **B**, Rectified and integrated CMUP activity in the lower limb muscles as a function of the stimulus frequency, given in proportion to the value obtained at 2.1 Hz. Subject #3/session #2, stimulating cathode at L3/4 level. **C**, Difference in rectified and integrated CMUP activity recorded in hamstring and quadriceps (or triceps surae and tibial anterior, respectively) in response to different stimulus strengths (6–9 V) and frequencies (2.1–53 Hz). Subject #3/session #2, stimulating cathode at L3/4 segmental level. Q, quadriceps; H, hamstring; TA, tibial anterior; TS, triceps surae.

In those recordings where the leg muscle groups were also activated by the external stimulus, an analogous response behaviour was found for triceps surae as compared to tibial anterior. Increasing the frequency of the stimulus train from single stimuli to 5–15 Hz resulted in a decline in the EMG output which was markedly weaker in triceps surae than in tibial anterior. The augmentation factors for the ankle extensor were higher than those for the ankle flexor within this frequency range. In one recording, even a slight increase of the triceps surae EMG activity was observed (augmentation factor = 1.04 when the frequency was 5.5 Hz) while the one in tibial anterior was reduced to 0.94 times its value for single stimuli.

The analysis was subsequently expanded also to recordings for which stimulus intensities lower than the maximum ones had been applied. Although the above described input-output characteristics with respect to the amount of EMG activity were, in principal, the same as for the maximum stimulus strength, they were increasingly less pronounced for lower intensities. **Fig. 2.4C** illustrates this finding in terms of the difference in the EMG output between hamstring and quadriceps (left hand side), or triceps surae and tibial anterior (right hand side), respectively. The dominance of hamstring over quadriceps is strongest for the highest stimulus strength that has been tested (9 V), progressively decreasing with decreasing intensity. Within the range of those frequencies which effectively elicited the EMG extension pattern in both the thigh and the leg muscles, the difference between the hamstring and quadriceps EMG activities reaches its maximum. This is true for all intensities between 6 and 9 V. The higher the strength, the larger this maximum, although the actual frequency at which this maximum occurs may shift a little with changing stimulus strength. The picture for the leg muscle groups is analogous. Note that the observed dominance pattern is reversed to a "flexion pattern" (i.e., the EMG activity in tibial anterior is larger than the one in triceps surae) when the stimulus frequency exceeds a certain level which is strength-dependent.

Taken together, the respective antagonistic muscle groups acting at the hip, knee and ankle joints responded differently to a low-frequency stimulus train. Regardless of the stimulus strength, as long as quadriceps and hamstring were activated, the observed "selective augmentation" of hamstring—and triceps surae if the leg muscles were activated, too—was strongest between 5 and 15 Hz (in most cases). The resulting dominance of hamstring and triceps surae over quadriceps and tibial anterior, respectively, was favoured by applying higher stimulus intensities.

Table 2.1. Relative amount of rectified and integrated EMG activity in quadriceps and hamstring in response to different stimulus frequencies

Frequency	Subject #4		Subject #2		Subject #3 (sess #2)	
[Hz]	Q	H	Q	H	Q	H
single	1.00	1.00	1.00	1.00	1.00	1.00
5–6	0.95	1.10			1.08	1.44
11	0.92	1.40	0.37	1.01	0.79	1.47
16–17	0.48	1.36	0.22	0.57	0.36	0.87
22–23	0.14	1.39	0.07	0.31	0.15	0.60

Single, single stimulus pulse; Q, quadriceps; H, hamstring. The amount of EMG activity is given in proportion to the respective value obtained for single pulses. Stimulus strength: subject #4, 7 V; subject #2, 8 V; subject #3, 9 V.

2.3.3 Content of the responses during implemented extension

So far we had analysed the amplitude of the observed posterior root muscle reflex responses. At this stage of the study, we were interested in the "content", including latency times, duration and shape, of the CMUPs elicited by the externally applied stimulus under different parameter combinations.

When the subject's lower extremities were placed in flexed position prior to the stimulation, and the subsequently applied train of electrical stimuli induced *sustained* lower limb extension, the EMG recorded in parallel revealed at least three qualitatively different phases (see **Fig. 2.3B**). Immediately after the onset of the stimulation, hamstring and triceps surae responded to the respective stimulus frequency with a "selective augmentation" as described in the previous section (first phase). During the second phase of induced extension antagonistic muscle groups tended toward each other with respect to their rectified and integrated EMG activities. When the actual limb movement was finished (i.e., the limb was in end position), the activity within each muscle group remained fairly constant. Continued stimulation actively retained this position, which was reflected in a temporally stable EMG pattern. In the following we will refer to this third phase of induced extension as the phase of "implemented extension". We must admit that a clear distinction between these three phases was quite difficult in some cases. Particularly the first and second phases frequently appeared unified ("fused") into one, or the first phase was very short, including only two or three responses.

We also analysed recordings where the subject's lower limbs were not initially flexed, but rested on the examination bed in extended position throughout the (stimulation and recording) session. In these recordings, the above introduced second and third phases could generally not be distinguished. The phase of selective augmentation in hamstring and triceps surae immediately merged into the phase of implemented extension. The results from the analysis of these recordings are presented first.

In each lower limb muscle group of a particular subject, the CMUPs recorded during implemented extension had roughly the same shape, latency time and duration. The quadriceps responses were either tri- or tetra-phasic, the fourth phase (i.e., the phase with the longest latency time) often having an amplitude lower than 10 % of the overall peak-to-peak amplitude ("$A_{0.1}$") of the response. In those cases where the fourth phase was higher than $A_{0.1}$, its amplitude was independent from the stimulus frequency, while the other phases were not. The hamstring responses were tri- or tetra-phasic, with either the first or the fourth phase frequently being lower than 10 % of the overall peak-to-peak amplitude of the response. The tibial anterior and triceps surae responses were generally tri-phasic. In triceps surae, a fourth phase with a latency time above 50 ms post stimulus was occasionally observed. Although this general description of the recorded CMUPs is true for all subjects under examination, certain differences in the shape of corresponding CMUPs were found between the subjects.

The response latencies of the leg muscles were about 9 (± 1) ms longer than the ones of the thigh muscles, while the duration of the responses was remarkably shorter in the former as compared to the latter. The actual values for the latency times and response durations depended on the particular subject, as well as on the stimulus frequency applied in the particular case. The averaged latency times (compared for similar frequencies) differed by up to 1.9 ms in the thigh muscles, and 0.5 ms in the leg muscles, respectively. However, in all subjects and regardless of the frequency, the recruitment order of the lower limb muscle groups in response to each (test) stimulus within the applied pulse train was: quadriceps—hamstring—tibial anterior—triceps surae (**Fig. 2.5A**).

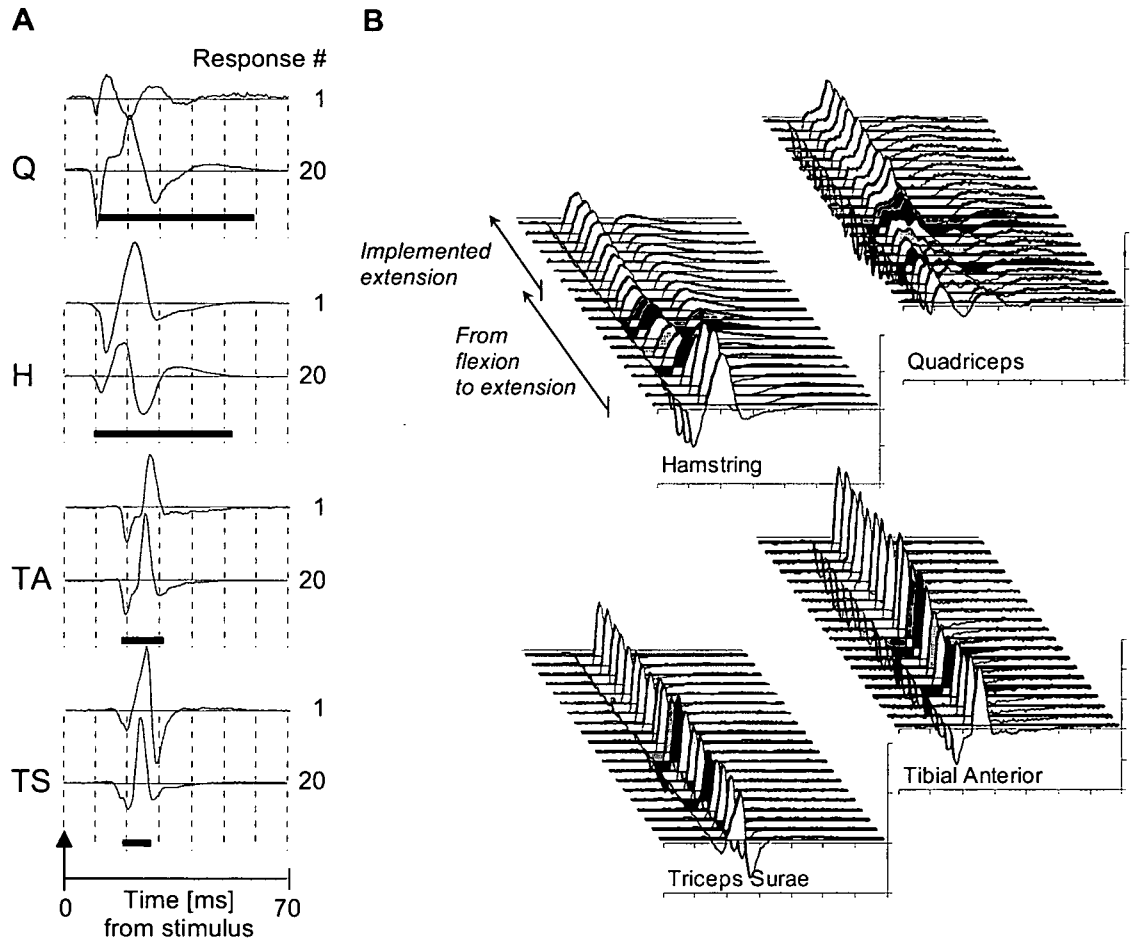

Fig. 2.5. Latency time, duration and shape of the CMUPs recorded during induced lower limb extension. First (initial) and 20th (steady-state) CMUPs (**A**), and transitional responses (**B**; first response in front) recorded during SCS-induced lower limb extension. The bars in **A** indicate mean latency time and duration of the steady-state responses. Subject #3/session #1, stimulus strength/frequency: 10 V/5 Hz, stimulating cathode at L3/4 segmental level. Vertical axes: 500 μV/division (hamstring, triceps surae); 200 μV/division (quadriceps); 100 μV/division (tibial anterior). Horizontal axes: 10 ms/division.

Comparing the quadriceps and hamstring responses to single stimuli with the responses to stimulus trains which induced a sustained lower limb extension, we found that both muscle groups responded significantly earlier to the single stimuli than to the (test) stimuli within the train. **Table 2.2a** shows the prolongation of the response latencies in the thigh muscles which occurred when the stimulus frequency was increased from single pulses to 5.2 Hz. A further increase to 10 Hz, i.e., *within* the frequency range of sustained lower limb extension, resulted in another (significant) latency shift.

Differences in the effect of different stimulus frequencies were also found with respect to the *duration* of the CMUPs recorded in the lower limb muscles. **Table 2.2b** demonstrates that the quadriceps, hamstring and triceps surae responses to a 10 Hz-stimulus train ended earlier than single muscle twitches. In hamstring and triceps surae this was also true for 5.2 Hz-trains, and at this frequency, even the tibial anterior responses ended earlier. Taken together with the observed

Table 2.2. Content of the steady-state lower limb CMUP responses to SCS at different frequencies

Table 2.2a. Latency

	Single pulse	5.2 Hz	10 Hz
Q	8.6 ± 0.2	8.7 ± 0.3	9.0 * ° ± 0.2
H	9.2 ± 0.2	9.3 ± 0.3	9.5 ° ± 0.2
TA	18.5 ± 0.3	18.1 ± 0.2	18.2 ± 0.3
TS	19.4 ± 0.5	18.8 ± 0.3	19.0 ± 0.4

Table 2.2b. End of response

	Single pulse	5.2 Hz	10 Hz
Q	58 ± 2	59 ± 1	55 * ° ± 2
H	55 ± 1	52.4 * ± 0.6	49.3 * ° ± 0.7
TA	34 ± 6	30.9 * ± 0.9	32 ± 2
TS	28.3 ± 0.3	27.3 * ± 0.4	27.6 * ± 0.3

Table 2.2c. Response duration

	Single pulse	5.2 Hz	10 Hz
Q	49 ± 2	50 ± 1	46 * ° ± 2
H	46 ± 1	43.1 * ± 0.9	39.8 * ° ± 0.9
TA	14.6 ± 0.9	12.8 * ± 0.9	13 ° ± 1
TS	9.0 ± 0.5	8.4 * ± 0.6	8.6 ° ± 0.5

Q, quadriceps; H, hamstring; TA, tibial anterior; TS, triceps surae. Entries are times in [ms], given as mean ± standard deviation. Recorded in subject #3/session #2, stimulus strength: 8 V.

Column '5.2 Hz': * The change in latency, response duration etc. as compared to responses to single pulses was *significant*.

Column '10 Hz': * The change in latency, response duration etc. as compared to the 5.2 Hz responses was *significant*. ° The change in latency time, response duration etc. as compared to responses to single pulses was *significant*.

latency prolongations, it follows that the frequency increase from single pulses to about 10 Hz significantly reduced the duration of the CMUPs in each of the four muscle groups. In subject #3 (**Table 2.2c**) this reduction amounted to 3, 6, 2 and 0.6 ms, for quadriceps, hamstring, tibial anterior and triceps surae, respectively. Thereby, the differences in the latency times contributed less to the decrease in the response duration than the fact that the 10 Hz-CMUPs ended earlier than the single muscle twitch responses. **Fig. 2.6** illustrates how particular peaks within the CMUPs were shifted in time in response to changes of the stimulus frequency. The analysis of those peaks of the CMUPs which were shifted in comparison with the ones which were invariant was not a matter of this study, though it might give some insights into the mechanisms underlying the observed "synchronisation" within the responses.

The analysis of the recordings where the subject's lower limbs were initially placed in flexed position was restricted to the thigh muscles as there was no information available on any ankle extension (foot plantar flexion) movement that might have been induced by the stimulation. (The ankle joint was not instrumented, and the foot was not placed in dorsiflexed position prior to the stimulation.) At this stage of the study, we were primarily interested in whether the content of the responses observed during implemented extension depended on the initial position of the leg.

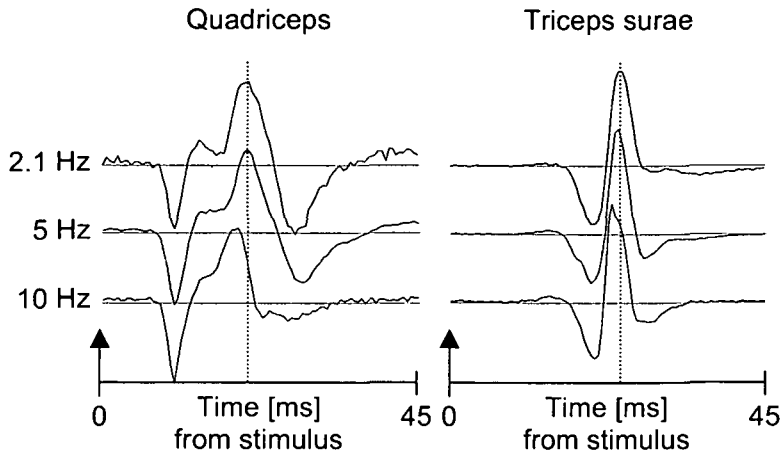

Fig. 2.6. SCS-induced synchronisation of motor unit activity. Average CMUP responses recorded during SCS at 2.1 Hz, and during implemented lower limb extension induced at 5 and 10 Hz, respectively. Within each muscle group, responses to different stimulus frequencies have been normalised to the same peak-to-peak amplitude. Subject #3/session #1, stimulus strength: 10 V, stimulating cathode at L3/4 segmental level.

The data analysis revealed that, regardless of the initial position of the lower limbs, the EMG responses in quadriceps and hamstring remained fairly constant as soon as the extension of the limb was fully implemented. During this phase, the shape of the observed CMUPs was more or less the same for both initial conditions. However, this needed not be the case for their latency time and duration. In some recordings, the responses observed in quadriceps and/or hamstring during implemented extension started later and were shorter when the lower limbs were initially flexed, as compared to the other initial condition (**Table 2.3**). Again, this reduction of the response duration went along with particular peaks of the CMUPs being shifted towards shorter latency times. In other recordings, however, the described effect of the "history" of the implemented extension (limb *movement* from flexed to extended position vs. limb already fully extended) was not found.

Taken together, the frequency of the externally applied stimulus train had a significant influence on the duration of the CMUPs recorded in the lower limb muscles in response to the stimulation. Increasing the stimulus frequency to a level of 5–10 Hz resulted in a reduction of the response duration, particularly in the thigh muscles. In some cases, this reduction ("synchronisation") was even more pronounced when the extended position of the subject's lower limbs was actively retained after their actual movement from full flexion to extension. Not least this finding led us to analyse the quadriceps and hamstring responses during the externally induced transition of the lower limbs from the fully flexed to the extended position.

2.3.4 Content of the responses during the transition from flexed to extended lower limb position

Comparing the EMG responses recorded during implemented extension with the ones during the preceding transition from the flexed to the extended position of the lower limb, it was most obvious that the shape of the responses changed substantially during the actual extension movement, while they remained fairly constant once the limb was in end position (**Fig. 2.3B**; "transitional" and "steady-state" responses). In the thigh muscles, particularly in quadriceps, the

observed changes were more pronounced than in the leg muscles. In general, the responses recorded in quadriceps at the outset of the extension movement were five- or six-phasic, with their second, third and fourth phases gradually fusing to one phase in the course of the transition. In hamstring, the transitional responses were either tri- or tetra-phasic. In all four muscle groups, the transition from the first CMUP, recorded immediately after the onset of the stimulation, to the steady-state responses appeared "smooth" (**Fig. 2.3B**).

The variations in latency time and duration between the responses recorded during the actual extension movement were much larger than between the ones recorded during implemented extension. However, the majority of the transitional responses in quadriceps and hamstring were significantly longer than the steady-state ones.

2.3.5 Analysis of the temporal changes in the EMG patterns observed during the actual extension movement

When we fitted the simple model (2.1) to a sequence of CMUPs recorded in a given muscle group during the induced transition from the flexed to the extended lower limb position the respective r^2-values frequently amounted to less than 0.8 (**Fig. 2.7A–C**). In other words, the two CMUPs actually recorded at the beginning and end of this transition, respectively, could not explain the whole set of CMUPs but roughly. However, performing a PCA on this set revealed that it *was* two-dimensional. That is, each response observed during the actual extension movement was a weighted sum of only two "components" which were common to the whole sequence of responses. Moreover, after filtering out the "noise" included in these CMUPs, the responses recorded at the beginning and end of the movement, respectively, could be chosen as the common components. Thus, the SCS-induced transition from the flexed to the extended position of the lower limbs was accompanied by the gradual substitution of one CMUP by another. In all four lower limb muscle groups, this explanation yielded an average goodness of fit (r^2-value) above 0.9.

An illustrative example is given in **Fig. 2.7D–F**. The recorded sequence of 20 quadriceps responses could be decomposed into two, with the first one losing and the second one gaining momentum. Note that within each of these sequences, only the amplitude of the CMUPs is modulated while their shape remains unchanged. The first sequence represents the gradual suppression of that CMUP which was observed at the *onset* of the SCS-induced extension movement while the second one depicts the gradual build-up of the CMUP observed at the *end* of this movement. This is also reflected in the corresponding sequences of weighting coefficients. The superimposition of the two processes, which is equivalent to the summation of

— *next page* →

Fig. 2.7. The set of CMUPs recorded during induced lower limb extension is basically two-dimensional. **A**, Sequential CMUP responses recorded in quadriceps during SCS-induced lower limb extension. First response in front; subject #3/session #1, stimulus strength/frequency: 10 V/5 Hz, stimulating cathode at L3/4 segmental level. **B**, Sequential and mean (–·–·–) r^2-values resulting from linear regression of the CMUPs given in **A** on the span of *(i)* the first and 20th responses (◆), and *(ii)* the first two principal components (▲), respectively. **C**, **D**, Approximation of the CMUPs given in **A** by linear regression on the span of *(i)* the first and 20th responses (**C**), and *(ii)* the first two principal components (**D**), respectively. **E**, First resp. 20th of the potentials given in **C** (◆) and **D** (▲) superimposed. The latter (▲) are referred to as the *adjusted CMUP responses*. **F**, Sequences into which the series given in **D** can be decomposed. Note that within each sequence the potentials do not change their shape.

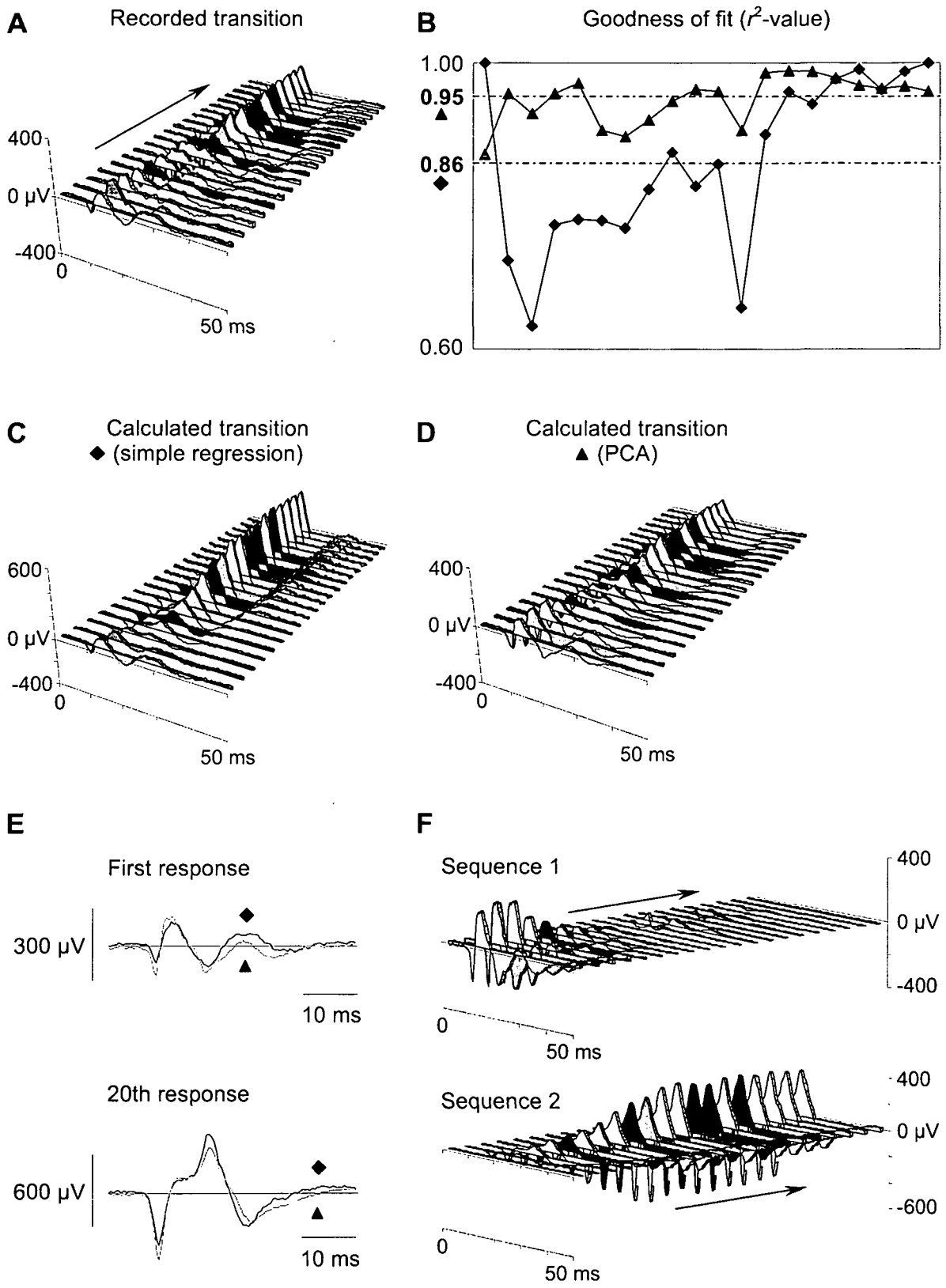
A
Recorded transition
400
0 µV
-400
0
50 ms
B
Goodness of fit (r^2-value)
1.00
0.95
0.86
0.60
C
Calculated transition
◆ (simple regression)
600
0 µV
-400
0
50 ms
D
Calculated transition
▲ (PCA)
400
0 µV
-400
0
50 ms
E
First response
300 µV
10 ms
20th response
600 µV
10 ms
F
Sequence 1
400
0 µV
-400
0
50 ms
Sequence 2
400
0 µV
-600
0
50 ms

the respective CMUPs, gives a good approximation (mean r^2 = 0.95) of the original data recorded during the transition from flexion to extension. Furthermore, the correlation between the processes of suppression and build-up, as verified by Pearson's correlation coefficient, amounts to –0.92.

When we compared the sequences of weighting coefficients obtained in different muscle groups during the *same* recording we found that they were strongly correlated to each other. In **Fig. 2.8** the correlation coefficients between the corresponding weights in quadriceps and hamstring amounted to 0.96 (for the first component) and 0.99 (for the second component), respectively. This observation led us to ask whether it would be possible to explain the whole spatiotemporal CMUP pattern during the SCS-induced extension movement on the basis of two "muscle synergies". We therefore conducted an according PCA, which confirmed this notion (based on a requested mean r^2-value of 0.9). Consequently, the changes observed in different muscle groups followed the same "time course" from the onset of the movement to the steady state.

We also asked if our observations depended on *(i)* the rostrocaudal level of the stimulation, or *(ii)* the stimulus frequency, respectively. As we have already mentioned above, the result of the set of CMUPs during the extension movement being basically two-dimensional was obtained for quite distinct vertebral levels of the stimulating cathode (ranging from T11/12 through lower L1) although the actually revealed components (resp. their span) could differ to some extent. To illustrate this, **Table 2.4** compares the results of a PCA which was separately applied to data recorded in response to T11/12 and L1 stimulation with the ones of the respective simultaneous analysis. When an r^2-value of at least 90 % was demanded, each of the quadriceps CMUP sets for the two spinal levels could be explained on the basis of two components, while a third component was required to explain the variation within the union of these sets. In hamstring, the goodness of fit achieved with two regressors similarly decreased from 99 resp. 97 % to 90 %.

Differences in the number of components to explain sequential CMUPs were also observed in response to different stimulus frequencies. The example given in **Table 2.5** is based on recordings in subject #3 at 5, 10 and 16 Hz while the other stimulation parameters were held constant. The extension movement evoked at 16 Hz was weaker than the ones observed at lower frequencies (67 °, 63 °, and 43 ° at 5, 10, and 16 Hz, respectively). This was accompanied by the fact that more than two (namely four) components essentially contributed to the quadriceps (but not the hamstring) responses recorded at 16 Hz. The according simultaneous analysis confirmed the union of the CMUP sets for 5, 10 and 16 Hz in quadriceps being 4-dimensional. Based on an r^2-value of at least 90 %, an additional (third) component was also found for hamstring. Obviously, the sequential CMUPs recorded at 5, 10 and 16 Hz were *not* composed of the *same*

Table 2.3. Content of the steady-state hamstring responses to SCS at 5 and 10 Hz, comparing different initial conditions

	5 Hz		10 Hz	
	Ext	Fl	Ext	Fl
Latency	12.1 ± 0.3	16.7 * ± 0.3	12 ± 1	16.6 * ± 0.7
End	51 ± 1	36 * ± 2	47.9 ± 0.9	37 * ± 2
Duration	38 ± 1	19 * ± 2	36 ± 1	20 * ± 2

Ext, lower limb initially extended; Fl, lower limb initially flexed. Entries are times in [ms], given as mean ± standard deviation. Recorded in subject #5, stimulus strength: 6 V.

* The change in latency time, response duration etc. as compared to the other initial condition was *significant*.

two components. Taken together, increasing the stimulus frequency beyond 10–15 Hz resulted in the emergence of additional influences on the induced motor unit activity which apparently counteracted the implementation of a sustained lower limb extension.

2.4 Discussion

The presented results may be classified into three categories. First, we have established the relationship between the SCS-induced initiation of a sustained hip/knee extension and the application of particular stimulus parameters (i.e., frequency, strength and segmental level of stimulation). Second, we have elaborated specific features of the steady-state (i.e., temporally stable) EMG responses to SCS at 5–15 Hz which were not observed outside this frequency range. Third, we have analysed the spatiotemporal pattern of CMUP responses during the actual implementation of the evoked extension movement.

As to item one, stimulation of the upper lumbar cord segments such that quadriceps and hamstring respond with single muscle twitches proved sufficient for the initiation of lower limb extension within a certain range of stimulus frequencies. On the other hand, the stimulation ought not to be weaker than required to activate at least one of these muscle groups. Extension was evoked from quite distinct segmental levels ranging from L2/3 through L5/S1. The strength of stimulation determined whether the extension induced at a particular frequency was sustained or eventually replaced by a flexion movement. In general, the range of frequencies effective for a *sustained* extension was broader if weaker stimuli were applied. From lower L5 segmental level, the evoked extension was never "disrupted", even in response to a 50 Hz train.

As to the second point, responses to 5–10 Hz stimulation were of significantly shorter duration than single CMUPs or responses to higher frequencies. With respect to the amount of rectified and integrated EMG activity above baseline, hamstring and triceps surae responses were selectively augmented compared to the ones in quadriceps and tibial anterior as the stimulus frequency approached 5–10 Hz. Outside this range the EMG amplitudes in all four muscle groups decreased as the interstimulus interval was reduced. Finally, the responses during the transition toward the extended lower limb position underwent repeatable morphologic changes. In terms of principal components, the changes in either muscle group were basically two-dimensional. That is, with pretty high accuracy, all transitional CMUPs were built up by the potentials observed at the onset of the movement and when the extension was ultimately implemented. The modulations simultaneously recorded in different muscle groups were highly correlated. Increasing the frequency beyond 15 Hz the temporal EMG pattern in the hip and ankle flexors became more complex (i.e. higher-dimensional) whereas, referring thereto, the extensors remained unaffected in the first instance.

On the basis of these results we hypothesise that *(i)* epidural stimulation of the human lumbosacral cord at 5–15 Hz and sufficient strength induced previously inactive lumbar interneuronal circuits to reorganise and form a "functional unit" [see Hultborn 2001] capable of generating lower limb extension; *(ii)* this extension was not just triggered but dynamically controlled by the newly-established organisation; *(iii)* its effects were plurisegmental—motor unit activity was coordinated between antagonistic thigh and leg muscles; and *(iv)* initiation of extension from either upper or lower lumbosacral cord levels probably share a common mechanism. In the following we are going to justify these hypotheses in detail.

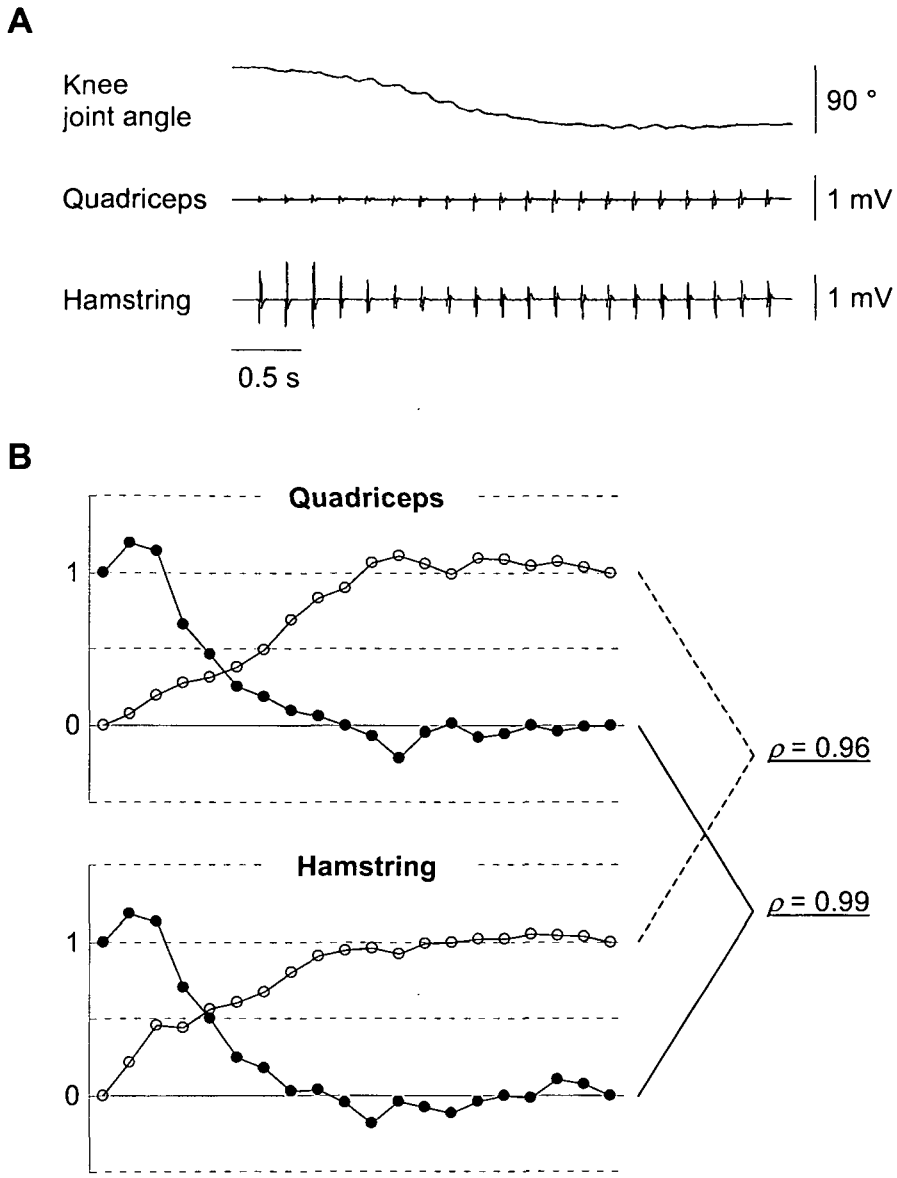

Fig. 2.8. Changes in the content of the CMUPs recorded in quadriceps and hamstring are strongly correlated. **A**, EMG and goniometric recording during SCS-induced lower limb extension. Downward deflexion of the knee joint angle indicates extension. Subject #3/session #1, stimulus strength/frequency: 10 V/5 Hz, stimulating cathode at L3/4 segmental level. **B**, Sequential weighting coefficients of the first (●) and second (O) principal components, which have been calculated *separately* for the quadriceps and hamstring responses given in **A**. ρ, Pearson's correlation coefficient.

2.4.1 Frequency-dependent motor unit synchronisation

Differences in the duration between CMUPs may either be due to variations in (overall) amplitude (while the potentials may share the same shape) or be the consequence of "internal" morphologic differences. Generally, a contribution from both sources has to be taken into account. With the definition of "duration" used in the present study the first possibility has been excluded. However, changes in the shape of EMG-recorded motor unit potentials may have

Table 2.4. Goodness of fit achieved with the individual principal components, comparing responses recorded in two subjects

Subject #3 (sess #1; T11/12; separate PCA)

Q1	65 %	H1	67 %
Q2	26 %	H2	32 %
Q3	3 %	H3	< 1 %

Subject #4 (L1; separate PCA)

Q1	68 %	H1	79 %
Q2	27 %	H2	18 %
Q3	3 %	H3	2 %

Subjects #3 and 4 (simultaneous PCA)

Q1	49 %	H1	53 %
Q2	34 %	H2	37 %
Q3	10 %	H3	7 %

T11/12 and L1, vertebral position of the stimulating cathode; Q1–Q3 and H1–H3, first three principal components calculated separately for quadriceps and hamstring. Stimulus strength/frequency: subject #3, 10 V/5 Hz; subject #4, 5 V/5 Hz. Upper tables: PC analyses performed separately for CMUP sets recorded in subjects #3 and 4. Lower table: PCA performed on the union of these sets.

different origin as well. First, the geometrical relations between the EMG electrodes and the muscle fibres which contribute to the EMG signal determine the actually observed CMUP waveform. The parameters of the volume conductor surrounding the muscle fibres (conductances of muscle and skin, in particular) are decisive as well [Roeleveld *et al.* 1997, Lowery *et al.* 2002]. If varying recording conditions can be ruled out, one has to consider alterations in the time and order at which the contributing motor units had been recruited [Windhorst 1991]. In a simple case, a reduced potential duration results from the omission of individual components at the outset or cessation of the CMUP while its morphology remains constant otherwise. In general, variations in motor unit recruitment will alter the waveform in a more complex manner.

Table 2.5. Goodness of fit achieved with the individual principal components, comparing responses to different stimulus frequencies

5 Hz (separate PCA)

Q1	65 %	H1	67 %
Q2	26 %	H2	32 %
Q3	3 %	H3	< 1 %
Q4	2 %	H4	< 1 %
Q5	1 %	H5	< 1 %

10 Hz (separate PCA)

Q1	73 %	H1	60 %
Q2	19 %	H2	38 %
Q3	6 %	H3	< 1 %
Q4	1 %	H4	< 1 %
Q5	1 %	H5	< 1 %

16 Hz (separate PCA)

Q1	61 %	H1	62 %
Q2	16 %	H2	34 %
Q3	8 %	H3	3 %
Q4	5 %	H4	< 1 %
Q5	2 %	H5	< 1 %

5, 10, and 16 Hz (simultaneous PCA)

Q1	53 %	H1	51 %
Q2	20 %	H2	38 %
Q3	10 %	H3	7 %
Q4	7 %	H4	3 %
Q5	2 %	H5	< 1 %

Q1–Q5 and H1–H5, first five principal components calculated separately for quadriceps and hamstring. Recorded in subject #3/session #1, stimulus strength: 10 V. Upper tables: PC analyses performed separately for CMUP sets recorded at 5–16 Hz. Lower table: PCA performed on the union of these sets.

In the present study, it is very unlikely that the reduction in CMUP duration as the stimulus frequency approached 5–10 Hz was due to changes in the geometrical conditions. In the corresponding recordings, the subjects' lower limbs were initially moved to the point of complete extension, then the stimulation was applied leaving them resting on the examination bed. This procedure was applied independently from the stimulus frequency, and only steady-state responses were included in this part of the study. Thus, differences in the spatiotemporal pattern of motor unit recruitment putatively accounted for the CMUPs observed at 5–10 Hz being shorter than single muscle twitch responses. Consecutive positive or negative phases which appeared separated at 2.1 Hz fused as the stimulus frequency was increased. In parallel, particular peaks were shifted toward shorter latency times, suggesting the reduced duration to result from an increased synchronisation of the activity in the motor units contributing to the EMG-recorded potentials.

Phase-dependent short-term (about 12 ms) synchronisation of activity in different motor units of the same lower limb muscle group has been demonstrated during walking in normal subjects. As verified by cross-correlation analysis, EMG-recorded motor unit discharges were highly synchronised toward the end of the swing phase. During mid swing, in contrast, they were largely asynchronous, which led the authors to suppose "a central physiological process" underlying this kind of phase-dependent modulation [Hansen *et al.* 2001, Halliday *et al.* 2003]. Short-term synchronisation was also observed during weak isometric contractions in lower and upper limb (forearm, hand and finger) muscles [Datta *et al.* 1991, Kakuda *et al.* 1999, Kilner *et al.* 1999, Kim *et al.* 2001; reviewed by Farmer 1998]. It was more pronounced when the muscle was activated in co-contraction rather than in an isolated agonist movement [Nielsen and Kagamihara 1994, see also Kilner *et al.* 1999]. Thereby, corticospinal tract fibres, or fibres which intimately depend on their function, appeared to play a significant role—as indicated by studies in subjects with central nervous lesions [Datta *et al.* 1991, Farmer *et al.* 1993]. Synchrony of voluntarily controlled discharges in extensor digitorum communis was preserved in clinically complete paraplegics, but it was absent in tibial anterior in response to reflex excitation [Davey *et al.* 1990]. This was explained by the severance of branched descending tract fibres directly projecting onto the motoneuronal pools or last-order interneurones under normal conditions [see also Kim *et al.* 2001]. In principle, however, the joint arrival of EPSPs which underlies motor unit synchronisation could also be accomplished via sufficiently branching segmental pathways [Hansen *et al.* 2001]. In cats, increased segmental afferent input was shown to promote short-term synchronisation [Ellaway and Murthy 1985].

As to the synchronisation of motor unit activity which accompanied the SCS-induced lower limb extension, we therefore arrived at the following hypothesis: Applying a train of electric stimuli at a frequency of 5–10 Hz to the lumbosacral cord not just evoked monosynaptic PRMRRs [Rattay *et al.* 2003, Minassian *et al.* 2003] but also induced the lumbar interneuronal network to exert a synchronising influence on the motoneuronal pools related to the lower limb muscles. Appropriate functional configuration of the internuncial circuitry was triggered via collaterals of the afferents primarily activated by the epidural stimulation. This explanation extends our previous suggestion of "the same afferent volleys being synaptically transmitted to spinal interneurones, which set up the relation in responsiveness between flexor and extensor motor nuclei to attain lower limb extension" [Jilge *et al.* 2003]. Configuration of the lumbar interneuronal system into functional units for lower limb extension was not induced unless a specific "code" (here: interstimulus interval) was provided. This has been demonstrated not least by the fact that both the initiation of extension and increased motor unit synchronisation depended on particular stimulus frequencies to be applied.

2.4.2 Frequency-dependent selective augmentation of extensor activity

With respect to the amount of induced CMUP activity, antagonistic muscle groups responded differently to the common input provided by SCS. This observation provides another clue to a newly-established "central" organisation generating lower limb extension. Let us suppose for a moment that hamstring was subject to stronger artificial input than quadriceps, and that this difference accounted for the extensors exhibiting larger EMG output than then flexors. Does this assumption explain why this dominance was greatly increased in response to stimulus frequencies of 5–10 Hz, and why it was reversed in the ankle antagonists at 35 Hz and above? Obviously, it does not. Two alternatives have previously been considered as possible explanations for the higher forces in the antigravity muscles during induced lower limb extension. First, the same stimulus strength would activate extensors stronger than flexors due to the inherent properties of the respective monosynaptic reflex arcs. Second, the same level of input to the muscle fibres would result in the extensors generating larger forces than the flexor muscles [see Jilge *et al.* 2003]. However, as the dominance of extensor activity was strongly determined by the applied stimulus frequency, these alternatives appear equally inadequate.

It is therefore much more likely that epidural stimulation at 5–10 Hz initiated the reorganisation of lumbar interneuronal circuits to form a system capable of recruiting a larger population of motor units in the extensor than in the flexor muscles. Stronger stimuli probably recruited a larger number of those afferents the activation of which reinforces the process of network configuration. This is indicated by an even more pronounced augmentation of extensor activity as the stimulus strength was stepped up. Unfortunately, the available data did not include whether an extension movement (i.e. foot plantar flexion) was also induced at the ankle joint. At least, as in the thigh muscles, the CMUP activity in triceps surae *was* augmented (as compared to tibial anterior) in response to a stimulus train at 5–10 Hz.

2.4.3 Changes in motor unit recruitment as the induced movement unfolded

During the SCS-induced transition of the lower limbs from the flexed to the extended position the initial shape of the CMUPs recorded in the thigh and leg muscles is gradually replaced by another. Although, in particular, changing muscle fibre length contributes to morphologic alterations [Gerilovsky *et al.* 1977, Dumitru and King 1999], it has been argued that varying geometrical relations (see *Frequency-dependent motor unit synchronisation*) cannot solely account for the observed modulations [Jilge *et al.* 2003]. Comparable temporal modulations, which resulted in prolonged latency times in that case, were previously found during epidurally evoked rhythmical, stepping-like EMG activity [Minassian *et al.* 2003].

For the present study, we conclude (as above) that the spatiotemporal pattern according to which motor units of the lower limbs were recruited changed as the movement unfolded. Moreover, we speculate that this process can be explained on the basis of Henneman's [1999] size principle. That is, the afferents which are primarily activated by epidural stimulation of the lumbar cord (i.e., large group I afferents from the lower limb muscles) predominantly project to fast-twitch (so-called 'type II') motor units [Desmedt 1983, Loeb and Ghez 2000]. The CMUPs recorded at the beginning of the induced movement putatively arose from motor units of that type, which are mobilised to implement strong and brisk movements. Later on, when the limb was in end position, retention of this position and joint stabilisation required lower forces, which are usually provided by slow-twitch ('type I') motor units. Presumably, the observed morphologic changes reflect the gradual transition from 'type II' to 'type I' motor units.

Regardless of the type of motor units actually involved, the temporal changes observed in different (synergistic and antagonistic) muscle groups being highly correlated suggests that a common "central" mechanism was activated (by the stimulation) which not just triggered but actively controlled the SCS-evoked extension. As soon as the movement was completed and the lower limb was in extended position, the recorded CMUPs revealed remarkably constant latency times, duration and shape. Given that these potentials reflected individual muscle reflex responses, such stability in neurophysiological parameters requires a high degree of organisation within the ensemble of the involved neuronal structures. Thus, the above "central mechanism" may be the consequence of a configuration process within the lumbar interneuronal network toward a new, stable organisation which was initiated by the external stimulation.

2.4.4 Reciprocal relation between stimulus strengths and frequencies inducing a sustained lower limb extension

As described above, the initiation of a hip/knee extension was closely related to the activation of the quadriceps and/or hamstring muscles. Both theoretical [Rattay *et al.* 2000] and clinical [Minassian *et al.* 2003] studies have revealed the respective muscle twitch thresholds to be lower if stimulation was applied at lower lumbar or upper sacral cord levels as compared to L1–L3 stimulation. This would explain why lower stimulus intensities were sufficient to induce lower limb extension from lower L5 segmental level.

One might consider different mechanisms to contribute to the extension movements we observed, depending on whether the upper or lower lumbar cord was stimulated. It may be an inherent property of the lumbar cord to adopt a "hip strategy" when the upper segments are stimulated and an "ankle strategy" when the lower segments are stimulated. According to the half-center model for locomotor rhythm generation [reviewed in Orlovsky *et al.* 1999], such a "hip strategy" would involve augmenting the output of the extensor half-center, whereas the "ankle strategy" would correspond to the extension known to be evoked at that point of the step cycle where the heel of the swinging leg hits the ground and becomes the center of weight bearing [Harkema *et al.* 1997, Pearson and Collins 1993].

On the one hand, studies in incomplete SCI subjects verify that the ankle strategy adopted when the foot touches the floor during externally induced stepping can be very powerful [Pinter *et al.* 1998]. During walking in humans with intact nervous system, the activity of group Ia afferents increases when the ankle extensors are lengthening at the beginning of the stance phase, and short latency pathways open in both directions between extensors of the knee and ankle [Brooke and McIlroy 1985]. Facilitation from ankle to knee in the resting human has been reported by Pierrot-Deseilligny *et al.* [1981, 1983] and Mao *et al.* [1983]. On the other hand, upper lumbar cord segments can be activated via their dorsal roots by electrically stimulating the cauda equina. This stimulation pathway has to do with the rostrocaudal parallel orientation of the dorsal root trajectories at this level, combined with the properties of the electric field applied [Maertens de Noordhout *et al.* 1988].

However, the present study brought about basically the same findings regardless of the rostrocaudal position of the stimulating cathode over the lumbosacral cord. Thereby, we particularly refer to the reduced CMUP duration and the selective augmentation of extensor activity in response to stimulus frequencies of 5–10 Hz, the low dimensionality of the transitional responses as the induced movement unfolded, and the large amount of correlation between the changes observed in different muscle groups during this transition. It is therefore unlikely that entirely separate mechanisms accounted for the evoked extension movements.

Moreover, independent from the segmental level of the stimulation (keeping the same constant), the so-called 'flexion threshold' frequency was lower as stronger stimuli were applied. While in **Fig. 2.3C** the extension induced at 4 V was sustained over the whole range of frequencies tested (5–50 Hz), it was disrupted by a flexion of the limb in response to 9 V and 16 Hz (and above). In our previous studies, SCS-induced stepping-like movements were usually preceded by such a 're-flexion' [Jilge *et al.* 2003]. A corresponding result has been reported by Dimitrijevic *et al.* [1998] who investigated the effect of epidural lumbar cord stimulation with respect to the initiation of stepping-like movements. In their Fig. 4, the authors gave an example in which 30 Hz stimulation of the upper lumbar cord at 4.5 V resulted in an EMG "extension pattern" of the lower limbs which turned rhythmical as the stimulus strength was increased to 5 V.

May we speculate that the above re-flexion—and subsequent rhythmical movements—of the lower limbs were not evoked until a certain minimum amount of synaptic current was provided to the lumbar interneuronal network? Thereby, it may have been less important whether this current was accumulated by spatial or temporal summation. Stepping up the intensity of the stimulation increased the number of recruited afferents [Minassian *et al.* 2003] and may thus have enhanced the amount of spatially summated current. On the other hand, reducing the interstimulus interval may have promoted temporal summation. However, currently only vague hints to this matter are available. Further examination of the stimulation parameters' physiological "meaning" is necessary until a conclusive answer to this question can be given.

In contrast to upper lumbar cord stimulation, re-flexion was never initiated from lower L5 segmental level—although quadriceps and hamstring were activated (e.g., ~2 V above the muscle twitch thresholds) under both conditions. This observation underlines once more the different requirements for evoking extension and flexion movements, respectively, by SCS. To initiate rhythmical, locomotor-like EMG activity in complete SCI subjects it has been shown to be crucial that the electric stimuli be applied over the second lumbar cord segment. Deviation from L2 readily resulted in a synchronous rather than an alternating activation of antagonistic muscle groups [Dimitrijevic *et al.* 1998]. In fact, the relative effect of the applied electric field on primary afferents on different cord segments strongly depends on the rostro-caudal level of stimulation. Distinct levels may result in quite different spatial (i.e. plurisegmental) patterns of dorsal root fibre recruitment [Minassian *et al.* 2003]. However, the importance of activating the afferents of a particular segment in the generation of SCS-induced movements is not understood yet. Unfortunately, recordings in which, for example, hamstring was but quadriceps was not activated by the stimulus train were not available in the present study. Moreover, the relevance of ("subthreshold") stimulation which does not directly evoke muscle twitches remains to be investigated.

Appendix: Principal component analysis of the temporal EMG patterns

A1 Analysis of the output of a single EMG channel

A system of linear regression models

Having divided the recording from a single EMG channel into successive time windows (of equal length) in such a way that the margins of the windows indicate when the external stimuli were applied, let p and $y_{1j},\ldots,y_{nj}$ denote the number of time windows obtained, and the values

(i.e. n samples, $n > p$) of the EMG potential within the j-th window, respectively. Let furthermore

$$x_{ij} = \frac{y_{ij} - \bar{y}_j}{\sqrt{s_j^2}} \quad \text{with} \quad \bar{y}_j = \frac{1}{n}\sum_{k=1}^{n} y_{kj} \quad \text{and} \quad s_j^2 = \frac{1}{n-1}\sum_{k=1}^{n}(y_{kj} - \bar{y}_j)^2$$

i.e., $x_{1j},\ldots,x_{nj}$ are obtained from $y_{1j},\ldots,y_{nj}$ by standardisation. In the following we assume that it is possible to decompose the $n \times p$-matrix $X = (x_{ij})$ as

$$X = Z_m V_m + U \tag{A1a}$$

where $Z_m = (z_{ik})$, $V_m = (v_{kj})$ and $U = (u_{ij})$ are suitable, yet unknown matrices of the dimensions $n \times m$, $m \times p$ and $n \times p$, respectively. With

$$\mathbf{x}_j = \begin{pmatrix} x_{1j} \\ \vdots \\ x_{nj} \end{pmatrix}; \quad \mathbf{v}_j^{(m)} = \begin{pmatrix} v_{1j} \\ \vdots \\ v_{mj} \end{pmatrix} \quad \text{and} \quad \mathbf{u}_j = \begin{pmatrix} u_{1j} \\ \vdots \\ u_{nj} \end{pmatrix}$$

for $j = 1,\ldots,p$, (A1a) can be regarded as a system of p classical linear regression models involving the same regressors,

$$\begin{aligned} \mathbf{x}_1 &= Z_m \mathbf{v}_1^{(m)} + \mathbf{u}_1 \\ &\vdots \\ \mathbf{x}_p &= Z_m \mathbf{v}_p^{(m)} + \mathbf{u}_p \end{aligned} \tag{A1b}$$

However, at this point of the analysis appropriate regressors

$$\mathbf{z}_k = \begin{pmatrix} z_{1k} \\ \vdots \\ z_{nk} \end{pmatrix}, \quad k = 1,\ldots,m$$

which secure a high goodness of fit (as documented by the value of the r^2-statistic—see below) remain to be determined. We even do not know the smallest *number* of regressors required to achieve a given r^2-value α. Note that it *is* possible to represent X with maximum accuracy (i.e. with $r^2 = 1$) as an affine (i.e. inhomogeneous) linear combination if $m = p$ regressors are used: $X = XE + O$ where E and O denote the unit and zero matrices, respectively. For $\alpha < 1$, $m < p$ regressors may be sufficient.

Definition of orthogonal regressors

As a method to find a small number of regressors securing a given r^2-value we use the principal component analysis [Timischl 2000]. This method starts with the trivial solution $X = XE$, which is equivalent to the vectors $\mathbf{x}_i = (x_{i1}, \cdots, x_{ip})$ being represented as linear combinations of the elements $\mathbf{e}_1 = (1,0,\cdots,0)$; ...; $\mathbf{e}_p = (0,\cdots,0,1)$ of the canonical basis $\mathfrak{B}$ of $\mathbf{R}^p$,

$$\mathbf{x}_i = \sum_{j=1}^{p} x_{ij}\,\mathbf{e}_j, \quad i = 1,\ldots,n. \tag{A2}$$

In general, giving up one of these regressors results in a considerable worsening of the r^2-value. One therefore seeks to improve the situation by changing from $\mathfrak{B}$ to another basis $\mathfrak{B}^*$ which allows to leave some of the regressors out without the GOF dropping to a level below α. In the following we are going to describe how to find the new basis $\mathfrak{B}^*$.

Let R denote the $p \times p$-sample correlation matrix of the columns of X, i.e.

$$R = \frac{1}{n-1} X^T X.$$

As R is symmetric, all its eigenvalues are real numbers; they are non-negative, and there are p eigenvectors $\mathbf{v}_1 = (v_{11}, \cdots, v_{1p})$;...; $\mathbf{v}_p = (v_{p1}, \cdots, v_{pp})$ of R which form an orthonormal (ON) basis of $\mathbf{R}^p$. Note that in the case of p different eigenvalues $\lambda_1,\ldots,\lambda_p$ of R, the eigenvectors with length 1 are unique except for their orientation. Let us assume that $\det V > 0$ where $V = (v_{kj})_{k=1,\ldots,p;\,j=1,\ldots,p}$. With $\mathfrak{B}^* = \{\mathbf{v}_1,\ldots,\mathbf{v}_p\}$ this means that the change from $\mathfrak{B}$ to $\mathfrak{B}^*$ describes a rotation of $\mathbf{R}^p$.

With respect to $\mathfrak{B}^*$ the vectors $\mathbf{x}_i$ have new coordinates,

$$\mathbf{x}_i = \sum_{k=1}^{p} z_{ik}\,\mathbf{v}_k, \quad i = 1,\ldots,n, \tag{A3a}$$

which is, with $Z = (z_{ik})$, equivalent to

$$X = ZV. \tag{A3b}$$

As V is orthogonal, i.e. $V^{-1} = V^T$, the assumption $R\,\mathbf{v}_k^T = \lambda_k\,\mathbf{v}_k^T$ (for all $k = 1,\ldots,p$) implies

$$Z = XV^T, \quad \mathbf{z}_k = X\,\mathbf{v}_k^T \tag{A4}$$

and

$$\mathbf{z}_i^T \mathbf{z}_k = \mathbf{v}_i X^T X \mathbf{v}_k^T = (n-1)\mathbf{v}_i R \mathbf{v}_k^T = (n-1)\lambda_j \mathbf{v}_i \mathbf{v}_k^T = (n-1)\lambda_j \delta_{ik} \tag{A5}$$

where δ_{ik} denotes Kronecker's symbol ($\delta_{ik} = 0$ if $i \neq k, \delta_{kk} = 1$). This means that the columns of Z are orthogonal. In the literature, these columns are usually referred to as the *principal components* of the matrix X or the *common components* of the columns of X.

Smallest number of regressors required to achieve a given goodness of fit

Defining for each natural number $m < p$ and $j = 1,\ldots,p$

$$Z_m = \begin{pmatrix} z_{11} & \vdots & \cdots & \vdots & z_{1m} \\ \vdots & & & & \vdots \\ z_{n1} & & & & z_{nm} \end{pmatrix} = \begin{pmatrix} \mathbf{z}_1 & \vdots & \cdots & \vdots & \mathbf{z}_m \end{pmatrix}; \qquad \mathbf{v}_j^{(m)} = \begin{pmatrix} v_{1j} \\ \vdots \\ v_{mj} \end{pmatrix}; \qquad \mathbf{x}_j^{(m)} = Z_m \mathbf{v}_j^{(m)}$$

as well as

$$b_j(m) = \frac{\mathbf{x}_j^{(m)T} \mathbf{x}_j^{(m)}}{\mathbf{x}_j^T \mathbf{x}_j} \quad \text{and} \quad \bar{b}(m) = \frac{1}{p}\sum_{j=1}^{p} b_j(m)$$

for the r^2-value of the regression problem

$$\mathbf{x}_j = Z_m \mathbf{v}_j^{(m)} + \mathbf{u}_j$$

and the mean over these values, respectively, one can easily find that

$$b_j(m) = \sum_{k=1}^{m} v_{kj}^2 \lambda_k \tag{A6}$$

and

$$\bar{b}(m) = \frac{1}{p}\sum_{j=1}^{p}\sum_{k=1}^{m} v_{kj}^2 \lambda_k = \frac{1}{p}\sum_{k=1}^{m}\sum_{j=1}^{p} v_{kj}^2 \lambda_k = \frac{1}{p}\sum_{k=1}^{m}\left(\lambda_k \sum_{j=1}^{p} v_{kj}^2\right) = \frac{\lambda_1 + \ldots + \lambda_m}{p}. \tag{A7}$$

This means that the average goodness of fit achieved if the m regressors $\mathbf{z}_1,\ldots,\mathbf{z}_m$ are used, is equal to the proportion of $p = \lambda_1 + \ldots + \lambda_p$ which is made up by the corresponding m eigenvalues of the correlation matrix R. (Note that the $\mathbf{v}_k$ have unit length, i.e. $\Sigma_{j=1,\ldots,p} v_{kj}^2 = 1$ for all $k = 1,\ldots,m,\ldots,p$.) In order to secure an accuracy of α the smallest number m of regressors to be chosen from the set $\{\mathbf{z}_1,\ldots,\mathbf{z}_m\}$ will consequently be such that

$$\frac{\lambda_1 + \ldots + \lambda_m}{p} < \alpha, \tag{A8}$$

if $\lambda_1 \geq \lambda_2 \geq \ldots \geq \lambda_p$.

Additional remarks

The achieved r^2-value does not change if one uses m linearly independent linear combinations of $\mathbf{z}_1, \ldots, \mathbf{z}_m$ instead. E.g., in those cases of the present study when only 2 regressors were required we used

$$\mathbf{x}_1^{(2)} = Z_2\, \mathbf{v}_1^{(2)} \quad \text{and} \quad \mathbf{x}_p^{(2)} = Z_2\, \mathbf{v}_p^{(2)} \tag{A9}$$

instead of the principal components $\mathbf{z}_1$ and $\mathbf{z}_2$. In general, if one replaces $\mathbf{z}_1, \ldots, \mathbf{z}_m$ by $\mathbf{a}_1, \ldots, \mathbf{a}_m$,

$$\left(\mathbf{a}_1 \;\vdots\; \cdots \;\vdots\; \mathbf{a}_m \right) = W \left(\mathbf{z}_1 \;\vdots\; \cdots \;\vdots\; \mathbf{z}_m \right), \tag{A10}$$

with W being invertible, the weights $\mathbf{v}_j^{(m)}$, $j = 1, \ldots, p$, convert to $W^{-1}\, \mathbf{v}_j^{(m)}$. Note that, in (A9), W is a sub-matrix of V, namely

$$W = \left(\mathbf{v}_1^{(2)} \;\vdots\; \mathbf{v}_p^{(2)} \right). \tag{A11}$$

In terms of the original EMG data $y_{1j}, \ldots, y_{nj}$, $j = 1, \ldots, p$, (A1) finally becomes

$$\begin{aligned} \mathbf{y}_1 &= \sqrt{s_1^2}\, Z_m\, \mathbf{v}_1^{(m)} + \sqrt{s_1^2}\, \mathbf{u}_1 + \overline{\mathbf{y}}_1 \\ &\vdots \\ \mathbf{y}_p &= \sqrt{s_p^2}\, Z_m\, \mathbf{v}_p^{(m)} + \sqrt{s_p^2}\, \mathbf{u}_p + \overline{\mathbf{y}}_p \end{aligned} \tag{A12a}$$

where

$$\overline{\mathbf{y}}_j = \begin{pmatrix} \overline{y}_j \\ \vdots \\ \overline{y}_j \end{pmatrix} \in \mathbf{R}^n. \tag{A12b}$$

By definition, the r^2-values with respect to the original "coordinates" are equal to the $b_j(m)$.

A2 Analysis of muscle synergies

To examine if the temporal changes in the CMUP patterns of different muscle groups were correlated to each other we performed the principal component analysis *simultaneously* on the EMG recordings of these muscle groups. Details of this approach will be described in the following.

If $(\mathbf{y}_K)_j \in \mathbf{R}^n$ denotes the samples (within the j-th time window) of the EMG potential recorded from muscle group $\#K$, and if there are L muscle groups to be analysed simultaneously,

$$Y = \begin{pmatrix} (\mathbf{y}_1)_1 & \cdots & (\mathbf{y}_1)_p \\ \vdots & \ddots & \vdots \\ (\mathbf{y}_L)_1 & \cdots & (\mathbf{y}_L)_p \end{pmatrix},$$

we are looking for a decomposition

$$X = Z_m V_m + U \tag{A13a}$$

of the matrix X which is, as above, obtained from Y by standardisation of its columns. Note that X is of the dimension $nL \times p$ since the values of the EMG potentials recorded in different muscle groups have been arranged one below the other. On the other hand, solving (A13) is equivalent to decomposing the sub-matrices X_K, $K = 1,\ldots,L$, consisting of the 1st n, the 2nd n, …, and the last n rows of X into

$$\begin{aligned} X_1 &= (Z_1)_m (V_1)_m + U_1 \\ &\vdots \\ X_L &= (Z_L)_m (V_L)_m + U_L \end{aligned} \tag{A14a}$$

under the restriction that

$$(V_1)_m = (V_2)_m = \ldots = (V_L)_m. \tag{A14b}$$

Applying the method which has been described in the previous section will therefore give representations

$$(\mathbf{y}_K)_j = \alpha_j \begin{pmatrix} (z_K)_{11} & \vdots & \cdots & \vdots & (z_K)_{1m} \\ \vdots & & & & \vdots \\ (z_K)_{n1} & & & & (z_K)_{nm} \end{pmatrix} \begin{pmatrix} v_{1j} \\ \vdots \\ v_{mj} \end{pmatrix} + \beta_j \begin{pmatrix} (u_K)_{1j} \\ \vdots \\ (u_K)_{nj} \end{pmatrix} \tag{A15}$$

for $j = 1,\ldots,p$ and $K = 1,\ldots,L$ using the same sequence of weighting coefficients for the muscle groups #1–L although the corresponding principal components may be very different. In this communication we refer to the columns

$$\begin{pmatrix} (\mathbf{z}_1)_j \\ \vdots \\ (\mathbf{z}_L)_j \end{pmatrix}, \quad j = 1,\ldots,p, \quad \text{where } (\mathbf{z}_K)_j = \begin{pmatrix} (z_K)_{1j} \\ \vdots \\ (z_K)_{nj} \end{pmatrix} \quad \text{for } K = 1,\ldots,L,$$

which include the respective principal components of all L muscle groups, as 'muscle synergies'.

Acknowledgements. We gratefully acknowledge the funding supports from the Austrian Science Fund (FWF research project P15469), and the Kent Waldrep National Paralysis Foundation in Addison, Texas, USA.

References

Brooke JD, McIlroy WE (1985) Locomotor limb synergism through short latency afferent links. Electroenceph clin Neurophysiol 60: 39–45

Burke RE (1999) The use of state-dependent modulation of spinal reflexes as a tool to investigate the organization of spinal interneurons. Exp Brain Res 128: 263–277

Burke RE, Degtyarenko AM, Simon ES (2001) Patterns of locomotor drive to motoneurons and last-order interneurons: Clues to the structure of the CPG. J Neurophysiol 86: 447–462

Datta AK, Farmer SF, Stephens JA (1991) Central nervous pathways underlying synchronization of human motor unit firing studied during voluntary contractions. J Physiol 432.1: 401–425

Davey NJ, Ellaway PH, Friedland CL, Short DJ (1990) Motor unit discharge characteristics and short term synchrony in paraplegic humans. J Neurol Neurosurg Psychiatry 53(9): 764–769

Dekin MS (1991) Comparative neurobiology of invertebrate motor systems: Implications for the control of breathing in mammals. In: Haddad GG, Farber J (eds) Development Neurobiology of the Control of Breathing. Dekker, New York, pp 111–154

Delcomyn F (1980) Neural basis of rhythmic behavior in animals. Science 210: 492–498

Desmedt JE (1983) Size principle of motoneuron recruitment and the calibration of muscle force and speed in man. In: Desmedt JE (ed) Motor Control Mechanisms in Health and Disease. Raven Press, New York, pp 227–251

Dimitrijevic MR (1994) Motor control in chronic spinal cord injury patients. Scand J Rehabil Med Suppl 30:53–62

Dimitrijevic MR, Gerasimenko Y, Pinter MM (1998) Evidence for a spinal central pattern generator in humans. In: Kien O, Harris-Warrick RM, Jordan L, Hultborn H, Kudo N (eds) Neuronal Mechanism for Generating Locomotor Activity. Annals of the New York Academy of Sciences, vol 860, pp 360–376

Dimitrijevic MR, Nathan PW (1967) Studies of spasticity in man. 1. Some features of spasticity. Brain 90:1–30

Dumitru D, King JC (1999) Motor unit action potential duration and muscle length. Muscle Nerve 22: 1188–1195

Ellaway PH, Murthy KSK (1985) The source and distribution of short term synchrony between gamma motoneurones in the cat. Q J Exp Physiol 70: 233–247

Farmer SF, Swash M, Ingram DA, Stephens JA (1993) Changes in motor unit synchronization following central nervous lesions in man. J Physiol 463: 83–105

Farmer SF (1998) Rhythmicity, synchronization and binding in humans and primate motor systems. J Physiol 509.1: 3–14

Feldman JL (1986) Neurophysiology of respiration in mammals. In: Bloom FE (ed) Handbook of Physiology, Section 1: The Nervous System, Am Physiol Soc, Bethesda, vol 4, pp 463–524

Gerilovsky L, Gydikov A, Radicheva N (1977) Changes in the shape of the extraterritorial potentials of tonic motor units, M- and H-responses of triceps surae muscles at different muscle lengths and under conditions of voluntary activation. Exp Neurol 56: 91–101

Getting PA (1986) Understanding central pattern generators: insights gained from the study of invertebrate systems. In: Grillner S, Stein PSG, Stuart DG, Forssberg H, Herman RM (eds) Neurobiology of Vertebrate Locomotion. Macmillan, Hong Kong, pp 231–244

Getting PA (1988) Comparative analysis of invertebrate central pattern generators. In: Cohen AH, Rossignol S, Grillner S (eds) Neural Control of Rhythmic Movements in Vertebrates. Wiley, New York, pp 101–128

Grillner S (1981) Control of locomotion in bipeds, tetrapods and fish. In: Brooks VB (ed) Handbook of Physiology, Section 1: The Nervous System, Motor Control. Am Physiol Soc, Bethesda, vol 2, pp 1179–1236

Grillner S (1985) Neurobiological bases of rhythmic motor acts in vertebrates. Science 228: 143–149

Grillner S, Cangiano L, Hu GY, Thompson R, Hill R, Wallén P (2000) The intrinsic function of a motor system – from ion channels to networks and behavior. Brain Res 886: 224–236

Grillner S, Wallén P (1985) Central pattern generators for locomotion, with special reference to vertebrates. Annu Rev Neurosci 8: 233–261

Halliday DM, Conway BA, Christensen LOD, Hansen NL, Petersen NP, Nielsen JB (2003) Functional coupling of motor units is modulated during walking in human subjects. J Neurophysiol 89(2): 960–968

Hansen NL, Hansen S, Christensen LOD, Petersen NT, Nielsen JB (2001) Synchronization of lower limb motor unit activity during walking in human subjects. J Neurophysiol 86: 1266–1276

Harkema SJ, Hurley SL, Patel UK, Requejo PS, Dobkin BH, Edgerton VR (1997) Human lumbosacral spinal cord interprets loading during stepping. J Neurophysiol 77: 797–811

Henneman E (1999) The size-principle. In: Adelman G, Smith BH. Encyclopedia of Neuroscience, 2nd Edition. Elsevier, pp 1868–1871

Hultborn H (2001) State-dependent modulation of sensory feedback. J Physiol 533.1: 5–13

Jilge B, Minassian K, Rattay F, Pinter MM, Gerstenbrand F, Binder H, Dimitrijevic MR (2003) Initiating extension of the lower limbs in subjects with complete spinal cord injury by epidural lumbar cord stimulation. Exp Brain Res (in press)

Kakuda N, Nagaoka M, Wessberg J (1999) Common modulation of motor unit pairs during slow wrist movement in man. J Physiol 520.3: 929–940

Kennedy D, Davis WJ (1977) Organization of invertebrate motor systems. In: Geiger SR, Kandel ER, Brookhart JM, Mountcastle VB (eds) Handbook of Physiology, Section I, Part 2. Am Physiol Soc, Bethesda, vol 1, pp 1023–1087

Kien O, Kjaerulff O (1998) Distribution of central pattern generators for rhythmic motor outputs in the spinal cord of limbed vertebrates. In: Kien O, Harris-Warrick RM, Jordan L, Hultborn H, Kudo N (eds) Neuronal Mechanism for Generating Locomotor Activity. Annals of the New York Academy of Sciences, vol 860, pp 110–129

Kilner JM, Baker SN, Salenius S, Jousmäki V, Hari R, Lemon RN (1999) Task-dependent modulation of 15–30 Hz coherence between rectified EMGs from human hand and forearm muscles. J Physiol 516.2: 559–570

Kim MS, Masakado Y, Tomita Y, Chino N, Pae YS, Lee K (2001) Synchronization of single motor units during voluntary contractions in the upper and lower extremities. Clin Neurophysiol 112: 1243–1249

Kuhn R (1950) Functional capacity of the isolated human spinal cord. Brain 1:1–51

Loeb GE, Ghez C (2000) The motor unit and muscle action. In: Butler J, Lebowitz H (eds) Principles of Neural Science, 4th Edition. McGraw-Hill, pp 674–694

Lowery MM, Stoykov NS, Taflove A, Kuiken TA (2002) A multi-layer finite-element model of the surface EMG signal. IEEE Trans Biomed Eng 49(5): 446–454

Mao CC, Ashby P, Wang M, McCrea D (1983) Synaptic connection from muscle afferents to the motoneurones of various leg muscles in man. Electroenceph clin Neurophysiol 56: 130

McCrea DA (2001) Spinal circuitry of sensorimotor control of locomotion. J Physiol 533.1: 41–50

Minassian K, Jilge B, Rattay F, Pinter MM, Binder H, Gerstenbrand F, Dimitrijevic MR (2003) Stepping-like movements in humans with complete spinal cord injury induced by epidural stimulation of the lumbar cord: Electromyographic study of compound muscle action potentials. Spinal cord (submitted)

Nielsen J, Kagamihara Y (1994) Synchronization of human leg motor units during co-contraction in man. Exp Brain Res 102(1): 84–94

Orlovsky GN, Deliagina TG, Grillner S (1999) Limb Controller. In: Neuronal Control of Locomotion. From Mollusc to Man. Oxford University Press, pp 175–204

Pearson KG (1993) Common principles of motor control in vertebrates and invertebrates. Annu Rev Neurosci 16: 265–297

Pearson KG (2000) Neural adaptation in the generation of rhythmic behavior. Annu Rev Physiol 62: 723–753

Pearson KG, Collins DF (1993) Reversal of the influence of group Ib afferents from plantaris on activity in medial gastrocnemius muscle during locomotor activity. J Neurophysiol 70: 1009–1017

Pierrot-Deseilligny E (1983) Reflex control of bipedal gait. In: Desmedt JE (ed) Motor Control Mechanisms in Health and Disease. Raven, New York, pp 699–716

Pierrot-Deseilligny E, Morin C, Bergego C, Tankov N (1981) Pattern of group I fibre projections from ankle flexor and extensor muscles in man. Exp Brain Res 42: 337–350

Pinter MM, Dimitrijevic MR, Dimitrijevic MM (1998) Effect of motor task on externally induced stepping movement in spinal cord subjects. Soc Neurosci Abstr 24: 838

Rattay F, Minassian K, Dimitrijevic MR (2000) Epidural electrical stimulation of posterior structures of the human lumbosacral cord: 2. quantitative analysis by computer modeling. Spinal Cord 38: 473–489

Rattay F, Minassian K, Jilge B, Pinter MM, Dimitrijevic MR (2003) EMG analysis of lower limb muscle responses to epidural lumbar cord stimulation. Proceedings of the IEEE EMBS Conference, Cancun (Mexico)

Roeleveld K, Blok JH, Stegeman DF, van Oosterom A (1997) Volume conduction models for surface EMG; confrontation with measurements. J Electromyogr Kinesiol 7(4): 221–232

Rossi A, Decchi B (1994) Flexibility of lower limb reflex responses to painful cutaneous stimulation in standing humans: evidence of load-dependent modulation. J Physiol 481.2: 521–532

Rothwell JC, Traub MM, Day BL, Obeso JH, Thomas PK, Marsden CD (1982) Manual motor performance in an deafferented man. Brain 105: 515–542

Sanes JN, Mauritz KH, Dalakas MC, Evarts EV (1985) Motor control in humans with large-fiber sensory neuropathy. Hum Neurobiol 4: 101–114

Selverston A, Moulins M (1985) Oscillatory neural networks. Annu Rev Physiol 47: 29–48

Timischl W (2000) Biostatistics. An introduction for biologists and physicians, 2nd edition. (Biostatistik. Eine Einführung für Biologen und Mediziner. Zweite, neubearbeitete Auflage. In German.) Springer Lehrbuch Biologie, Wien/New York

Windhorst UR (1991) What are the output units of motor behavior and how are they controlled? In: Humphrey DR, Freund HJ (eds) Motor Control: Concepts and Issues. John Wiley & Sons, pp 101–120

Zehr EP, Komiyama T, Stein RB (1997) Cutaneous reflexes during human gait: electromyographic and kinematic responses to electrical stimulation. J Neurophysiol 77: 3311–3325

Chapter 3

Frequency-dependent selection of alternative spinal pathways with common periodic sensory input

Bernhard Jilge[1], Karen Minassian[1,2], Frank Rattay[1], Milan R. Dimitrijevic[3,4,5]

[1] TU-BioMed Association for Biomedical Engineering, Vienna University of Technology, Vienna, Austria

[2] Ludwig Boltzmann Institute for Electrical Stimulation and Physical Rehabilitation, Vienna, Austria

[3] Ludwig Boltzmann Institute for Restorative Neurology and Neuromodulation, Vienna, Austria

[4] University Institute for Clinical Neurophysiology, Clinical Centre Ljubljana, Slovenia

[5] Department of Physical Medicine and Rehabilitation, Baylor College of Medicine, Houston, Texas, USA

Abstract. Electrical stimulation of the lumbar cord at distinct frequency ranges has been shown to evoke either rhythmical, stepping-like movements (25–50 Hz) or a sustained extension (5–15 Hz) of the paralysed lower limbs in complete spinal cord injured subjects. Frequency-dependent activation of previously "silent" spinal pathways was suggested to contribute to the differential responsiveness to distinct neuronal "codes" and the modifications in the electromyographic recordings during the actual implementation of the evoked motor tasks. In the present study we examine this idea by means of a simplified biology-based neuronal network. Involving two basic mechanisms, temporal summation of synaptic input and presynaptic inhibition, the model exhibits several patterns of mono- and/or disynaptic motor output in response to different interstimulus intervals. It thus reproduces fundamental input-output features of the lumbar cord isolated from the brain. The results confirm frequency-dependent spinal pathway selection as a simple mechanism which enables the cord to respond to distinct neuronal codes with different motor behaviours, and to control the actual performance of the latter.

3.1 Introduction

The ability to adapt spinal reflexes to the requirements of an ongoing postural or movement task is a common feature of the central nervous systems of vertebrates and invertebrates. In both groups of animals numerous examples for state-dependent reflex modulation have been presented, and several mechanisms have been proposed to account for the variability of spinal reflex responses [for a review, see Pearson 1993, Hultborn 2001, or McCrea 2001]. That is, in

particular, *(i)* the activation of previously "silent" (i.e., present, but not responding) reflex pathways during certain motor tasks in parallel with the suppression of previously operating ones, and *(ii)* the presynaptic inhibition of synaptic transmission from primary afferents to motoneurones. Back in 1973, Lundberg suggested that, under normal conditions, command signals that descend during voluntary movement activate interneurones in one of several alternative spinal reflex paths while "inhibitory interactions" suppress the transmission in the collateral ones. Meanwhile, this concept of coexisting parallel pathways that can be differentially modulated according to the "central state" of the spinal cord is widely accepted [Hultborn 2001]. Moreover, presynaptic mechanisms which influence synaptic transmission from primary afferent neurones have been shown to constitute an integral part of the "central programs" of various voluntary and reflex movement tasks [reviewed by Nusbaum *et al.* 1999, or Rudomin and Schmidt 1999; for details on identified spinal interneurones that mediate presynaptic inhibition see Jankowska 1992 and 2001].

According to these views, a given sensory input to the spinal cord may result in different motor outputs, depending on which one of several alternative pathways has previously been "opened". Recently, Dimitrijevic and collaborators have demonstrated that a sustained regular train of electrical stimuli, epidurally applied to primary afferents of the L2–L3 segments, can have a "conditioning" effect on the lumbar cord in subjects with a complete spinal cord injury [Minassian *et al.* 2001b]. Using stimulus frequencies within distinct ranges (25–50 Hz or 5–15 Hz, respectively), they induced either rhythmical, stepping-like movements of the lower limbs [Dimitrijevic *et al.* 1998], or a sustained lower limb extension [Jilge *et al.* 2003]. Most interestingly, the lower limb surface EMG recorded in parallel to the spinal cord stimulation (SCS)-induced movements revealed single compound motor unit potentials (CMUPs). Each of them could unequivocally be related to the pulse within the stimulus train which had triggered it. Moreover, as the evoked extension unfolded, the recruitment order of the motor units which contributed to the recorded CMUPs changed in a characteristic, reproducible manner. The authors explained this with the SCS-induced afferent volleys being displayed not only monosynaptically to the corresponding motor nuclei, but also to interneuronal structures, which governed the spatiotemporal CMUP pattern via premotoneuronal mechanisms [Jilge *et al.* 2003].

Similarly, Minassian *et al.* [2002] supposed that—during SCS-evoked rhythmical lower limb muscle EMG activity—the afferent volleys delivered by the epidural electrode were no longer transmitted via the monosynaptic reflex arc but "re-routed" through spinal pathways which involve more centrally situated interneurones [see also Minassian *et al.* 2001a]. The individual steady-state CMUP responses to SCS at 25–50 Hz revealed latency times which were prolonged by about 10 ms compared to lower stimulus frequencies. During the transition toward the equilibrium, the motor responses included both short- and long-latency components, with the first one gradually losing and the second one gradually gaining momentum.

There are two remarkable aspects in these studies: First, as any descending control of the lumbar premotor centre was excluded, the externally applied pulse train itself must have accomplished the "opening", or selection, of particular spinal pathways, and the "closing" of others. Second, the activation/inactivation hinged on the stimulus train to be applied within a specific frequency range. In the present communication, we demonstrate that this behaviour is yet exhibited by a simplified network of neurones involving two basic mechanisms: temporal summation of postsynaptic potentials, and presynaptic inhibition.

In the following sections we present a simplified, biology-based computational model to reproduce the above-described input-output features of the human lumbar cord in complete spinal cord injured subjects. Therein, summation processes rely on the elementary properties of the leaky integrate-and-fire neurone, the capacity of which has repeatedly been investigated [see, e.g., Scharstein 1979, Rospars and Lánský 1993, Bressloff 1995, Lánský and Rodriguez 1999a,b, Shimokawa *et al.* 2000, Burkitt and Clark 2000, Feng and Brown 2000, Feng 2001, Pakdaman 2001]. Details on the biophysics of excitable cell membranes—during primary afferent depolarisations and shunting inhibition in particular [Atwood *et al.* 1984, Atwood and Tse 1988, Segev 1990, Graham and Redman 1994, Walmsley *et al.* 1995, Lamotte d'Incamps *et al.* 1998, 1999, Cattaert *et al.* 2001]—are omitted.

3.2 Methods

3.2.1 Model description

The network is composed of three model neurones denoted as the sensory neurone, the motoneurone, and the interneurone, respectively (**Fig. 3.1**). Via parallel pathways the sensory neurone provides both mono- and disynaptic excitatory input to the motoneurone. In addition, monosynaptically transmitted volleys are subject to presynaptic inhibition (PSI) by the activity of the interneurone within the disynaptic pathway. The moto- and interneurones are modelled as discrete-time single-point leaky-integrate-and-fire neurones [Rescigno 1970, Knight 1972, Softky and Koch 1995] *without* resetting of the state variable after action potential (AP) initiation. That is, at all evaluation times $t_k = k\Delta t$, $k = 0, 1, 2, \ldots$, after the onset of the sensory volley the firing behaviour of neurone n is determined by its postsynaptic potential $P_n(t_k)$

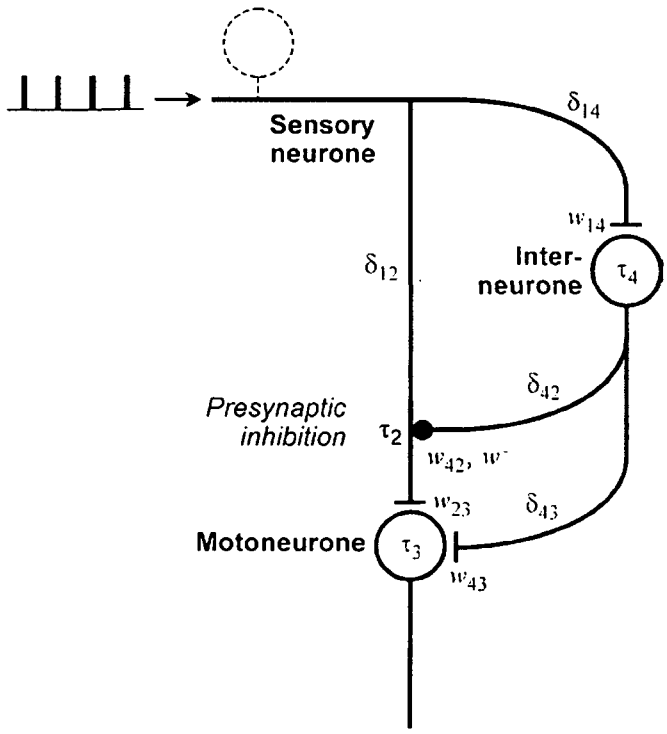

Fig. 3.1. Architecture of the model network. Excitatory connection between a sensory and a motor neurone is made via both a mono- and a disynaptic pathway. In addition, the interneurone which is part of the latter exerts inhibitory influence on the afferent terminals on the motoneurone. The individual network elements are modelled as leaky integrate-and-fire neurones, with τ_n denoting the respective (linear) leakage coefficient. w_{mn} and w^- describe the mapping from the pre- to the induced postsynaptic potentials, and the "strength" of the presynaptic mechanism, respectively. Between the model neurones different delays δ_{mn} are considered.

(reduced by the resting potential of the postsynaptic membrane). The evolution of $P_n(t_k)$ is described by the recursive equation

$$P_n(t_k) = P_n(t_{k-1})\exp\left(-\frac{\Delta t}{\tau_n}\right) + \sum_m w_{mn}V_{mn}(t_k). \tag{3.1}$$

Thereby, $V_{mn}(t_k)$ denotes the synaptic input provided by neurone m, $w_{mn}V_{mn}(t_k)$ represents the induced EPSP, and $\tau_n > 0$ is the time constant for the repolarisation of the postsynaptic membrane. An AP is initiated when the postsynaptic potential (PSP) attains the firing threshold V^{thr}. (The associated changes of the membrane potential at the trigger zone are not included in the model.) The network input, i.e. the sensory volley, as well as in- and output of the inter- and motoneurones are represented by sequences consisting of the elements 0 and V^{AP} only. Different delays in the model neurones caused by the initiation of an AP and its final integration, are taken into account.

At the site of presynaptic inhibition, the above-described scheme of the summation process is applied to the input from the interneurone only. At all times, however, the resulting PSP is weighted by a constant coefficient w^-, and subtracted from the current sensory input amount. If the difference attains the firing threshold—which requires both the arrival of a sensory AP and the interneuronal influence being sufficiently weak—the AP is propagated to the motoneurone; otherwise, monosynaptic input to the latter is completely blocked at that time.

The behaviour of the single-point model without potential reset is compared with the two-compartment model with partial reset described by Bressloff [1995]. In brief, it is defined in the following way:

$$\begin{aligned}\frac{dx_{n1}}{dt}(t) &= -\frac{x_{n1}(t)}{\tau_n} + \frac{x_{n2}(t) - x_{n1}(t)}{\tau_n^r} + \sum_m w_{mn}v_{mn}(t)\\ \frac{dx_{n2}}{dt}(t) &= -\frac{x_{n2}(t)}{\tau_n} + \frac{x_{n1}(t) - x_{n2}(t)}{\tau_n^r}\end{aligned} \tag{3.2}$$

where

$$\int_{t_k}^{t_{k+1}} v_{mn}(t)dt = V_{mn}(t_k), \tag{3.3}$$

x_{n1}, x_{n2} denote the membrane potentials of the two compartments representing neurone n, and τ_n^r is the intercompartmental junctional time constant. When $x_{n2}(t)$ attains V^{thr} it is reset to zero while $x_{n1}(t)$ continues in its evolution.

In a second step, the model is refined by introducing a stochastic element in the summation process to improve the fit of the network behaviour to the neurophysiologically observed features. The EPSP induced in the interneurone and at the site of PSI, respectively, by a presynaptic AP is decomposed into a constant c_{vmn} and a random factor. In the computer simulations the latter is assumed to follow a Poisson distribution with mean and standard deviation being equal to $w_{mn}c_{vmn}^{-1}V_{mn}(t_k)$. It is re-evaluated at any t_k, particularly each time when

an AP is integrated. The supposed distribution thus determines the firing probability of the model neurone in response to a presynaptic AP. In the theoretical analyses the Poisson distribution is substituted by a Gaussian one. Furthermore, each model neurone is regarded as a representative of a larger population of functionally equivalent neurones. According to this view, the above-mentioned firing probability is interpreted as the relative size of the subpopulation generating spikes in response to an incoming AP. For details see the model formulation in the Appendix.

3.2.2 Computer simulations

The behaviour of the model neurones and their interactions in response to a periodical series of sensory APs were simulated using MATLAB 6.1 (THE MATHWORKS, INC., NATIC, MA). Thereby, given a pair of input frequencies $f_{lo} < f_{hi}$, we aim at reproducing the following scenario:

1. In response to either frequency of the sensory volley, the network eventually develops a steady-state behaviour. At any time, the output is phase-locked to the input signal. However, each single motor response to an individual sensory pulse may have more than one component.
2. At f_{lo}, the whole population of motoneurones reveals solely monosynaptic responses.
3. At f_{hi}, the immediate motor responses are still of monosynaptic origin. In the following an increasingly larger subpopulation additionally demonstrates disynaptic responses. In parallel, the monosynaptic component becomes more and more suppressed—until it vanishes completely. During the transition from the mono- to the disynaptic pathway the motoneurones fire twice per sensory AP: once with a shorter latency time and once with a longer one—corresponding to the mono- and disynaptic paths, respectively.

As higher input frequencies are applied,

4. disynaptic motor responses appear earlier (i.e., within shorter time from the onset of the sensory volley), and
5. the disynaptic component becomes larger, while the monosynaptic one decreases.

Following previous neurophysiological results [Minassian *et al.* 2001b, 2002; Jilge *et al.* 2002, 2003], we consider two different frequency pairs (f_{lo}, f_{hi}), namely (2 Hz, 10 Hz) and (10 Hz, 25 Hz). The "spatial extension" of the neuronal populations in the stochastic model is simulated by performing 200 test runs under equal conditions. Throughout the simulations the delays δ_{mn} are set to the following values: $\delta_{12} = 7$ ms, $\delta_{14} = 11$ ms, $\delta_{42} = 4$ ms, $\delta_{43} = 4$ ms. A firing threshold of 30 mV is applied to each model neurone. Each test run is started under resting conditions, i.e. $P_n(0) = 0$ for all n. For details on the determination of suitable values for the model parameters see the Appendix, Determination of parameter settings.

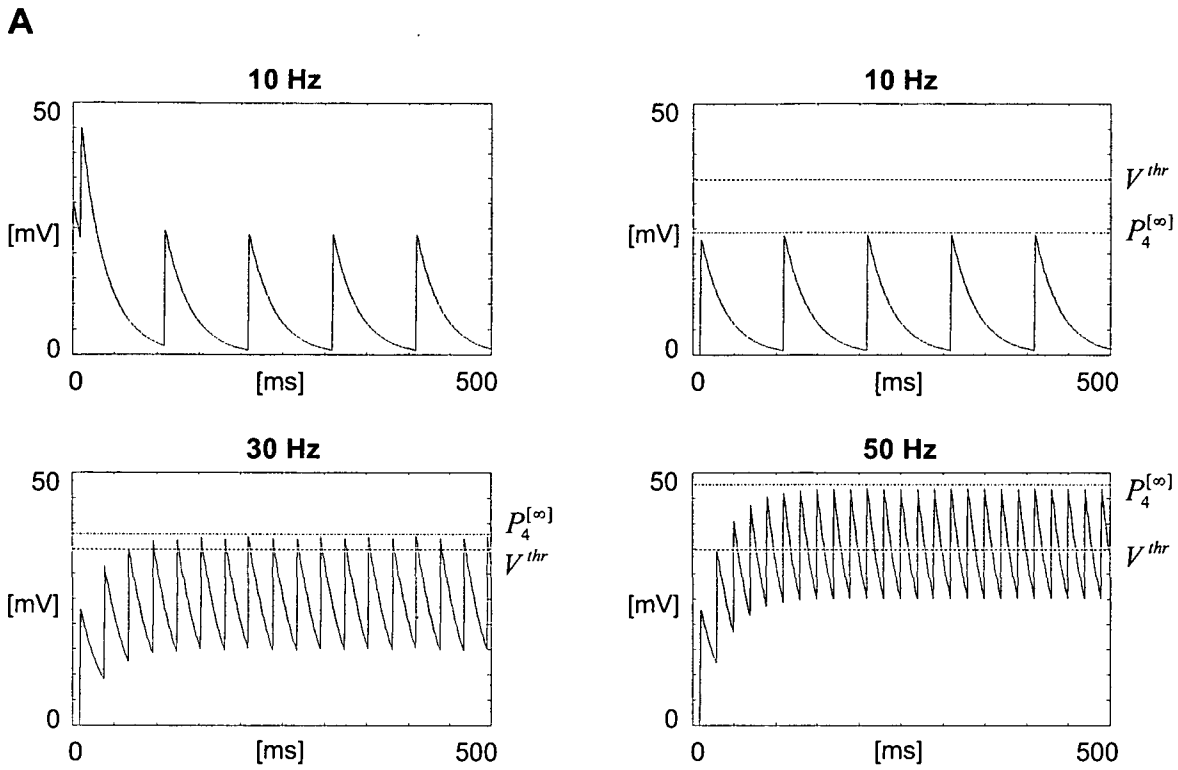
A
10 Hz
50
[mV]
0
0
[ms]
500
10 Hz
50
[mV]
0
0
[ms]
500
V^{thr}
$P_4^{[\infty]}$
30 Hz
50
[mV]
0
0
[ms]
500
$P_4^{[\infty]}$
V^{thr}
50 Hz
50
[mV]
0
0
[ms]
500
$P_4^{[\infty]}$
V^{thr}

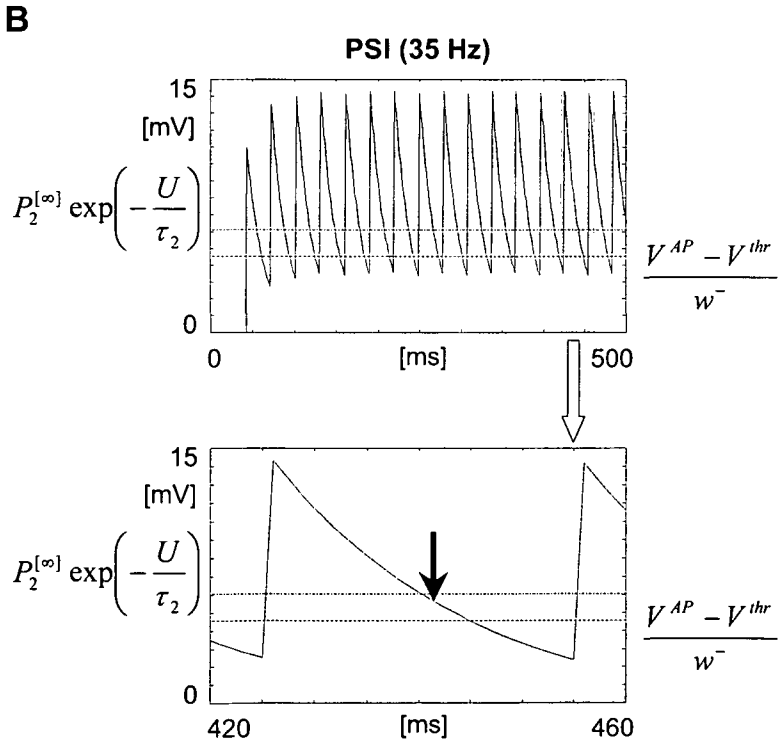
B
PSI (35 Hz)
15
[mV]
$P_2^{[\infty]} \exp\left(-\frac{U}{\tau_2}\right)$
0
0
[ms]
500
$\frac{V^{AP} - V^{thr}}{w^-}$
15
[mV]
$P_2^{[\infty]} \exp\left(-\frac{U}{\tau_2}\right)$
0
420
[ms]
460
$\frac{V^{AP} - V^{thr}}{w^-}$

Fig. 3.2. Behaviour of the key elements of the deterministic model in response to a periodical sensory volley. **A**, Time course of the PSP of the model interneurone for different initial conditions, $P_4(0) = 30$ mV (10 Hz, *left hand side*) and $P_4(0) = 0$ (resting condition; 10 Hz, *right hand side*), and different input frequencies (10, 30, 50 Hz), respectively. The *broken horizontal lines* mark the assumed firing threshold of 35 mV, while the *dotted* ones indicate the frequency-dependent PSP peak values during the equilibrium. Parameter settings: $\tau_4 = 30$ ms, $w_{14}V^{AP} = 59.4$ mV. For representation purposes, relatively large values have been chosen for the time constant and a single EPSP, respectively. However, the qualitative results are independent from the actual settings of these parameters. **B**, Time course of the PSP at the site of PSI. The *dotted horizontal lines* indicate its frequency-dependent steady-state value at the time instants when a sensory spike passes the target site of PSI (*arrow*). The *broken horizontal lines* mark the threshold which has to be attained to block passing APs (see Eqn. 3.9). Parameter settings: $\tau_2 = 20$ ms, $w_{42}V^{AP} = 11.0$ mV, $w^- = 17.0$; $U = 21$ ms.

← *previous page* —

3.3 Results

3.3.1 Theoretical analysis of the network behaviour

Let t_{k_j}, $j = 0, 1, 2, \ldots$, denote the subsequence of those time instants t_k when a sensory AP arrives at the interneurone. Apparently, the interneuronal PSP $P_4(t_k)$ is largest (i.e., has its "peaks") at these times. Independently from the model parameters and the input frequency f, the respective values $P_4^{[j]} = P_4(t_{k_j})$ tend toward an equilibrium which is equal to

$$P_4^{[\infty]} = w_{14}V^{AP}\left[1 - \exp\left(-\frac{1}{f\tau_4}\right)\right]^{-1}. \tag{3.4}$$

If the interneurone starts from the resting potential—i.e. $P_4(0) = 0$, which we will assume henceforth—the PSP peak amplitudes increase monotonic toward their limit (which in turn does not depend on the initial value anyhow). $P_4^{[\infty]}$ obviously increases with f or τ_4, respectively (**Fig. 3.2A**). As to the speed of convergence, it takes

$$N = -f\tau_4 \ln\frac{1-\gamma}{100} \tag{3.5}$$

sensory pulses until the PSP of the interneurone equals γ per cent of $P_4^{[\infty]}$. In this sense, the PSP peak amplitudes converge slower in response to higher-frequency sensory volleys. However, this is not true with respect to the corresponding *time* $t = N/f$, which does not depend on f. If

$$f > \left[-\tau_4 \ln\left(1 - \frac{w_{14}V^{AP}}{V^{thr}}\right)\right]^{-1} \tag{3.6}$$

(i.e. $P_4^{[\infty]} > V^{thr}$) for a given combination of the model parameters, the time t^* until the interneurone starts to fire becomes

$$t^* \approx \delta_{14} - \tau_4 \ln\left\{1 - \frac{V^{thr}}{w_{14}V^{AP}}\left[1 - \exp\left(-\frac{1}{f\tau_4}\right)\right]\right\}. \tag{3.7}$$

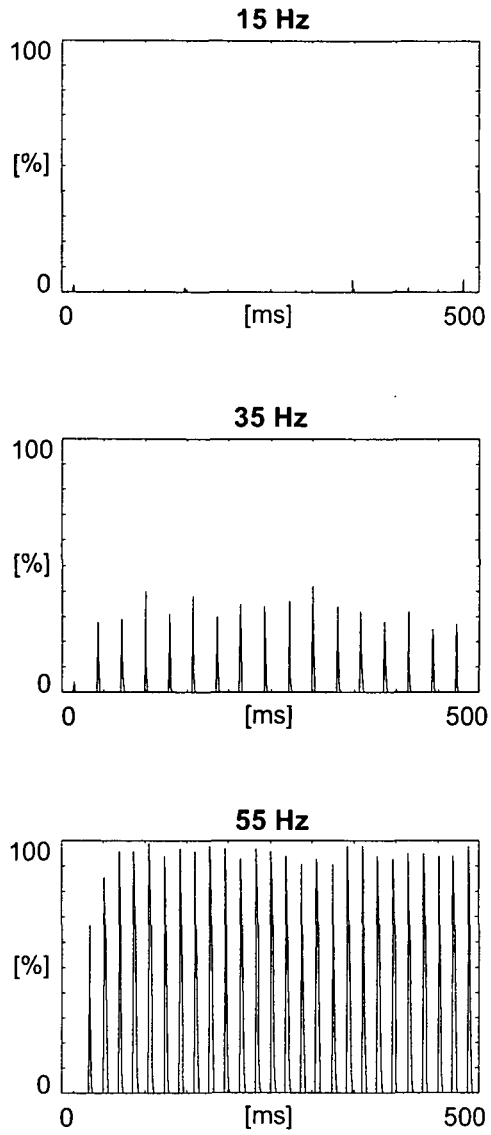

Fig. 3.3. Behaviour of the interneuronal population in the stochastic model in response to different input frequencies. The proportion of interneurones which generate APs is plotted versus the time from the onset of the sensory volley. As the frequency is stepped up, an increasingly larger subpopulation responds to the periodical input. Calculated with the same parameter settings as **Fig. 3.2**.

As expected, the higher the frequency of an excitatory ($w_{14} > 0$) sensory volley, the earlier the interneurone generates APs: $t^* = 78$ and 31 ms for 30 and 50 Hz, respectively (**Fig. 3.2A**). Until t^* has elapsed, the motor responses (if present) are solely monosynaptic. Later, both the site of PSI and the motoneurone receive "input" from two sources, and the output of the latter may also include APs of disynaptic origin.

The PSP $P_2(t_k)$ at the site of PSI shows an analogous behaviour (**Fig. 3.2B**). As soon as the interneurone has started to fire, passing sensory APs will not be blocked until an additional period of

$$t^{**} \approx \delta_{42} - \tau_2 \cdot \ln\left\{1 - \frac{V^{AP} - V^{thr}}{w^- \cdot w_{42} V^{AP}} \cdot \exp\left(\frac{U}{\tau_2}\right) \cdot \left[1 - \exp\left(-\frac{1}{f\tau_2}\right)\right]\right\}. \tag{3.8}$$

time units has elapsed. Thereby, U denotes the delay between the arrival of an interneuronal spike and the directly following transient sensory pulse, $w_{42}V^{AP}$ is the amount by which a single interneuronal AP changes the PSP at the site of PSI, and w^- represents the weighting coefficient for PSI as explained in the Methods. Furthermore, we have assumed that the interneurone does not generate more than one spike in response to a single sensory AP, and that $P_2(t_k)=0$ until the first interneuronal spike arrives at the site of PSI. ("Repetitive firing" of the interneurone will be excluded if the repolarisation time constant of its postsynaptic membrane is sufficiently small.) As soon as PSI is effective, sensory pulses are no longer monosynaptically transmitted to the motoneurone, and the transition from the mono- to the disynaptic responses is completed. However, on condition that

$$\frac{V^{AP}-V^{thr}}{w^-}\exp\left(\frac{U}{\tau_2}\right)\geq P_2^{[\infty]} \text{ where } P_2^{[\infty]}=w_{42}V^{AP}\left[1-\exp\left(-\frac{1}{f\tau_2}\right)\right]^{-1}, \tag{3.9}$$

passing APs will never be blocked, and, in general, the steady-state motoneuronal output will include both mono- and disynaptic components.

Taken together, each model neurone exhibits—after an initial "tuning" phase—a stationary firing behaviour which depends on the frequency of the sensory volley. This particularly applies to the motoneurone and thus to the network output. Whether the latter is solely monosynaptic or includes a disynaptic component primarily depends on the time constant at which the postsynaptic membrane of the interneurone repolarises. The smaller this time constant, the larger the frequency of the sensory volley has to be in order to "activate" the interneurone and thus „open" the disynaptic pathway. The model parameters for PSI (i.e., the time constant at the site of PSI and the respective synaptic weights) determine if the output of the interneurone can suppress the monosynaptic transmission of the sensory volley to the motoneurone. This presynaptic suppression also requires temporal summation during which sensory APs are transmitted via both the mono- and the disynaptic pathway. Provided suitable parameter settings, the motor responses consequently include two components with different latency times:

—— *next page* ——→

Fig. 3.4. Deterministic model for $f_{lo}=10$ Hz and $f_{hi}=25$ Hz. *Left hand side*: Time course of the PSP in the inter- (*upper panel*) and motoneurones (*lower panel*) and at the site of PSI (*intermediate panel*) in response to a sensory volley at 10 Hz (**A**), 22 Hz (**B**) and 25 Hz (**C**). *Right hand side*: Enlargement of the vertices of the PSPs given at the left hand side (**A**; **B**; **C**, *upper and intermediate panels*). The *broken horizontal line* in the *upper and intermediate panels* indicates the firing threshold V^{thr} imposed on the interneurone, and the threshold which has to be attained by the PSP at the site of PSI to block passing APs (see Eqn. 3.9), respectively. The *lower panel* in **C** shows a single PSP peak at an enlarged *time* scale. The time instant at which the triggering sensory pulse has been applied is marked by an *arrow*. At 10 Hz, the PSP of the interneurone does not attain the firing threshold. Consequently, all motor responses are of monosynaptic origin. At 25 Hz, the interneurone *is* activated, and the PSP at the site of PSI eventually attains the threshold for suppression of passing APs. Therefore, the motor output pattern reveals three phases in which purely monosynaptic, both mono- and disynaptic (transitional phase), resp. purely disynaptic responses (steady-state phase) are observed. At the intermediate frequency of 22 Hz, the steady-state network output reveals both short- and long-latency components as the inhibitory action of the interneurone is too weak to eliminate the transmission via the monosynaptic pathway. Parameter settings: $\tau_4=10$ ms, $\tau_2=20$ ms, $\tau_3=2$ ms, $w_{14}V^{AP}=29.7$ mV, $w_{42}V^{AP}=11.0$ mV, $w^-=31.3$, $w_{23}V^{AP}=w_{43}V^{AP}=79.2$ mV, $V^{thr}=30$ mV.

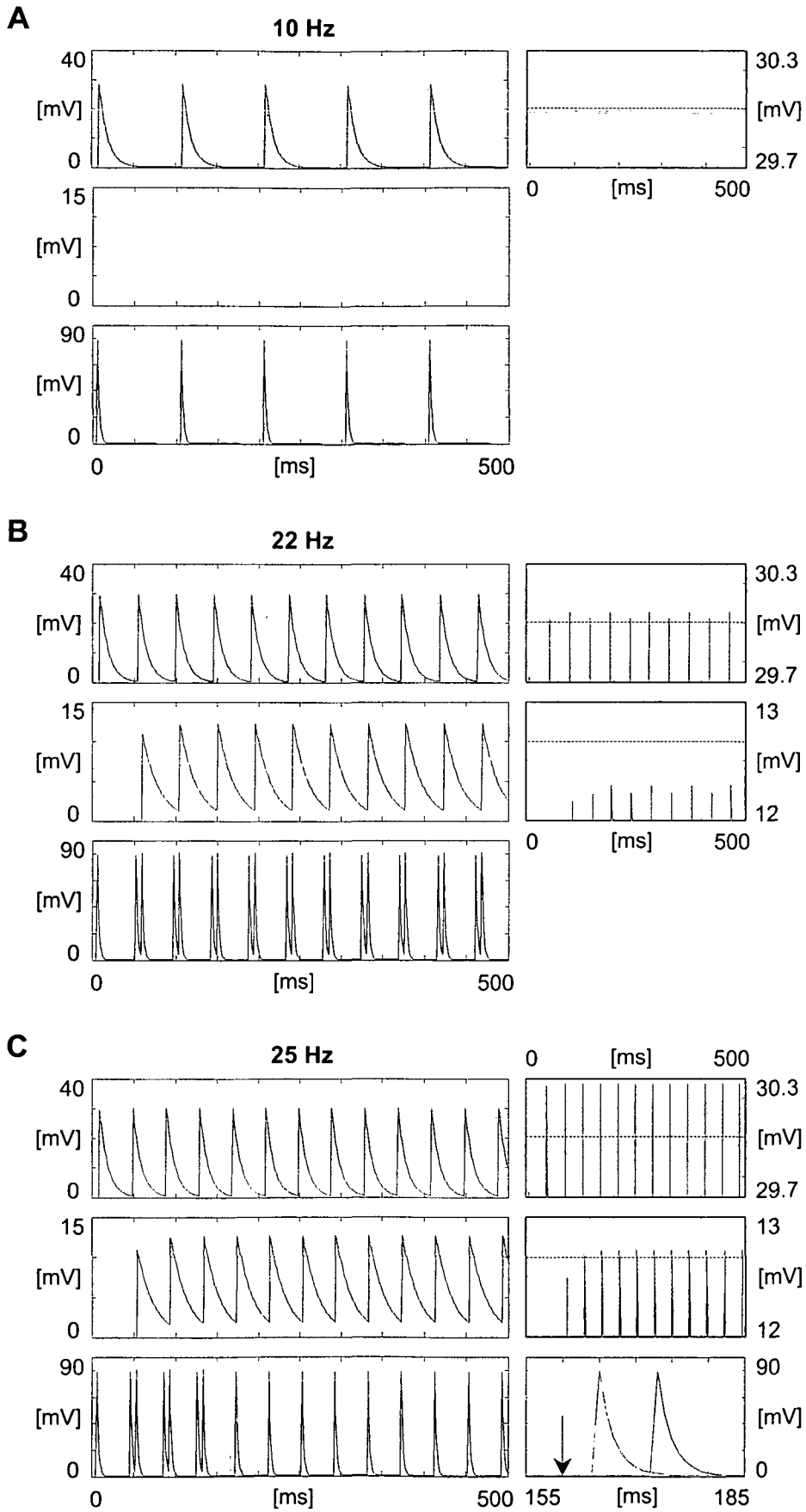
A
10 Hz
40
[mV]
0
15
[mV]
0
90
[mV]
0
0
[ms]
500
30.3
[mV]
29.7
0
[ms]
500
B
22 Hz
40
[mV]
0
15
[mV]
0
90
[mV]
0
0
[ms]
500
30.3
[mV]
29.7
13
[mV]
12
0
[ms]
500
C
25 Hz
40
[mV]
0
15
[mV]
0
90
[mV]
0
0
[ms]
500
0
[ms]
500
30.3
[mV]
29.7
13
[mV]
12
90
[mV]
0
155
[ms]
185

a monosynaptic and a disynaptic one.

In the stochastic model, the PSP of each model neurone is represented by a discrete-time stochastic process, whereas the sensory volley remains deterministic. Thus, instead of calculating the time instant when the PSP of the interneurone attains the firing threshold for the first time, we are interested in the *probability* that this will occur at a given time t_{k_j} (see above). The steady-state value of this probability, which is approximately equal to

$$p = 1 - \Phi\left(\left[\frac{V^{thr}}{\sqrt{c_{v14}}} - \frac{w_{14}V^{AP}}{\sqrt{c_{v14}}}\left(1 - e^{-\frac{1}{f\tau_4}}\right)^{-1}\right] \cdot \sqrt{w_{14}V^{AP}\left(1 - e^{-\frac{2}{f\tau_4}}\right)}\right), \tag{3.10}$$

can subsequently be interpreted as the proportion of interneurones that fire in response to the sensory pulses. Thereby, $w_{14}V^{AP}$ and c_{v14} are the mean EPSP induced in the interneurone by a single presynaptic AP, and the constant factor in the summation process (as described in the Methods), respectively; and Φ denotes the cumulative distribution function of the Gaussian distribution with mean 0 and variance 1. In the Appendix we show that p increases with f, which means that the transition from the mono- to the disynaptic pathway will be more "complete" if the interneuronal population is excited at a higher frequency (**Fig. 3.3**).

3.3.2 Computer simulations

Deterministic model

Fig. 3.4 illustrates the behaviour of the deterministic model in response to $f_{lo} = 10$ Hz and $f_{hi} = 25$ Hz. Each sensory pulse within a train at 10 Hz evokes just one motor response at a latency time of 7 ms (= the delay via the sensory axon). **Fig. 3.4A** demonstrates that these responses are in fact of monosynaptic origin as the PSP of the interneurone never attains the firing threshold ($P_4^{[\infty]} = 29.7$ mV), and the disynaptic pathway consequently remains "closed". At an input frequency of 25 Hz, however, the steady-state responses of the motoneurone are disynaptic—as confirmed by the prolonged latency time of 15 ms (= 11 ms delay via the sensory axon to the interneurone + 4 ms onward to the motoneurone; **Fig. 3.4C**). At that frequency, the PSP of the interneurone exceeds the firing threshold for the first time in response to the second sensory pulse ($P_4^{[\infty]} = 30.3$ mV). Subsequently, the site of PSI is subject to both excitatory and inhibitory influence from the sensory and interneurones, respectively. In parallel, the interneurone provides excitatory synaptic input to the motoneurone inducing motor responses of disynaptic origin. The inhibitory input to the site of PSI soon blocks the propagation of the sensory APs via the monosynaptic pathway ($P_2^{[\infty]} = 12.72$ mV while the respective threshold calculated from (3.9) amounts to 12.68 mV). Accordingly, from the response to the fifth sensory pulse, the network output is solely disynaptic. During the short transitional phase from the mono- to the disynaptic responses it reveals two components at latency times of 7 and 15 ms, respectively.

When the frequency of the sensory volley is reduced to 22 Hz, the interneurone is still activated, but its presynaptic inhibitory influence on the transmission within the monosynaptic pathway is

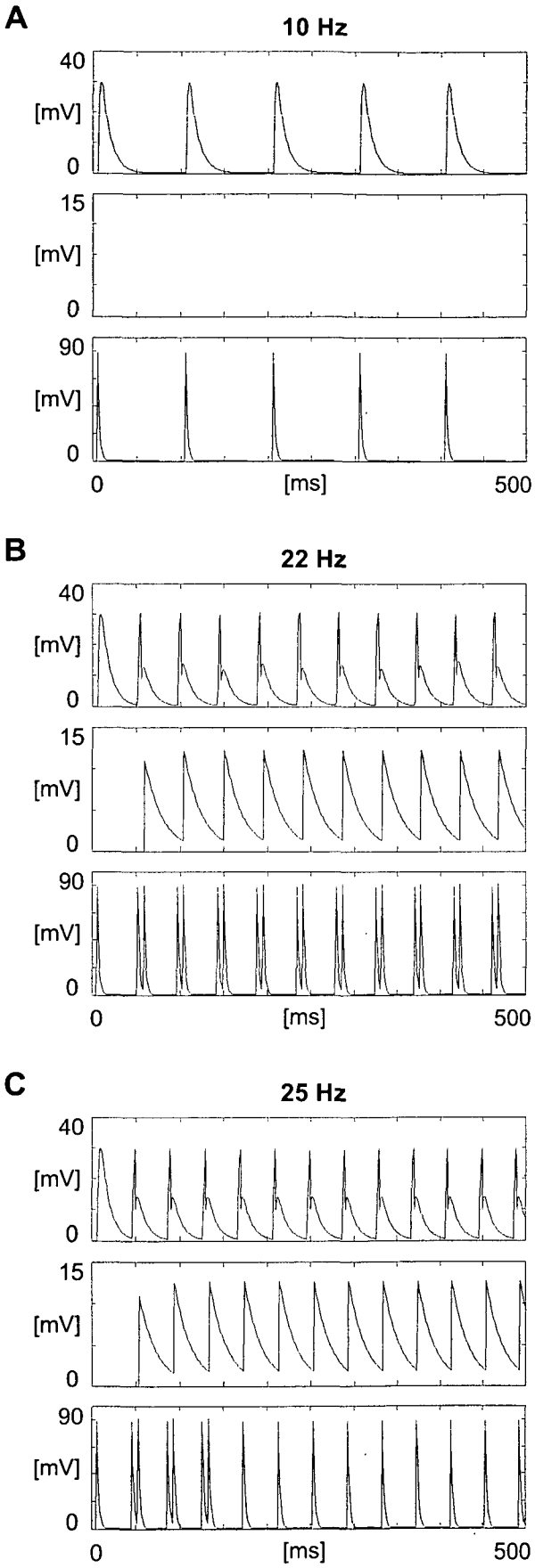

Fig. 3.5. Deterministic model for $f_{lo} = 10$ Hz and $f_{hi} = 25$ Hz, applying the two-point model with partial potential reset to the interneurone. Time course of the potential $x_{41}(t)$ at the integration zone of the interneurone (*upper panel*), PSP in the motoneurone (*lower panel*) and at the site of PSI (*intermediate panel*) in response to a sensory volley at 10 Hz (**A**), 22 Hz (**B**) and 25 Hz (**C**). Having adjusted $w_{14}V^{AP}$, the network reveals the same behaviour as for the one-point interneurone (compare **Fig. 3.4**). Due to the potential reset at the trigger zone, $x_{41}(t)$ sharply decreases and immediately "recovers" after spike initiation. Parameter settings: $\tau_4 = 10$ ms, $\tau_2 = 20$ ms, $\tau_3 = 2$ ms, $w_{42}V^{AP} = 11.0$ mV, $w^- = 31.3$, $w_{23}V^{AP} = w_{43}V^{AP} = 79.2$ mV, $V^{thr} = 30$ mV—as in **Fig. 3.4**; $\tau_4^r = 3$ ms, $w_{14}V^{AP} = 59.4$ mV.

insufficient to suppress the short-latency network responses ($P_2^{[\infty]} = 12.3$ mV). Both the mono- and the disynaptic component are therefore included in the steady-state output (**Fig. 3.4B**).

Applying the two-point model with partial potential reset to the interneurone does not change the network behaviour significantly (**Fig. 3.5**). However, using $\tau_4^r = 3$ ms, the EPSP induced by a single sensory AP has to be about twice as large to have the same effect. Moreover, δ_{14} has to be reduced by 3 ms as a respective delay is incorporated in the compartment model. Though the membrane potential at the trigger zone is reset immediately after spike initiation, it soon "recovers" due to its connectivity with the "dendritic" (i.e. postsynaptic) compartment (**Fig. 3.5B** and **C**).

Stochastic model

Steady-state motor responses which comprise both components are more readily obtained in the stochastic model. According to the results of the theoretical analysis, the transition from the mono- to the disynaptic pathway is the more "complete" the higher the frequency of the sensory volley. Thereby, "steady-state response" refers to the behaviour of an ensemble of neurones rather than of a single one. The motoneuronal population as a whole tends to an equilibrium while its elements may fire irregularly.

Random factors have been imposed on the summation process in the interneurone and at the site of PSI, otherwise the same parameter settings as in **Fig. 3.4** were used. As in the deterministic model, the network output remains roughly stable after an initial tuning phase. When the sensory volley is applied at 10 Hz, 45 % of the interneurones fire during the equilibrium, yet leaving the transmission via the monosynaptic pathway unaffected (**Fig. 3.6A**). As the input frequency is stepped up, increasingly more interneurones generate APs, while the monosynaptic component progressively diminishes (**Fig. 3.6B–D**). At 25 Hz, 55 and 75 % of the motoneurones eventually respond at the short (7 ms) and the prolonged (15 ms) latency time, respectively. Obviously, as 55 % + 75 % > 100 %, some motoneurones exhibit both components (**Fig. 3.6C**). At 35 Hz, the respective proportions amount to 25 and 77 % yet (**Fig. 3.6D**). In line with (3.10), the disynaptic component is fully implemented when sensory volleys at more than 56 Hz are applied. During the tuning phase of the network, the proportion of those motoneurones—or equivalently, the size of that motoneuronal subpopulation—which reveal disynaptic responses increases toward the frequency-dependent equilibrium.

In contrast to the deterministic model, a long-latency component of considerable size *is* observed here in response to f_{lo}. Even at lower input frequencies disynaptic responses are not excluded as, according to (3.10),

$$\lim_{f \to 0} p = 1 - \Phi\left(\frac{V^{thr} - w_{14} V^{AP}}{\sqrt{c_{v14} w_{14} V^{AP}}}\right) \tag{3.11}$$

still amounts to 45 % under the present simulation conditions. Similarly, short-latency responses are not eliminated by applying sensory pulses at f_{hi}, though at 56 Hz and above this is

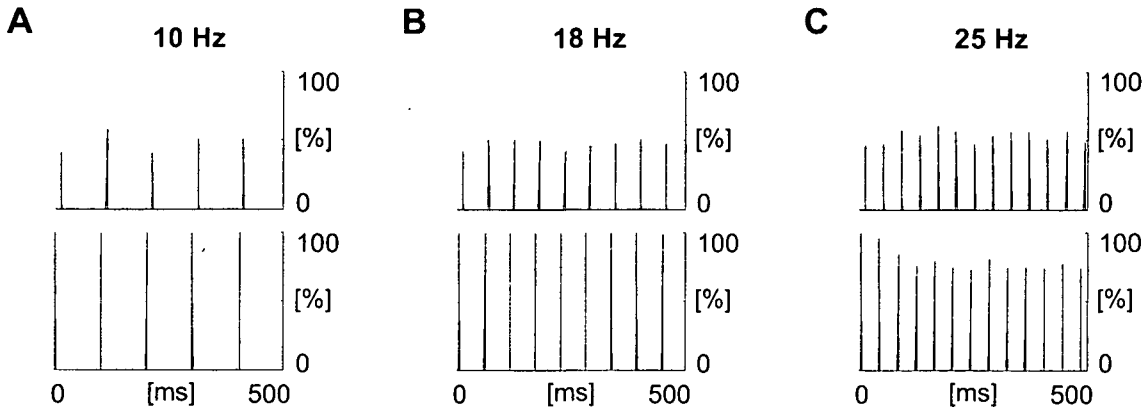
A
10 Hz
B
18 Hz
C
25 Hz
100
[%]
0
0
[ms]
500

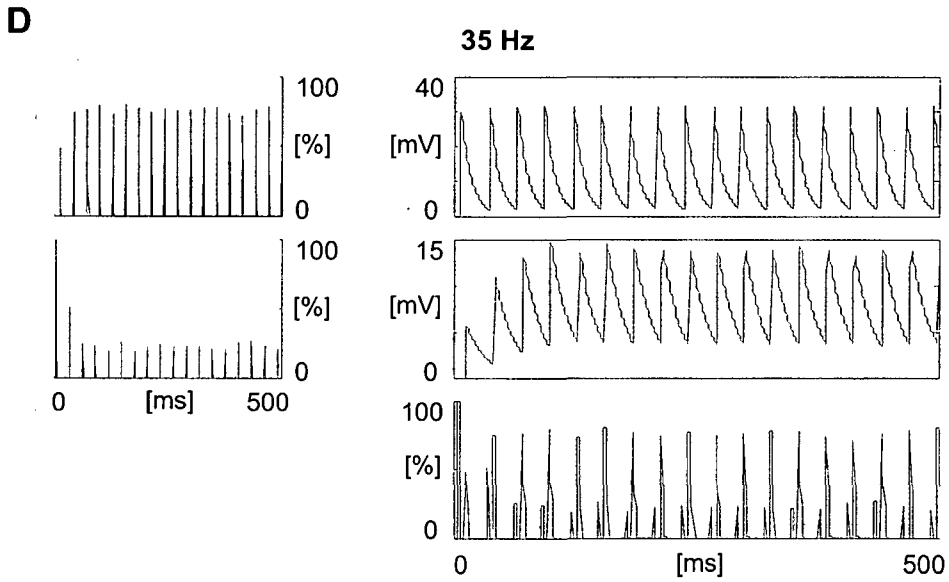
D
35 Hz
100
[%]
0
40
[mV]
15
0
[ms]
500

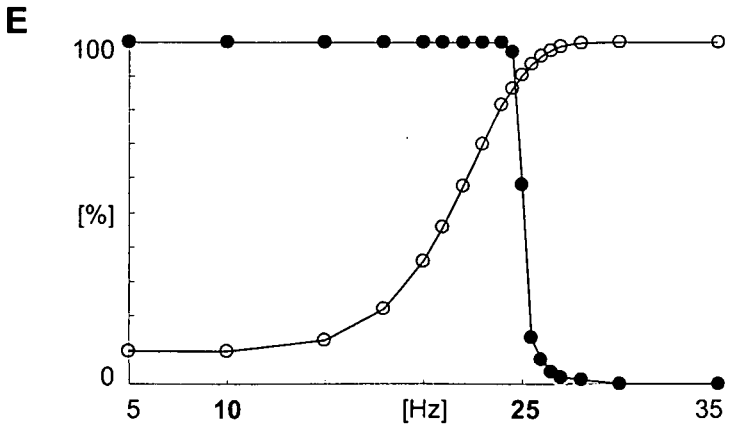
E
100
[%]
0
5
10
[Hz]
25
35

Fig. 3.6. Stochastic model for f_{lo} = 10 Hz and f_{hi} = 25 Hz. **A–C, D** (*left hand side*), Proportion of interneurones which generate APs in response to a sensory volley at 10, 18, 25 and 35 Hz (*upper panel*), and proportion of sensory pulses which remain unaffected by the PSI (*lower panel*), as a function of time. **D** (*right hand side*), Time course of the PSP in the interneurone (*upper panel*) and at the site of PSI (*intermediate panel*), averaged over 200 test runs. Proportion of motoneurones which fire in response to the sensory volley, plotted versus the time from its onset (*lower panel*). Parameter settings: $\tau_4 = 10$ ms, $\tau_2 = 20$ ms, $\tau_3 = 2$ ms, $w^- = 31.3$, $w_{23}V^{AP} = w_{43}V^{AP} = 79.2$ mV, $V^{thr} = 30$ mV—as in **Fig. 3.4**; $c_{v14} = c_v w'_{14} = 0.39$ mV, $c_{v42} = c_v w'_{42} = 0.14$ mV, $w_{14}V^{AP} = 29.7$ mV, $w_{42}V^{AP} = 11.0$ mV. **E**, Proportion p of interneurones which fire during the equilibrium (O), and proportion of sensory pulses which remain unaffected by the PSI (●), as a function of the input frequency. In contrast to **A–D**, c_v has been set to 1 % of its original value while keeping the other parameters constant. As higher input frequencies are applied, the disynaptic network output gradually evolves while the monosynaptic one is attenuated. By reducing c_v the range $\lim_{f\to\infty} p(f) - \lim_{f\to 0} p(f)$ is enlarged (see Eqn. 3.10).

← *previous page* —

accomplished. Analogous results are obtained for the other frequency pair, $f_{lo} = 2$ Hz and $f_{hi} = 10$ Hz (**Fig. 3.7**). The long-latency component in response to f_{lo} does not vanish ($p(f_{lo}) = 0.49 = \lim_{f\to 0} p(f)$; **Fig. 3.7A**), and PSI is ineffective. At f_{hi}, the interneurones are far away from „acting in concert"—as it would be the case in the deterministic model ($p(f_{hi}) = 0.51 < 1$), and the presynaptic suppression of the short-latency component is not successful but in approximately 60 % of the sensory terminals (**Fig. 3.7B**).

A possibility how to reduce p at f_{lo} and, in parallel, increase p at f_{hi} is implied by (3.10), namely to reduce c_{v14} while keeping $w_{14}V^{AP}$ constant. This does not change the mean EPSP induced in the interneurone by a single presynaptic AP, but reduces its variability. Depending on the frequency f of the sensory volley, the term [...] is either positive ($f = f_{lo}$) or negative ($f = f_{hi}$). Consequently, changing c_{v14} has opposite effects on p in response to f_{lo} and f_{hi}. In **Fig. 3.6E**, c_{v14} and c_{v42} have been reduced to 1 % of their original values. At 10 Hz the interneuronal population remains practically "silent" ($p < 0.1$), whereas at 25 Hz its strong activation ($p > 0.9$) suppresses the monosynaptic motor responses to a large extent. The analogous result for $f_{lo} = 2$ Hz, $f_{hi} = 10$ Hz is shown in **Fig. 3.7D**.

To estimate the relative importance of the probabilistic elements in the interneurone and at the site of PSI we have additionally performed test runs in which only one of these neurones behaved stochastically while the other one remained deterministic. Deterministic PSI yields fairly the same network output as the stochastic one, provided that it is subject to stochastic interneuronal input (**Fig. 3.8A**). In the reverse situation, in contrast, the stronger activation of the interneuronal population inhibits the monosynaptic component much more effectively (**Fig. 3.8B**).

Duration of the tuning phase

In both the models for $f_{lo} = 2$ Hz, $f_{hi} = 10$ Hz and $f_{lo} = 10$ Hz, $f_{hi} = 25$ Hz, the equilibrium is quickly reached. In the deterministic model for the latter frequency pair, the steady states are adopted within one ($f = 22$ Hz) or four ($f = 25$ Hz) sensory pulse(s), respectively (**Fig. 3.4B** and **C**). If one assumes V^{AP} and V^{thr} to be invariant, (3.7) and (3.8) imply that, in principle, the

tuning phase in response to a given input frequency can be prolonged either by increasing the time constants τ_4 and/or τ_2, or by reducing the synaptic weights w_{14} and/or $w_{42}w^-$. The demand for repetitive firing of the model neurones to be excluded actually leaves only little scope for changes of τ_4. However, adjustment of the size of the EPSP induced by a single presynaptic spike is indeed effective: A one-percent reduction of w_{14} and a 0.3-percent reduction of w^- yields an extension of t^* and t^{**} by the equivalent of 4 and 7 sensory pulses, respectively, under the present simulation conditions using a 25-Hz train of sensory input (**Fig. 3.9A**). The requirements that $P_4^{[\infty]}$ be above the firing threshold of the interneurone, and (3.9) not be fulfilled restrict the reduction of the synaptic weights by imposing lower boundaries to them. Nevertheless, the duration of the tuning phase can be prolonged indefinitely by sufficiently approaching these boundaries. Thereby, $P_4^{[\infty]}$ draws increasingly nearer to V^{thr}.

In contrast, with respect to the length of the tuning phase, the stochastic model appears unaffected by synaptic weight adaptation (compare **Figs. 3.6B** and **3.9B**) or by increasing the time constants. Even if combined with reduction of c_{v14}, a "smooth" transition is not obtained (**Fig. 3.9C**). Variation of these parameters, however, readily changes the size of the mono- and disynaptic motor output, respectively.

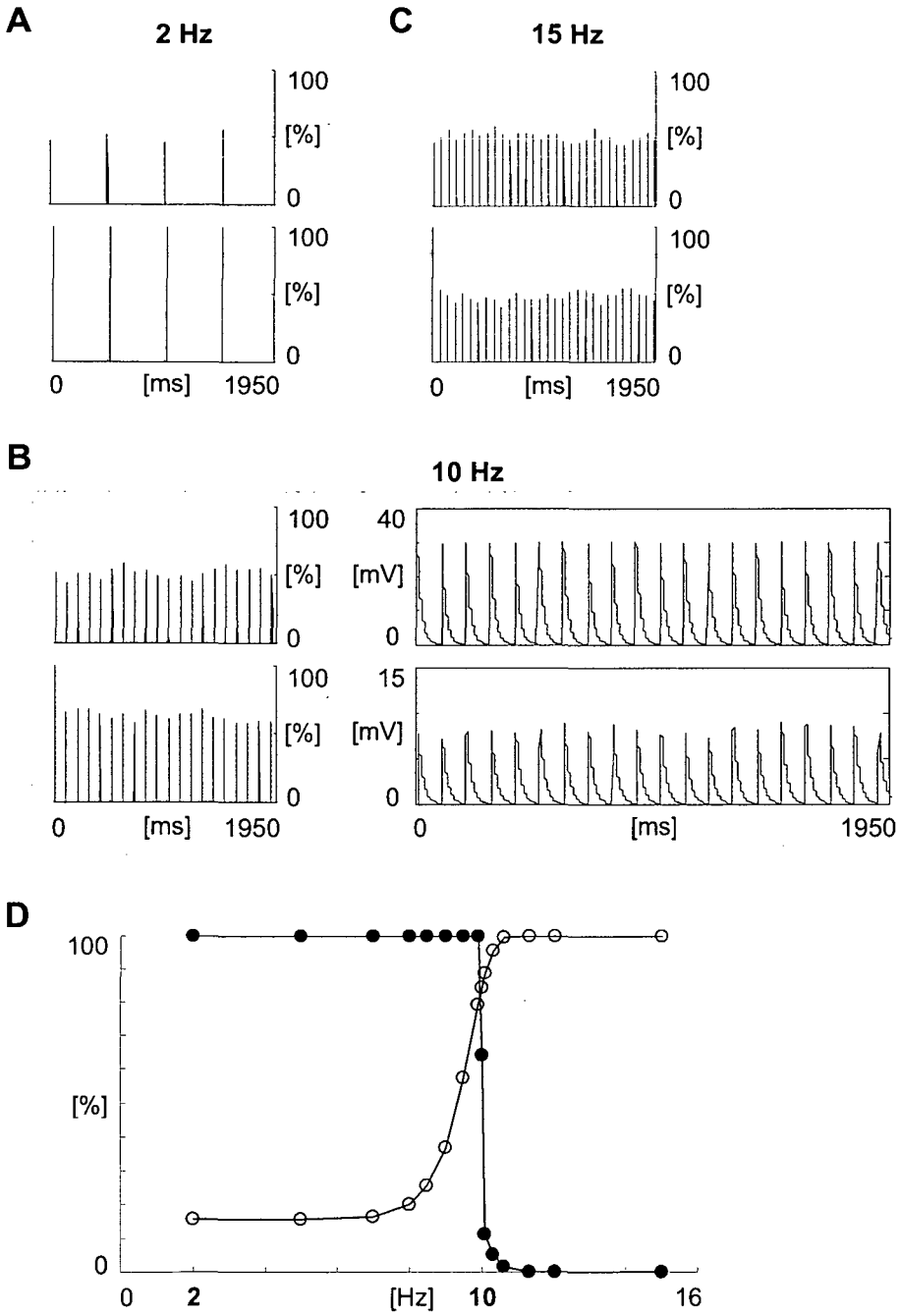

Fig. 3.7. Stochastic model for $f_{lo} = 2$ Hz and $f_{hi} = 10$ Hz. **A**, **B** (*left hand side*), **D**, Proportion of interneurones which generate APs (*upper panel*), and proportion of sensory pulses which remain unaffected by the PSI (*lower panel*), as a function of time from the onset of the sensory volley at 2 Hz (**A**), 10 Hz (**B**) and 15 Hz (**C**). **B** (*right hand side*), Time course of the PSP in the interneurone (*upper panel*) and at the site of PSI (*intermediate panel*), averaged over 200 test runs. Parameter settings: $\tau_4 = 10$ ms, $\tau_2 = 20$ ms, $\tau_3 = 2$ ms, $w^- = 31.3$, $c_{v14} = c_v w'_{14} = 0.39$ mV, $c_{v42} = c_v w'_{42} = 0.14$ mV, $w_{14} V^{AP} = 29.7$ mV, $w_{42} V^{AP} = 11.0$ mV, $w_{23} V^{AP} = w_{43} V^{AP} = 79.2$ mV, $V^{thr} = 30$ mV. **D**, Proportion p of interneurones which fire during the equilibrium (O), and proportion of sensory pulses which remain unaffected by the PSI (●), as a function of the input frequency. In contrast to **A–C**, c_v has been set to 10^{-5} % of its original value while keeping the other parameters constant. As higher input frequencies are applied, the disynaptic network output gradually evolves while the monosynaptic one is attenuated. By reducing c_v the range $\lim_{f\to\infty} p(f) - \lim_{f\to 0} p(f)$ is enlarged (see Eqn. 3.10).

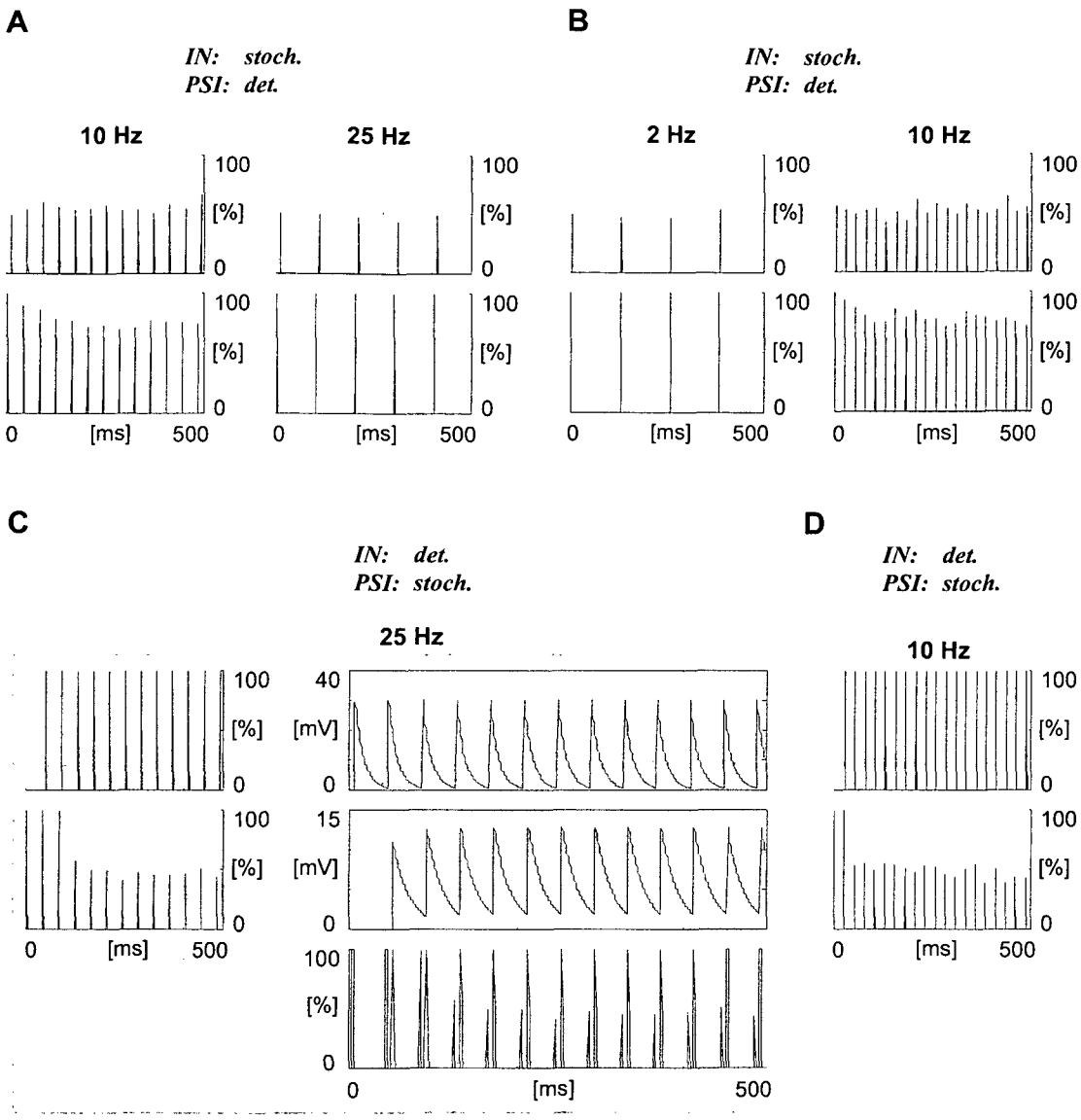

Fig. 3.8. Relative contribution of the stochastic elements imposed on the model neurones. **A**, **B**, **C** (*left hand side*), **D**, Proportion of interneurones which generate APs (*upper panel*), and proportion of sensory pulses which remain unaffected by the PSI (*lower panel*), as a function of time from the onset of the sensory volley at 10 and 25 Hz (**A**), 2 and 10 Hz (**B**), 25 Hz (**C**), and 10 Hz (**D**), respectively. **C** (*right hand side*) Time course of the PSP in the interneurone (*upper panel*) and at the site of PSI (*intermediate panel*), averaged over 200 test runs. Proportion of motoneurones which fire in response to the sensory volley, plotted versus the time from its onset (*lower panel*). Figures **A** and **C** are an extension of **Fig. 3.6**, using the same parameter values. Analogously, figures **B** and **D** are based on the same settings as **Fig. 3.7**. In **A** and **B**, however, the summation process at the site of PSI is assumed to be deterministic while the interneurone remains stochastic, whereas in **C** and **D**, the reverse situation is considered. Apparently, the fact whether PSI includes a stochastic element or not does not influence the network behaviour significantly.

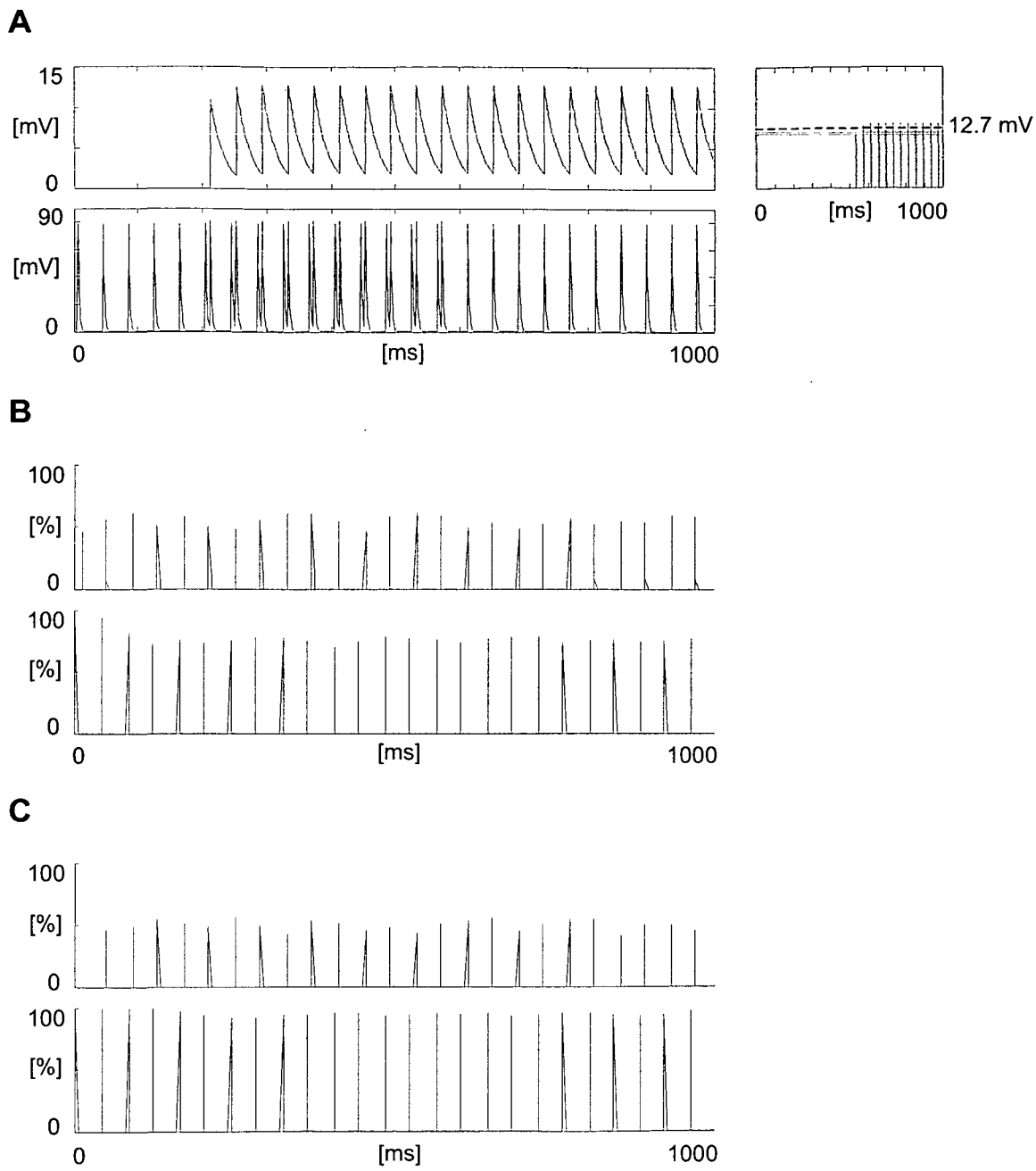

Fig. 3.9. Duration of the tuning phase. **A**, Simulation of the deterministic model for $f_{lo} = 10$ Hz and $f_{hi} = 25$ Hz, using the same parameter settings as in **Fig. 3.4**, except for the synaptic weights w_{14} and $w_{42}w^-$, which have been reduced by 1 % and 0.3 % of their original value, respectively. *Left hand side*: Time course of the PSP at the site of PSI (*upper panel*) and in the motoneurone (*lower panel*) in response to a sensory volley at 25 Hz. *Right hand side*: Enlargement of the vertices of the PSP at the site of PSI. The *broken horizontal line* indicates the threshold which has to be attained to block passing APs (see Eqn. 3.9). **B**, Proportion of interneurones which generate APs (*upper panel*), and proportion of sensory pulses which remain unaffected by the PSI (*lower panel*), as a function of time from the onset of the sensory volley at 25 Hz. Thereby, both the interneurone and the site of PSI are assumed to behave stochastically, using otherwise identical parameter settings as in **A**. **C**, As **B**, but with c_v set to 1 % of its original value. By reducing w_{14} or $w_{42}w^-$ in the deterministic model, the transitional phase until the network output remains stable can be prolonged arbitrarily. However, adjusting these parameters is not effective in the stochastic model. Additional reduction of c_v, which brings the model "closer" to the deterministic one, does not result in a "smoother" transition toward the equilibrium either.

3.4 Discussion

We have presented a simplified network capable of reproducing fundamental input-output features of the human lumbar cord which were observed in response to input at 2–50 Hz externally induced by epidural stimulation [Minassian *et al.* 2001b, 2002; Jilge *et al.* 2002, 2003]. Between a sensory and a motoneurone (or corresponding neuronal populations, respectively) two parallel pathways of different length, which we called "mono-" and "disynaptic", were considered. (Although we used the terms "mono- and disynaptic" throughout this communication, it might be more realistic to think of "oligo- and multisynaptic" paths, to which our results are easily generalised.) Each pulse within the input signal was transmitted via one or both of these pathways to become part of the network output. The latency time at which it arrived at the motoneurone thereby depended on whether the shorter or the longer path had actually been taken. The respective selection was determined by the length of the interpulse interval within the sensory volley. Simply spoken, a disynaptic component was observed in response to higher frequencies only, while responses to low-frequency input were of solely monosynaptic origin. This was accomplished by introducing an interneurone at the "gate" to the disynaptic pathway which acted in a frequency-dependent manner: the gate was not "opened" unless the input pulses arrived at sufficiently short intervals. Temporal summation of the input was required to activate the pathway alternative to the monosynaptic one. Thus, the network revealed different output patterns in response to distinct input frequencies.

As to the neurophysiological findings we aimed to reproduce in detail (see the Methods), both the deterministic and the stochastic model revealed responses phase-locked to the input signal. Starting with motor output of monosynaptic origin, they eventually demonstrated a steady-state behaviour. During the equilibrium, the size of the mono- and disynaptic components decreased and increased, respectively, as higher input frequencies were applied. At all times the output of the deterministic model followed the all-or-none firing principle, being either solely mono- or disynaptic, or including both components at the same size. Lowering the frequency of the sensory volley prolonged the tuning phase of the network. Not until a stochastic element was introduced in the summation process of the interneurone, the neurophysiologically observed gradation of the motor output was reproduced. However, a *gradual* transition toward the equilibrium was not accomplished in this model either. **Figs. 3.6–3.9** revealed rather step-like changes from the immediate to the stationary responses.

Apart from the stochastic nature of synaptic integration, two key mechanisms account for the described network behaviour: temporal summation of postsynaptic potentials, and presynaptic inhibition of primary afferent terminals. Temporal summation in the interneurone and at the site of PSI was implemented using the single-point leaky integrate-and-fire model (1-LIFM) *without* potential reset. The 1-LIFM is commonly regarded as the simplest biologically realistic neuronal model, and has extensively been investigated [e.g., Scharstein 1979, Ermentrout 1995, Burkitt and Clark 2000, Feng and Brown 2000, Shimokawa *et al.* 2000, Feng 2001, Pakdaman 2001]. However, in these studies the state variable *was* set to a constant 'postdischarge resetting potential' ($< V^{thr}$) after spike initiation. By this means one sought to account for the fact that, after the generation of an AP, the membrane of the axon hillock returns to the resting potential—though this is not true for the postsynaptic membrane at the dendrites. To overcome this unsatisfactory situation, in which the model neurone loses all "memory" of its history, *(i)* the reset condition could be omitted, or *(ii)* the integration and trigger zones could be separated,

restricting the potential reset to the latter only. Alternative *(ii)* has been described as the 'two-point', or 'two-compartment', LIFM with 'partial', or 'somatic', potential reset [Bressloff 1995, Lánský and Rogdriguez 1999a,b; Rospars and Lánský 1993]. (A brief model definition is given in the Methods.) In the present study the two alternatives have not revealed substantial differences with respect to the behaviour of the considered network (**Fig. 3.5**).

As to the presumed subtractive effect of PSI on the size of a transient AP we leant on the theoretical results reported by Graham and Redman [1994]. Supposing both a chloride shunt and the possibility of sodium channel inactivation by PSI-induced depolarisation, they had demonstrated a roughly linear relationship between the chloride conductance in an en passant synaptic bouton and the AP amplitude [see also Walmsley *et al.* 1995, Lamotte D'Incamps *et al.* 1998, and Cattaert *et al.* 2001]. According to Segev's [1990] simulation studies, whether shunting PSI exerts graded control over the voltage at the premotoneuronal release site or rather operates in an "on-off" fashion strongly depends on the location of the axo-axonal synapse and the morphology and membrane properties of the axonal terminal [see also Atwood *et al.* 1984]. In the present model, an all-or-none effect was assumed, but—as a respective decision is made in the subsequent motoneurone anyhow—one can simply switch to the alternative presumption by properly adjusting the PSI parameter w^-.

Obviously, the model network cannot reproduce all details of the biological data on which the present simulation study is based. In particular, it does not explain how the activity within *several* cord segments is *differentially* controlled under constant stimulation conditions. During SCS-induced lower limb extension, hip and ankle extensor muscles exhibit larger CMUP activity and forces than the corresponding flexors. During the unfolding extension movement the responsiveness of the flexor muscles to the external stimulus increases while the extensors lose momentum. During SCS-evoked stepping-like movements, flexor and extensor motor nuclei are subject to rhythmically alternating excitation/inhibition [Dimitrijevic 1998, Jilge *et al.* 2003, Minassian *et al.* 2003]. Generating the underlying spatiotemporal patterns of motor unit activation requires control mechanisms within the spinal cord which are not yet understood.

The foregoing neurophysiological studies in complete spinal cord injured subjects have indicated that different "codes" provided to the same interneuronal system accomplish the initiation and retention of distinct types of motor output. Thereby, frequency-dependent selection between alternative spinal pathways was hypothesised to play an important role. In the present work this particular idea was investigated on the basis of a computational model. According to the results, the suggested mechanism could in fact contribute to the differential responsiveness of the lumbar cord to distinct neuronal codes, and to the modifications in the electromyographic recordings during the actual implementation of the evoked motor tasks.

Appendix: Theoretical analysis of the network behaviour

B1 Deterministic model

Model formulation

With $\Delta t > 0$ covering the duration of an AP (incl. refractory period), and $t_k = k\Delta t$, $k = 0, 1, 2, \ldots$, the network behaviour is defined by the equations

$$P_n(t_k) = P_n(t_{k-1}) \cdot \exp\left(-\frac{\Delta t}{\tau_n}\right) + \sum_{m \in N_n} w_{mn} V_{mn}(t_k) \quad \text{for} \quad n = 2, 3, 4 \quad \text{and} \quad k = 1, 2, \ldots \tag{B1}$$

$$V_{mn}(t_k) = \begin{cases} V^{AP} & \text{there is a } j \in \mathbf{N} \text{ so that } t_k = jT + \delta_{mn} \\ 0 & \text{otherwise} \end{cases} \quad \text{for} \quad (m,n) = (1,2); (1,4) \tag{B2}$$

$$V_{23}(t_k) = \begin{cases} V^{AP} & V_{12}(t_k - \delta_{23}) - w^- \cdot P_3(t_k - \delta_{23}) \geq V^{thr} \\ 0 & \text{otherwise} \end{cases} \tag{B3}$$

$$V_{mn}(t_k) = \begin{cases} V^{AP} & P_m(t_k - \delta_{mn}) \geq V^{thr} \\ 0 & \text{otherwise} \end{cases} \quad \text{for} \quad (m,n) = (4,2); (4,3) \tag{B4}$$

Thereby, the following abbreviations are used: $P_n(t_k)$, PSP of neurone n after the integration of any synaptic input which may have arrived at t_k; τ_n, time constant at which the postsynaptic membrane repolarises; $V_{mn}(t_k) \in \{0, V^{AP}\}$, input provided by neurone m to neurone n at t_k; $w_{mn}V^{AP}$, EPSP induced by a single presynaptic AP; $N_2 = \{4\}; N_3 = \{2, 4\}; N_4 = \{1\}$; V^{thr}, firing threshold imposed on each model neurone; $\delta_{mn} = z_{mn}\Delta t$ with the z_{mn} being natural numbers, synaptic delay due to the integration process in neurone m plus AP conduction time from neurone m to neurone n. Here, the site of PSI is referred to as "neurone 2".

According to (B2), an AP is initiated in the sensory neurone at the times $t_k = jT$, $j = 1, 2, \ldots$ where $T = z\Delta t = f^{-1}$ and for a (fixed) natural z. If the PSP of neurone m attains the firing threshold at $t_k - \delta_{mn}$, an AP is initiated and propagated to neurone n where it arrives at t_k (B4). If the amount $w^- \cdot P_3(t_k - \delta_{23})$, $w^- > 0$, by which the PSP at the site of PSI reduces a transient AP is sufficiently large, the latter is not propagated to the motoneurone (B3).

Explicit solutions of (B1) are given by

$$P_n(t_k) = P_n(0) \cdot \exp\left(-\frac{k\Delta t}{\tau_n}\right) + \sum_{l=0}^{k-1} \sum_{m \in N_n} w_{mn} V_{mn}(t_{k-l}) \cdot \exp\left(-\frac{l\Delta t}{\tau_n}\right); \quad n = 2, 3, 4; \quad k = 1, 2, \ldots \tag{B5}$$

Interneuronal integration

The interneurone is directly affected by the sensory volley, receiving input from only one source at most. Presynaptic APs increase $P_4(t_k)$ at the time instants $t_k = jT + \delta_{14}$, $j = 0, 1, 2, \ldots$ Taking into account that

$$V_{14}(t_{k-l}) = V_{14}(k\Delta t - l\Delta t) = \begin{cases} V^{AP} & \text{there is an } r \in \{0,1,\ldots,j-1\} \text{ so that } l\Delta t = rT \\ 0 & \text{otherwise} \end{cases}$$

the corresponding values $P_4^{[j]} = P_4(jT + \delta_{14})$ are

$$P_4^{[j]} = P_4(0) \cdot \exp\left(\frac{\delta_{14}}{\tau_4}\right) \cdot q_4^j + w_{14} V^{AP} \cdot \frac{1-q_4^j}{1-q_4}, \quad q_4 = \exp\left(-\frac{1}{f\tau_4}\right).$$

These are the local maxima of P_4, which tend to the supremum of the monotonically increasing sequence $w_{14}V^{AP}(1-q_4^j)(1-q_4)^{-1}$, $j = 1, 2, \ldots$,

$$P_4^{[\infty]} = \lim_{j\to\infty} P_4(jT + \delta_{14}) = \frac{w_{14}V^{AP}}{1-q_4}. \tag{B6}$$

Let us assume henceforth that $P_4(0) = 0$, and define

$$R_j = P_4^{[\infty]} - P_4^j; \quad j = 0, 1, 2, \ldots$$

As to the speed of convergence, we are looking for the smallest number j^* of sensory pulses that fulfils

$$R_{j^*} \le \varepsilon P_4^{[\infty]}, \text{ or equivalently, } P_4^{j^*} \ge (1-\varepsilon)P_4^{[\infty]}$$

for a given ε, $0 < \varepsilon < 1$. As

$$\frac{R_j}{P_4^{[\infty]}} = q_4^j,$$

we have

$$j^* = \lfloor -f\tau_4 \cdot \ln\varepsilon \rfloor,$$

where $\lfloor x \rfloor$ means the smallest integer equal to x or larger. If one is interested in the time instead of the number of pulses until P_4 reaches $(1-\varepsilon)P_4^{[\infty]}$, one has to divide j^* by the frequency f,

$$t^* = \delta_{14} + \frac{j^*}{f} \approx \delta_{14} - \tau_4 \cdot \ln\varepsilon.$$

This relation also allows to estimate the time instant when $P_4(t_k)$ attains the firing threshold V^{thr} for the first time. It depends on the ratio $\rho = V^{thr}/P_4^{[\infty]}$. If $\rho \ge 1$, $P_4(t_k)$ will obviously never reach V^{thr}. Otherwise, using (B6) and substituting $1-\rho$ for ε, one obtains that it will take

$$t^* \approx \delta_{14} - \tau_4 \cdot \ln\left\{1 - \frac{V^{thr}}{w_{14}V^{AP}} \cdot \left[1 - \exp\left(-\frac{1}{f\tau_4}\right)\right]\right\} \tag{B7}$$

time units to equal V^{thr}. If $w_{14} > 0$, the interneurone obviously fires earlier in response to a higher-frequency sensory volley. Once it has started to fire it will never stop.

Presynaptic inhibition

As for the interneurone, the PSP at the site of PSI—which determines whether a passing AP is propagated to the motoneurone or not—depends on the amount of input from only one source. Let us assume that the interneurone has just started to fire, that it does not generate more than one AP in response to a single sensory pulse, and that $P_2(t_k) = 0$ until the time u_0 when the first interneuronal spike arrives at the site of PSI. Then transient APs will not be blocked until an additional period of

$$t^{**} \approx \delta_{42} - \tau_2 \cdot \ln\left\{1 - \frac{V^{AP} - V^{thr}}{w^- \cdot w_{42} V^{AP}} \cdot \exp\left(\frac{U}{\tau_2}\right) \cdot \left[1 - \exp\left(-\frac{1}{f\tau_2}\right)\right]\right\} \tag{B8}$$

time units has elapsed after u_0. Thereby, U denotes the delay between the arrival of an interneuronal AP and the directly following passing sensory pulse, and therefore depends on the input frequency. In general, U is positive, i.e., the input to the site of PSI from different sources is asynchronous. This prolongs the transitional phase until the PSI is "effective". Note, however, that passing APs will never be blocked if

$$\frac{V^{AP} - V^{thr}}{w^- \cdot P_2^{[\infty]}} \cdot \exp\left(\frac{U}{\tau_2}\right) \geq 1 \tag{B9}$$

where

$$P_2^{[\infty]} = \lim_{j \to \infty} P_2(jT + \delta_{14} + \delta_{42}) = \frac{w_{42} V^{AP}}{1 - q_2}, \quad q_2 = \exp\left(-\frac{1}{f\tau_2}\right). \tag{B10}$$

B2 Stochastic model

Model formulation

In order to refine the model we decompose the synaptic weights w_{mn}, $m \in N_n$, as follows:

$$w_{mn} = c_\lambda c_v w'_{mn}, \text{ with } c_\lambda, c_v, w'_{mn} \in \mathbf{R}, \text{ for } (m,n) = (1,4); (2,3); (4,2); (4,3) \tag{B11}$$

Assuming a linear relationship between the pre- and postsynaptic membrane potentials, $c_\lambda V_{mn}(t_k)$ could, e.g., be the number of neurotransmitter vesicles that are released from the presynaptic terminal of an "average" neurone m at an "average" neurone n in response to the presynaptic potential $V_{mn}(t_k)$. However, this number may vary to a certain extent between individual synapses, and this fact is taken into account by introducing the w'_{mn}'s. Consequently, with c_v being the PSP which is caused by the content of a single vesicle, $w_{mn} V_{mn}(t_k)$ will be the PSP in response to a presynaptic $V_{mn}(t_k)$ at the synaptic contact of neurone m at neurone n.

We introduce random variables X_{14k} and X_{42k}, $k = 1, 2, \ldots$, and suppose that the former ones are stochastically independent, following Poisson distributions with respective parameters $c_\lambda V_{14}(t_k)$. At the site of PSI, the input from the interneurone is thus no longer deterministic, and the X_{42r}'s consequently follow the distributions

$$\mathbf{P}\{X_{42r} = i\} = \mathbf{P}\{X_{42r} = i | P_4(t_r - \delta_{42}) \geq V^{thr}\} \cdot \mathbf{P}\{P_4(t_r - \delta_{42}) \geq V^{thr}\} + \\ + \mathbf{P}\{X_{42r} = i | P_4(t_r - \delta_{42}) < V^{thr}\} \cdot \mathbf{P}\{P_4(t_r - \delta_{42}) < V^{thr}\}; \; i = 0, 1, 2, \ldots$$

at any time instant $t_r = jT + \delta_{14} + \delta_{42}$, $j = 1, 2, \ldots$ Assuming that

$$\mathbf{P}\{X_{42r} = i | P_4(t_k - \delta_{42}) < V^{thr}\} = 0$$

holds for all $i = 1, 2, \ldots$ we define

$$\mathbf{P}\{X_{42r} = i\} = \begin{cases} \dfrac{(c_\lambda V^{AP})^i}{i!} \cdot \exp(-c_\lambda V^{AP}) \cdot p_j^{(4)} & \text{for } i = 1, 2, \ldots \\ \exp(-c_\lambda V^{AP}) \cdot p_j^{(4)} + 1 - p_j^{(4)} & \text{for } i = 0 \end{cases}$$

while

$$\mathbf{P}\{X_{42k} = i\} = \begin{cases} 0 & \text{for } i = 1, 2, \ldots \\ 1 & \text{for } i = 0 \end{cases}$$

if t_k does not coincide with one of the time instants $jT + \delta_{14} + \delta_{42}$. By finally replacing $c_\lambda V_{mn}(t_k)$ in (B1) by the newly adopted random variables we arrive at the probabilistic recursive definitions

$$P_n(t_k) = P_n(t_{k-1}) \cdot \exp\left(-\frac{\Delta t}{\tau_n}\right) + w'_{mn} c_v X_{mnk} \quad \text{for } k = 1, 2, \ldots \tag{B12}$$

Interneuronal integration

As the input to the interneurone is still deterministic in this model, the respective explicit solution of (B12) can immediately be given:

$$P_4(t_k) = P_4(0) \cdot \exp\left(-\frac{k\Delta t}{\tau_4}\right) + \sum_{l=0}^{k-1} w'_{14} c_v X_{14(k-l)} \cdot \exp\left(-\frac{l\Delta t}{\tau_4}\right) \quad \text{for all } k = 1, 2, \ldots \tag{B13}$$

With the X_{14k}, the $P_4(t_k)$ are also random variables, and instead of calculating the time instant when the PSP of the interneurone attains the firing threshold V^{thr} for the first time we are now interested in the probability that this will occur at a given time t_k. As

$$\mathbf{P}\{P_4(t_k) \geq V^{thr}\} = 1 - \mathbf{P}\left\{\sum_{l=0}^{k-1} X_{14(k-l)} \cdot \exp\left(-\frac{l\Delta t}{\tau_4}\right) < \frac{1}{w'_{14}c_v}\left[V^{thr} - P_4(0)\cdot\exp\left(-\frac{k\Delta t}{\tau_4}\right)\right]\right\}$$

we define

$$\Gamma_k = \frac{1}{w'_{14}c_v}\left[V^{thr} - P_4(0)\cdot\exp\left(-\frac{k\Delta t}{\tau_4}\right)\right]$$

and approximate the Poisson distributions by Gaussian ones in the further calculation. The sum of Gaussian random variables also follows a Gaussian distribution, and so, with

$$\mathrm{M}_k = \mathbf{E}\left[\sum_{l=0}^{k-1} X_{14(k-l)} \cdot \exp\left(-\frac{l\Delta t}{\tau_4}\right)\right] = c_\lambda \sum_{l=0}^{k-1} V_{14}(t_{k-l}) \cdot \exp\left(-\frac{l\Delta t}{\tau_4}\right) \text{ and}$$

$$\Sigma_k^2 = \mathbf{V}\left[\sum_{l=0}^{k-1} X_{14(k-l)} \cdot \exp\left(-\frac{l\Delta t}{\tau_4}\right)\right] = c_\lambda \sum_{l=0}^{k-1} V_{14}(t_{k-l}) \cdot \exp\left(-\frac{2l\Delta t}{\tau_4}\right)$$

the above probability can be written as

$$\mathbf{P}\{P_4(t_k) \geq V^{thr}\} = 1 - \Phi\left(\frac{\Gamma_k - \mathrm{M}_k}{\sqrt{\Sigma_k^2}}\right)$$

where Φ symbolises the cumulative distribution function of the Gaussian distribution with mean 0 and variance 1. For the time instants $t_r = jT + \delta_{14}$, $j = 1, 2, \ldots$, in particular, this implies

$$p_j^{(4)} := \mathbf{P}\{P_4(t_r) \geq V^{thr}\} = 1 - \Phi\left(\frac{\Gamma_r - \mathrm{M}_r}{\sqrt{\Sigma_r^2}}\right),$$

$$\Gamma_r = \frac{V^{thr} - P_4(0)\cdot\exp\left(\frac{\delta_{14}}{\tau_4}\right)\cdot q_4^j}{w'_{14}c_v}, \quad \mathrm{M}_r = c_\lambda V^{AP}\cdot\frac{1-q_4^j}{1-q_4}, \quad \Sigma_r^2 = c_\lambda V^{AP}\cdot\frac{1-q_4^{2j}}{1-q_4^2}. \tag{B14}$$

The limit of $p_j^{(4)}$ as j approaches infinity, $p^{(4)}$, constitutes the proportion of interneurones which generate APs when the steady state has been reached. If $P_4(0) = 0$, this proportion increases monotonically as the transition from the mono- to the disynaptic pathway proceeds at the level of the interneurone. It is larger in response to larger frequencies of the sensory volley since

$$\mathrm{sgn}\left(\frac{dp}{df}(f)\right) = \mathrm{sgn}(-2q_4^2 + q_4 + 1) = 1 \quad \text{for} \quad 0 < q_4 < 1.$$

B3 Determination of parameter settings

Suitable parameter settings are determined on the basis of the following behaviour to be reproduced by the model network, given two input frequencies $f_{lo} < f_{hi}$:

(0) $P_n(0) = 0$ for $n = 2, 3, 4$

(I) In response to a single presynaptic AP, each of the model neurones fires once at most.

If f_{lo} is applied,

(II) the interneurone does not fire,

(III) each (but a finite number of) sensory pulses pass the site of PSI, and

(IV) the motoneurone fires in response to each (but a finite number of) APs which have passed the site of PSI.

If f_{hi} is applied,

(V) the interneurone fires in response to each (but a finite number of) sensory pulses,

(VI) not more than a finite number of sensory pulses pass the site of PSI, and

(VII) the motoneurone fires in response to each AP from the interneurone.

Repetitive firing of the interneurone in response to a single sensory pulse is excluded if (and only if) the following implication holds for all $k = 1, 2, \ldots$, regardless of the input frequency:

(I) If $P_4(t_k) \geq V^{thr}$ and $V_{14}(t_{k+1}) = 0$ then $P_4(t_{k+1}) < V^{thr}$.

If $P_4(t_k) \leq V^{thr} + a$ for all $k = 1, 2, \ldots$ and a positive real number a, this implication follows from

(Ia) $(V^{thr} + a)\exp\left(-\frac{\Delta t}{\tau_4}\right) < V^{thr}$ or, equivalently, $\tau_4 < \frac{1}{\ln(V^{thr} + a) - \ln V^{thr}}$.

With (B6), (II) and (V) follow from

(IIa) $\frac{c_\lambda c_v w'_{14} V^{AP}}{1 - \exp(-1/f_{lo}\tau_4)} = V^{thr} - b_1$ for a $b_1 \in (0, V^{thr})$

(which implies that $P_4(t_k)$ will be lower than V^{thr} for all $k = 1, 2, \ldots$ at f_{lo}), and

(Va) $\frac{c_\lambda c_v w'_{14} V^{AP}}{1 - \exp(-1/f_{hi}\tau_4)} = V^{thr} + a_1$ for a positive real number a_1,

respectively. (III) immediately follows from (II). With (B10), demand (VI) is fulfilled if

(VIa) $V^{AP} - w^- \cdot \frac{c_\lambda c_v w'_{42} V^{AP}}{1 - \exp(-1/f_{hi}\tau_2)} \cdot \exp\left(-\frac{U}{\tau_2}\right) = V^{thr} - b_2$ for a $b_2 \in (0, V^{thr})$

holds. Demands (IV) and (VII) are simply met if the motoneurone fires in response to each incoming AP, regardless of the frequency of their arrival and without the necessity for temporal summation, i.e., if

(IVa, VIIa) $c_\lambda c_v w'_{mn} V^{AP} \geq V^{thr}$ for $(m,n) = (2,3); (4,3)$.

In the computer simulations we set V^{AP} and V^{thr} to 110 and 30 mV, respectively, c_λ to 1.8 $(\text{mV})^{-1}$, c_v to 0.4 mV, τ_2 to 20 ms, and w'_{42} to 0.14. The increment Δt is set to 1 ms. Supposing $a = a_1 = a_2 = a_3 = b_1 = b_2$, we simultaneously choose τ_4 and a such that

$$a = V^{thr} \cdot \frac{(1-q_4^{lo}) - (1-q_4^{hi})}{(1-q_4^{lo}) + (1-q_4^{hi})} \quad \text{and} \quad \text{(Ia)}$$

holds. (Thereby, q_4^{lo} and q_4^{hi} abbreviate $\exp(-1/f_{lo}\tau_4)$ and $\exp(-1/f_{hi}\tau_4)$, respectively.) The remaining parameters of neurones 2 and 4 are computed on the basis of the above equations. Independently, the synaptic weights of the motoneurone are chosen in accordance with (IVa, VIIa), while τ_3 is first arbitrarily chosen and subsequently reduced until each incoming AP does not induce more than one motor response.

Acknowledgements. We gratefully acknowledge the funding supports from the Austrian Science Fund (FWF research project P15469), and the Kent Waldrep National Paralysis Foundation in Addison, Texas, USA.

References

Atwood HL, Stevens JK, Marin L (1984) Axoaxonal synapse location and consequences for presynaptic inhibition in crustacean motor axon terminals. J Comp Neurol 225(1): 64–74

Atwood HL, Tse FW (1988) Changes in binomial parameters of quantal release at crustacean motor axon terminals during presynaptic inhibition. J Physiol 402: 177–193

Bressloff PC (1995) Dynamics of a compartmental model integrate-and-fire neuron with somatic potential reset. Physica D 80: 399–412

Burkitt AN, Clark GM (2000) Calculation of interspike intervals for integrate-and-fire neurons with Poisson distribution of synaptic inputs. Neural Comput 12(8): 1789–1820

Cattaert D, Libersat F, El Manira A (2001) Presynaptic inhibition and antidromic spikes in primary afferents of the crayfish: a computational and experimental analysis. J Neurosci 21(3): 1007–1021

Dimitrijevic MR, Gerasimenko Y, Pinter MM (1998) Evidence for a spinal central pattern generator in humans. In: Kien O, Harris-Warrick RM, Jordan L, Hultborn H, Kudo N (eds) Neuronal Mechanism for Generating Locomotor Activity. Annals of the New York Academy of Sciences, vol 860, pp 360–376

Dimitrijevic MR, Minassian K, Jilge B, Rattay F (2002) Initiation of standing and locomotion like movements in complete SCI subjects by mimicking brain stem control of lumbar network with spinal cord stimulation. Proceedings of the 4th International Symposium on Experimental Spinal Cord Repair and Regeneration Brescia (Italy)

Ermentrout B (1995) Phase-plane analysis of neural activity. In: Arbib M (ed) The handbook of brain theory and neural networks. MIT Press, Cambridge, Mass., pp 732–738

Feng J, Brown D (2000) Integrate-and-fire Models with Nonlinear Leakage. Bull Math Biol 62: 467–481

Feng J (2001) Is the integrate-and-fire model good enough?—a review. Neural Netw 14: 955–975

Graham B, Redman S (1994) A simulation of action potentials in synaptic boutons during presynaptic inhibition. J Neurophysiol 71(2): 538–549

Hultborn H (2001) State-dependent modulation of sensory feedback. J Physiol 533.1: 5–13

Jankowska E (1992) Interneuronal relay in spinal pathways from proprioceptors. Progr Neurobiol 38: 335–378

Jankowska E (2001) Spinal interneuronal systems: identification, multifunctional character and reconfigurations in mammals. J Physiol 533.1: 31–40

Jilge B, Minassian K, Rattay F, Dimitrijevic MR (2002) Tonic and rhythmic motor units activity of the cord induced by epidural stimulation can alter posterior roots muscle reflex responses. Proceedings of the 7th Annual Conference of the IFESS Ljubljana (Slovenia)

Jilge B, Minassian K, Rattay F, Pinter MM, Gerstenbrand F, Binder H, Dimitrijevic MR (2003) Initiating extension of the lower limbs in subjects with complete spinal cord injury by epidural lumbar cord stimulation. Exp Brain Res (in press)

Knight B (1972) Dynamics of encoding in a population of neurons. J Gen Phys 59: 734–766

Lamotte D'Incamps B, Meunier C, Monnet ML, Zytnicki D, Jami L (1998) Reduction of presynaptic action potentials by PAD: model and experimental study. J Comp Neurosci 5: 141–156

Lamotte D'Incamps B, Meunier C, Zytnicki D, Jami L (1999) Flexible processing of sensory information induced by axo-axonic synapses on afferent fibers. J Physiol (Paris) 93: 369–377

Lánský P, Rodriguez R (1999a) The spatial properties of a model neuron increase its coding range. Biol Cybern 81: 161–167

Lánský P, Rodriguez R (1999b) Two-compartment stochastic model of a neuron. Physica D 132: 267–286

Lundberg A (1973) The significance of segmental spinal mechanisms in motor control. 4th International Symposium on Biophysics Moscow (Russia)—*Cited by Hultborn 2001*

McCrea DA (2001) Spinal circuitry of sensorimotor control of locomotion. J Physiol 533.1: 41–50

Minassian K, Rattay F, Dimitrijevic MR (2001a) Features of the reflex responses of the human lumbar cord isolated from the brain but during externally controlled locomotor activity. Proceedings of the World Congress on Neuroinformatics Vienna (Austria)

Minassian K, Rattay F, Pinter MM, Murg M, Binder H, Sherwood A *et al.* (2001b) Effective spinal cord stimulation (SCS) train for evoking stepping locomotor movement of paralyzed human lower limbs due to SCI elicits a late response additionally to the early monosynaptic response. Soc Neurosci Abstr 27: 935.12

Minassian K, Jilge B, Rattay F, Pinter MM, Gerstenbrand F, Binder H, Dimitrijevic MR (2002) Effective spinal cord stimulation (SCS) for evoking stepping movement of paralyzed human lower limbs: study of posterior root muscle reflex responses. Proceedings of the 7th Annual Conference of the IFESS Ljubljana (Slovenia)

Minassian K, Jilge B, Rattay F, Pinter MM, Binder H, Gerstenbrand F, Dimitrijevic MR (2003) Stepping-like movements in humans with complete spinal cord injury induced by epidural stimulation of the lumbar cord: Electromyographic study of compound muscle action potentials. Spinal cord (submitted)

Nusbaum MP, El Manira A, Gossard JP, Rossignol S (1999) Presynaptic mechanisms during rhythmic activity in vertebrates and invertebrates. In: Stein PSG, Grillner S, Selverston AI, Stuart DG (eds) Neurons, Networks and Motor Behavior. MIT Press, Cambridge, Mass., pp 257–267

Pakdaman K (2001) Periodically forced leaky integrate-and-fire model. Phys Rev E 63

Pearson KG (1993) Common principles of motor control in vertebrates and invertebrates. Annu Rev Neurosci 16: 265–297

Rattay F, Minassian K, Jilge B, Pinter MM, Dimitrijevic MR (2003) EMG analysis of lower limb muscle responses to epidural lumbar cord stimulation. Proceedings of the IEEE EMBS Conference Cancun (Mexico)

Rescigno AR, Stein RB, Purple RL, Poppele RE (1970) A neuronal model for the discharge patterns produced by cyclic inputs. Bull Math Biophys 32: 537

Rospars JP, Lánský P (1993) Stochastic model neuron without resetting of dendritic potential: application to the olfactory system. Biol Cybern 69(4): 283–294

Rudomin P, Schmidt RF (1999) Presynaptic inhibition in the vertebrate spinal cord revisited. Exp Brain Res 129: 1–37

Scharstein H (1979) Input-output relationship of the leaky-integrator neuron model. J Math Biol 8: 403–420

Segev I (1990) Computer study of presynaptic inhibition controlling the spread of action potentials into axonal terminals. J Neurophysiol 63(5): 987–998

Shimokawa T, Pakdaman K, Takahata T, Tanabe S, Sato S (2000) A first-passage-time analysis of the periodically forced noisy leaky integrate-and-fire model. Biol Cybern 83: 327–340

Softky W, Koch C (1995) Single-cell models. In: Arbib M (ed) The handbook of brain theory and neural networks. MIT Press, Cambridge, Mass., pp 879–884

Walmsley B, Graham B, Nicol MJ (1995) Serial E-M and simulation study of presynaptic inhibition along a group Ia collateral in the spinal cord. J Neurophysiol 74(2): 616–623

Epilogue

One has to be careful when interpreting the approach of applying sustained electrical stimulation to the lumbosacral cord below a spinal cord lesion as "mimicking", or "simulating", the missing tonic input which is normally provided by the brainstem. Obviously, the artificial "code" applied from outside can replace the complex dynamic process underlying postural control in a fragmentary manner only. Moreover, in response to a spinal cord injury, reorganisation of spinal circuitry takes place which generates new motor control strategies and new features of spinal reflex activity, respectively. Therefore, the situation of the electrically stimulated injured spinal cord is quite different from the normal condition. Apparently, definite evidence for the brain actually providing *simple* neuronal commands to the spinal cord in order to perform lower limb extension has not been supplied. Nor has the supraspinal-spinal communication been "decoded" which is aimed at implementing a standing posture. The results presented in this work may rather be regarded as clues to fundamental *principles* underlying the control of these postural and motor tasks by the central nervous system. Taking these principles into account when interacting with the injured spinal cord may open a new avenue to the neurorehabilitation of standing and walking in paraplegic subjects.

Curriculum vitae

Bernhard Jilge

born on **August 3, 1969** in Vienna; *citizenship:* Austria; *religion:* Roman Catholic
parents: Anita and Herbert Jilge, *brother:* Roman Jilge

Education

1975 – 1979	Primary school, Vienna 1050, Gassergasse 46
1979 – 1983	Grammar school "Josef Haydn-Gymnasium", Vienna 1050, Reinprechtsdorfer Straße 24
1983 – 1988	Commercial college "Vienna Business School", 1010, Akademiestraße 12
	June 7, 1988 **High school degree**
1988 – 1996	Study of Technical Mathematics (Economic Mathematics), Vienna University of Technology
	Study of Physics, University of Vienna (6 terms)
	June 27, 1996 **Graduation in Technical Mathematics (Dipl.-Ing.)** *Diploma thesis:* "Evolutionarily stable strategies" (Evolutionsstabile Strategien, in German)
1991 – 1994	Training for a teacher of social dancing, Vienna association of teachers of dancing
	June 4, 1994 **Certificate as a teacher of social dancing**
2001 – 2003	Doctoral program in Engineering sciences, Vienna University of Technology

Professional career

1984 – 1987	Practical training (during holidays) at the "Raiffeisen" building society, Vienna
1988 – 2001	Teacher at the dancing schools „Stanek" and „Watzek", Vienna
1993 – 1994	Freelance (editor) at Radio Lower Austria
1996 – 1997	Civil servant at the "Kaiser Franz Josef" hospital, Vienna
Jul/Aug 1997	Teacher of Mathematics and Cost/Accounting at "Lern 1", Vienna
1997 – 1998	Temporary worker at the "Raiffeisen" building society, Vienna
1998 – 2001	Managing director of dancing school „Watzek", Vienna
1998 – 2001	Systems analyst and sub-project leader at „Software Daten Service", Vienna
2001 – 2003	Scientific collaborator of Univ.-Prof. DDr. Frank Rattay, TU-BioMed Association for Biomedical Engineering, Vienna University of Technology
	Project: "Modelling LLPG activity in incomplete SCI subjects" (supported by the Austrian Science Fund FWF)

Publications

1. Jilge B., Länger H. (1996) Evolutionarily stable strategies. Diploma Thesis. (Evolutionsstabile Strategien, in German) Vienna University of Technology
2. Pinter M. M., Jilge B., Dimitrijevic M. R. (2001) Putative contribution of residual brain control below spinal cord injury to the involuntary movements of the paralyzed lower limbs. Proceedings of the World Congress on Neuroinformatics Vienna (Austria): 58
3. Jilge B., Pinter M. M., Dimitrijevic M. R. (2001) Involuntary movements of paralyzed lower limbs and residual brain control below spinal cord injury. Proceedings of the World Congress on Neuroinformatics Vienna (Austria): 62–63
4. Jilge B., Minassian K., Dimitrijevic M. R. (2001) Electrical stimulation of the human lumbar cord can elicit standing parallel extension of paralyzed lower limbs after spinal cord injury. Proceedings of the World Congress on Neuroinformatics Vienna (Austria): 281–283
5. Jilge B., Minassian K., Rattay F., Dimitrijevic M. R. (2002) Tonic and rhythmic motor units activity of the cord induced by epidural stimulation can alter posterior roots muscle reflex responses. Proceedings of the 7th Annual Conference of the IFESS Ljubljana (Slovenia): 267–268
6. Minassian K., Jilge B., Rattay F., Pinter M. M., Gerstenbrand F., Binder H., Dimitrijevic M. R. (2002) Effective spinal cord stimulation (SCS) for evoking stepping movement of paralyzed human lower limbs: study of posterior root muscle reflex responses. Proceedings of the 7th Annual Conference of the IFESS Ljubljana (Slovenia): 167–169
7. Dimitrijevic M. R., Minassian K., Jilge B., Rattay F. (2002) Initiation of standing and locomotion like movements in complete SCI subjects by mimicking brain stem control of lumbar network with spinal cord stimulation. Proceedings of the 4th International Symposium on Experimental Spinal Cord Repair and Regeneration Brescia (Italy): 25–27
8. Rattay F., Resatz S., Lutter P., Minassian K., Jilge B., Dimitrijevic M. R. (2003) Mechanisms of electrical stimulation with neural prostheses. *Neuromodulation* 6(1): 42–56
9. Jilge B., Minassian K., Rattay F., Pinter M. M., Gerstenbrand F., Binder H., Dimitrijevic M. R. (2003) Initiating extension of the lower limbs in subjects with complete spinal cord injury by epidural lumbar cord stimulation. *Exp Brain Res* (in press)
10. Jilge B., Rattay F., Dimitrijevic M. R. (2003) Initiating pattern generator activity by epidural lumbar cord stimulation. Proceedings of the European Workshop on Movement Sciences Muenster (Germany)
11. Rattay F., Minassian K., Jilge B., Pinter M. M., Dimitrijevic M. R. (2003) EMG analysis of lower limb muscle responses to epidural lumbar cord stimulation. Proceedings of the IEEE EMBS Conference Cancun (Mexico)
12. Minassian K., Jilge B., Rattay F., Pinter M. M., Binder H., Gerstenbrand F., Dimitrijevic M. R. (2003) Stepping-like movements in humans with complete spinal cord injury induced by epidural stimulation of the lumbar cord: Electromyographic study of compound muscle action potentials. *Spinal cord* (submitted)